Gas Chromatographic Electron Capture Negative Ionization Mass Spectrometric (GC/ECNI/MS) Determination of Unique Fluorinated Compounds in the Sediments of Lake Ontario

And

The Effect of High-Boiling Alcohols (as Injection Solvents) on Chromatographic Behaviour of Polycyclic Aromatic Hydrocarbons in Gas Chromatography

By

Rosalie Krystyna Zielinski-Lawrence

A Thesis Presented to the Department of Chemistry in Partial Fulfillment of the Requirements for the Degree of Master of Science

July 2009
Brock University
St. Catharines, Ontario

Abstract

Part I – Fluorinated Compounds

A method has been developed for the extraction, concentration, and determination of two unique fluorinated compounds from the sediments of Lake Ontario. These compounds originated from a common industrial landfill, and have been carried to Lake Ontario by the Niagara River. Sediment samples from the Mississauga basin of Lake Ontario have been evaluated for these compounds and a depositional trend was established. The sediments were extracted by accelerated solvent extraction (ASE) and then underwent clean-up, fractionation, solvent exchange, and were concentrated by reduction under nitrogen gas. The concentrated extracts were analyzed by gas chromatography – electron capture negative ionization – mass spectrometry.

The depositional profile determined here is reflective of the operation of the landfill and shows that these compounds are still found at concentrations well above background levels. These increased levels have been attributed to physical disturbances of previously deposited contaminated sediments, and probable continued leaching from the dumpsite.

Part II – Polycyclic Aromatic Hydrocarbons

Gas chromatography/mass spectrometry is the most common method for the determination of polycyclic aromatic hydrocarbons (PAHs) from various matrices. Mass discrimination of high-boiling compounds in gas chromatographic methods is well known. The use of high-boiling injection solvents shows substantial increase in the response of late-eluting peaks. These solvents have an increased efficiently in the transfer of solutes from the injector to the analytical column. The effect of 1-butanol, 1-pentanol, cyclopentanol, 1-hexanol, toluene and n-octane, as injection solvents, was studied.

Higher-boiling solvents yield increased response for all PAHs. 1-Hexanol is the best solvent, in terms of PAH response, but in this solvent PAHs were more susceptible to chromatographic problems such as peak splitting and tailing. Toluene was found to be the most forgiving solvent in terms of peak symmetry and response. It offered the smallest discrepancies in response, and symmetry over a wide range of initial column temperatures.

Acknowledgement

First and foremost, I would like to thank my supervisor, Dr. Ian Brindle, for the opportunity to work on this project, and for his direction and patience throughout. I must also thank Chris Marvin for his guidance throughout these past two years.

This project would not have been possible without support and cooperation from the people at Environment Canada in Burlington. Thanks to Donna Zaruk, Julia Jia, Joanne Schatschneider, and Ed Sverko.

I would like to express my most sincere thanks to Tim Jones for answering my many, many questions and for his understanding and encouragement. I would also like to thank Donna Vukmanic, Miles Snow, and the staff at the machine and electronics shops at Brock University.

This work is dedicated to my family, and especially my husband, Bryan. He has been beside me every step of the way, and has always instilled confidence in me. At times, I thought I would never finish. He was always there to encourage me. His confidence in me has driven me to accomplish things that I never thought I would be able to do.

Table of Contents

List of Tables

List of Figures

Chapter 1 – Introduction

Part I – Fluorinated Compounds

Historical Background

For over one hundred years the Niagara River has been, and continues to be, a source of contamination to Lake Ontario. The industrial revolution sparked the growth of industry along the shores of the Niagara River. A readily available source of process water drew industry to the area. During the 20th century, massive chemical and manufacturing plants were built along the shores of the river. The Niagara River became a highly industrialized area. Billions of gallons of chemical wastes have been dumped both directly into the river, and into open pits near the river. As cities expanded, residential neighbourhoods were developed around, and in some cases over, these buried wastes. Love Canal was, of course, the most infamous example of such an occurrence.

Now, a hundred years after the industrial revolution, although many of the industries have closed, or moved from the area, many have left behind dumpsites filled with organic wastes that continue to leach into the Niagara River, which are subsequently carried to Lake Ontario. If all industrial contamination were to completely stop, it has been estimated that it would take nearly 200 years in order for the Niagara River to rejuvenate itself [1].

Niagara River – Lake Ontario System

The condition of the Niagara River is important not only because it serves as a drinking water source for many people [2], but also as it is a major supply of water [3], and fine-grained sediments [4] to Lake Ontario. Fifty percent of all fine-grained sediment input [4], and approximately eighty-five percent of water input [5] to Lake Ontario comes from the Niagara River.

In addition to being a major source of drinking water for over 6.5 million people (in Canada and the United States) that live along its shores [6], Lake Ontario is also an important source for recreation, transport, and food [7].

Unfortunately, the very characteristics that make the Niagara River falls area an ideal location for the production of chemicals also make it the absolute worst place to have them buried. The area is like a giant sponge. It is composed of a shallow layer of sand and silt that covers Lockport dolomite which is fractured bedrock [8]. Vast amounts of water permeate through the ground and discharge into the river. Large volumes of liquid chemical wastes in landfills could, too, permeate through the ground in the form of APL (aqueous phase liquid), NAPL (non-aqueous phase liquid), and DNAPL (dense non-aqueous phase liquid) and follow the flow of groundwater into the river. Once chemical wastes have found their way into the river, either from being dumped or seeping though the ground, they can be transported to Lake Ontario in two ways: by water, or by sediment. Water-soluble contaminants can dissolve in the water and be carried away by the flow of the river. Contaminants that are not water-soluble can adsorb to fine particles in the water and settle to the bottom of the river. The sediments are then carried into Lake Ontario, by the rushing waters of the river.

Hyde Park Landfill

Most of the existing chemical waste sites along the Niagara River represent non-point sources for various contaminants. One dumpsite in particular, however, represents a point source for an array of fluorinated compounds that were never synthesized for industrial purposes. These compounds are byproducts of other chemical wastes that have been dumped at this site. This insidious dumpsite is called the Hyde Park landfill. Occidental Chemical Company (OCC), formerly Hooker Chemicals and Plastics, is responsible for this site, as well as the disaster at Love Canal (from which the company has incurred its notoriety).

The Hyde Park Landfill is located in the Northwest corner of the city of Niagara Falls, New York. It is situated a few blocks east of a residential community [9], and less than 1 km from the Niagara River [10].

The Hyde Park dump is of specific interest for the purpose of this study. This landfill was opened to replace the Love Canal. The Hyde Park landfill, formerly a quarry pit [11], is a 15 acre site that was used by Hooker Chemicals and Plastics to dump some 80 000 tons of chemical waste between 1953 and 1975 [8]. Of these 80 000 tons of waste, there are about 3300 tons of 2,4,5-trichlorophenol (2,4,5-TCP) wastes [12]. 2,3,7,8-tetrachlorodibenzo-*p*-dioxin (TCDD), an extremely potent carcinogen, is known to be present in significant amounts in TCP wastes, as it is a by-product in the synthesis of 2,4,5-TCP. The Hyde Park landfill is expected to contain 0.7-1.6 tons of TCDD [12], thus making it the largest dioxin dump in the world [1]. 2,4,5-TCP was used to make several herbicides, most notably 2,4,5-trichlorophenoxyacetic acid (2,4,5-T) which was a major component of Agent Orange [13].

The landfill is also known to contain 55 000 tons of halogenated wastes, about 10% of which is from the synthesis of 4-chloro-(trifluoromethyl)benzene [14].

Remediation of Hyde Park

In 1987, a Declaration of Intent was signed between the US EPA, the New York State Department of Environmental Conservation (NYSDEC), Environment Canada, and the Ontario Ministry of the Environment, to reduce the loading of toxic material into the Niagara River, under a cooperative effort [15]. The work plan was called the Niagara River Toxics Management Plan (NRTMP). Under this plan, the Hyde Park Landfill was one of thirty-three toxic dumpsites that were its focus. The US EPA sued OCC in 1979, requiring the clean up the Hyde Park

Landfill. The landfill was classified as a Category I site (the most severe category), under the NRTMP. Waste sites under this category were responsible for contributing more than 50lbs of toxic material to the Niagara River each day [12]. In 1986 an agreement was made between OCC, the US EPA, and the NYSDEC. This agreement involved the containment of the landfill, and not its excavation, which was highly desired by citizens of Canada and the United States who live along the shores of the Niagara River [11].

Monitoring, containment, and extraction wells have been established throughout the landfill. These wells are in place to ensure that contaminants in the overburden, and the plumes of APL and NAPL, do not migrate from the landfill [8]. An on-site leachate storage and handling facility has been built. Groundwater, which flows both in the overburden, and in the fractured bedrock below, is pumped and treated on site. NAPL is pumped and shipped, by truck, for incineration in Texas. Bloody Run Creek has been excavated, and any sewers linked to the landfill have been closed off [8]. The entire landfill, and the gorge where the groundwater drains to the Niagara River, has been fenced off. A three-foot thick layer of clay, and a vegetative cover cap the landfill. Remediation at the Hyde Park Landfill was complete according to the agreement between OCC and the US EPA and NYSDEC in 2003 [12]. The site is monitored, and reviewed every five years to ensure containment of toxins.

Fluorinated Compounds

In 1981, a study was conducted by Professor Ron Hites of Indiana University to determine what, if anything, might be leaching from various chemical waste sites in the New York area [3]. The Hyde Park Landfill was one of the dumpsites in question. In Bloody Run Creek, which (at that time) drained the Hyde Park Landfill to the Niagara River, Hites *et al.* found a series of fluorinated compounds [3]. The ten fluorinated compounds can be seen in Figure 1.

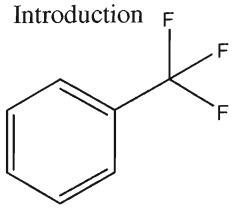

Benzotrifluoride
(98-08-8)

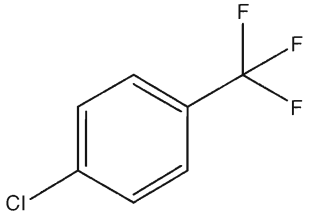

4-Chlorobenzotrifluoride
(98-56-6)

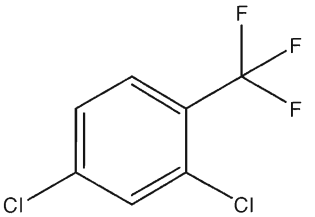

2,4-Dichlorobenzotrifluoride
(320-60-5)

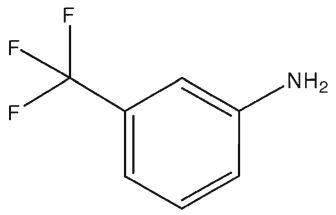

3-Aminobenzotrifluoride
(98-16-8)

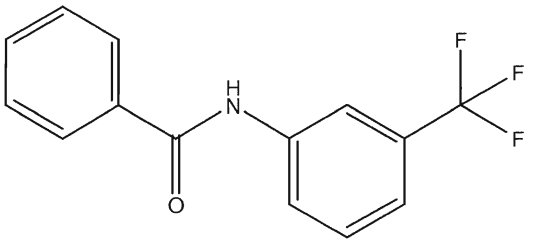

N-(3-trifluoromethyl)phenylbenzamide
(1939-24-8)

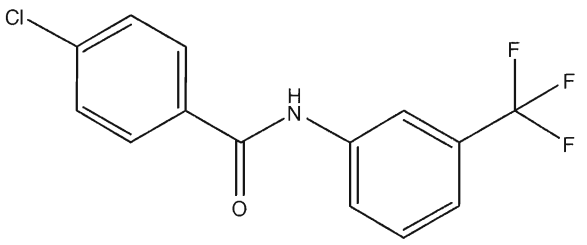

4-chloro-N-[3-(trifluoromethyl)phenyl]benzamide
(3830-65-7)

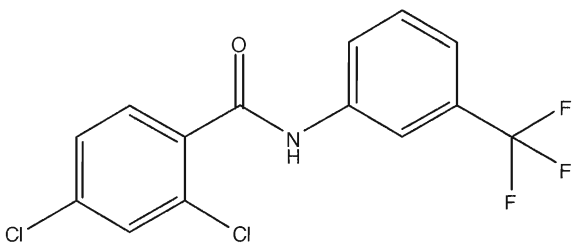

2,4-dichloro-N-[3-(trifluoromethyl)phenyl]benzamide
(1230-84-8)

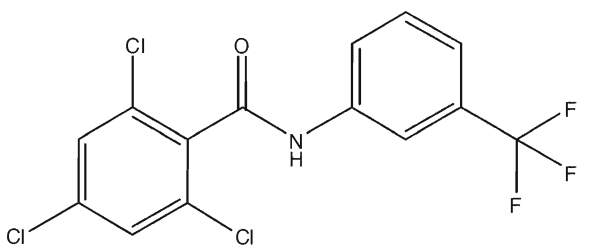

2,4,6-trichloro-N-[3-(trifluoromethyl)phenyl]benzamide
(unknown)

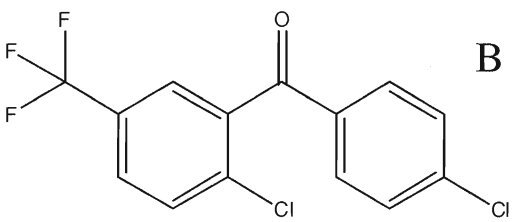

2,4'-dichloro-5-(trifluoromethyl)-benzophenone
(95998-69-9)

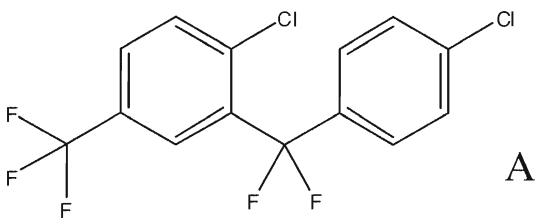

difluoro-2,4'-dichloro-5-(trifluoromethyl)diphenylmethane
(95998-70-2)

Figure 1 – Fluorinated compounds found 1n 1981 [3] (CAS No.)

Some of these compounds were expected, as the Hyde Park dump was known to contain thousands of tons of waste pertaining to the synthesis of p-chlorobenzotrifluoride. It was also not surprising that these benzotrifluoride derivatives were found in Bloody Run Creek, as they had been reported by Yurawecz [16] to be present in fish from the Niagara River.

In addition to the expected benzotrifluoride derivatives, however, were reported a couple of unusual fluorinated compounds (see Figure 2, compounds A and B). Bloody Run Creek was found to contain large quantities of these two compounds that, at that time, did not exist in the chemical literature. It was deduced by Hites *et al.* that these compounds were formed through "accidental synthesis," a Freidel-Crafts reaction between some of the by-products from the synthesis of p-chlorobenzotrifluoride, catalyzed by ferric chloride - resulting from the stainless steel barrels in which some of the chemical wastes were stored [3] (see Figure 2). These two compounds should be the most stable, of the ten fluorinated compounds found, and they became the focus of Hites' research over the next several years. There are no other known sources of these fluorinated compounds upstream, or downstream, of the Hyde Park landfill making it the point source for these contaminants.

In 1983, nearly ten years after the landfill was closed, these fluorinated compounds were detected in surficial sediments in the Niagara and Mississauga basins of Lake Ontario [17]. The compounds detected in the Mississauga basin of Lake Ontario were found over 80km from the entrance of the Niagara River to the lake. This clearly indicates that, despite initial remedial efforts by OCC, Hyde Park was still leaching significant amounts of material into the Niagara River at that time.

As it was clearly shown in 1983, that compounds from the Niagara River would accumulated to detectable levels in the sediments of Lake Ontario, Hites *et al.* turned their attention to sediment cores and fish from the lake. In 1985, the two unique fluorinated compounds, A and B, were found to be present in sediment

cores from all four sedimentation basins (Niagara, Mississauga, Rochester, and Kinston) of Lake Ontario [14].

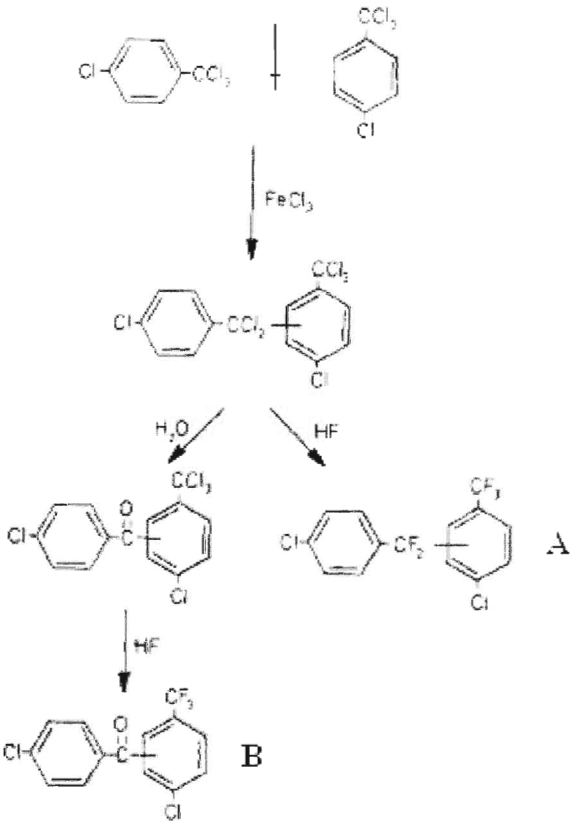

Figure 2 – Hites' proposed synthesis of compounds A and B [3].

In 1986, Hites *et al.* performed a study in which they set out to determine where compounds A and B would come to rest in Lake Ontario. The time taken for these compounds to reach their final resting place was also determined. It was found that, for the three major basins (not including Kingston), the year in which these compounds first appeared in sediments was 1958 and the year of maximum deposition was in 1970 ± 2 years [18]. After this time, there was a marked decrease in the concentration of these compounds found in the sediments.

Based on the time profile of compounds A and B in Lake Ontario, Hites *et al.* concluded that these compounds are transported into the lake via a particle-

associated pollutant transport mechanism [18]. It was found that compounds entering the Niagara River from Hyde Park would be carried into the lake where they would be quickly and evenly distributed amongst the Niagara, Mississauga, and Rochester basins. The compounds, adsorbed to suspended sediments in the lake, are distributed by mixing. Lower concentrations of the compounds are observed in the Kingston basin as this basin is not adjacent to the Southern nearshore zone, from which the compounds that enter the lake from the river are distributed. The Kingston basin is also missing a nepheloid layer of suspended sediments that is present in the other basins [18]. A nepheloid layer is a layer of suspended sediments above the lake floor.

As the Hyde Park landfill was opened in 1953, and closed in 1975, the values for the year of onset and maximum determined by Hites *et al.*, from core data, are realistic. Since these compounds are by-products of industrial processes, and have never been intentionally produced for commercial purposes [3], industrial processes cannot explain their depositional history. But, their depositional history reflects of the operation of Hyde Park dump. Although the dumpsite was opened in 1953, there are a couple of reasons that the compounds were not found in sediments until 1958. First of all, it is not known that these compounds were put into the dump when it was first opened. Secondly, deposition of fine-grained sediments entering the lake can be delayed by 1-2 years because of resuspension, and mixing [18].

Hites *et al.* also performed studies on sedentary fish from the Niagara River – Lake Ontario system. It was known that the fluorinated compounds were not only reaching, but accumulating over time in the sediments of the lake. The purpose of the studies with sedentary fish was to determine if these fluorinated compounds were bioavailable. The fat of non-migratory fish such as carp, goldfish, catfish, and suckers were analyzed for fluorinated compounds. Compound A was found in all fish samples near the Hyde Park dumpsite, downstream of the dumpsite, and in all streams off of Lake Ontario tested -

including the St. Lawrence River [18]. Concentrations as high as 160ng/g fish fat were found in fish from Fort Niagara, which is the Niagara River meets Lake Ontario.

Interestingly, compound B was only found in two fish samples out of fifteen taken from the Niagara River – Lake Ontario area. Both samples contained very low levels of compound B (3ng/g fish fat and less), relative to compound A [18].

Hites *et al.* had predicted, in 1986, that, if the constant rate of decrease in the concentration of fluorinated compounds observed between 1970 and 1986 were to continue, in the years following the concentration of the compounds in sediments should reach background values by the early 1990s [18]. In light of this, Hites *et al.* reopened the study, ten years later, in 1996 to see if the prediction had come true. It had not. It was found that the concentration of compounds A and B in sediments had decreased to twenty percent of its maximum and then leveled off [10]. Hites *et al.* suggested that, while the remedial efforts to contain the chemicals had dramatically reduced the amount of chemicals allowed to escape the landfill, that it was probable that leachate was still reaching the Niagara River.

This conclusion was vehemently disputed by researchers funded by OCC. Smith *et al.* claimed that the results published by Hites did not suggest that the landfill was still leaking, and that the concentration of chemicals in the sediments were decreasing in an expected manner (according to a first-order decrease) [19]. Interestingly, Smith *et al.* also stated, in the same paper, that adjustments to the bedrock remedy at Hyde Park were ongoing, at that time (1997), and that the adjustments would eliminate the flow of leachate through the bedrock to the Niagara River.

Significance of Fluorinated Compounds

As the Hyde Park landfill is the only known point source for these unique fluorinated compounds, A and B, they can provide important information about some other toxins of concern. This information is of significance as Hyde Park is the largest existing dioxin (TCDD) dump in the world [1]. If the fluorinated markers continue to accumulate in the sediments of Lake Ontario, this suggests that other toxins (like TCDD) from the landfill are also continuing to migrate from the landfill and subsequently ending up in the lake. A temporal trend of the markers would indicate the effectiveness of remedial strategies employed at Hyde Park.

Knowing that any leaching of compounds from the landfill will subsequently accumulate in Lake Ontario suggests an important question – why are OCC, USEPA, and/or NYSDEC not monitoring the sediments or suspended sediments of the lake for the markers to determine the impact that the dump had, and may still have, on the lake? As part of the ongoing remedial process, monitoring wells are used to ensure the containment of toxins in the landfill. But information collected from these wells cannot possibly confirm complete containment. Using such techniques, it is not possible to know of whether there are other potential transport routes from the landfill to the river.

Comparison of Compounds A and B

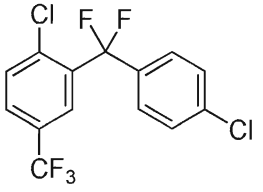

Compound A

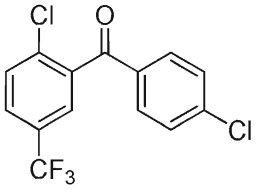

Compound B

Some information regarding these compounds can be obtained based on research done in the past. Hites *et al.* [14] found, in 1985, that in Bloody Run Creek, the concentration of compound B in sediments was three times higher than the concentration of compound A. However, in Lake Ontario samples, compound A was always found in concentrations that were approximately four times higher than compound B. The following year, Hites *et al.* [18] found that the concentration of compound B, relative to compound A, decreased from 56% in the Niagara Basin, to 37% in the Mississauga Basin, to 23% in the Rochester Basin in Lake Ontario. This information, suggests that compound B may be less stable than compound A and is probably more susceptible to degradation. Compound A, then, is more environmentally persistent. These compounds are expected to be associated with particulate matter, and since sediments are expected to be evenly distributed throughout the lake within a few months [18], much of compound B is broken down in this time. It is also possible that compound B has less affinity for sediments than compound A.

Also in 1985 Hites *et al.* [18] collected fish samples from major tributaries to Lake Ontario. Fish are exposed to compounds A and B through the intake of particles, to which these compounds are adsorbed, or by eating smaller contaminated species. Compound A was found in fish from all tributaries tested that were near, or downstream of, the Hyde Park landfill (some of which are over 300km from the landfill). Not only was it found in all of the fish samples, it was found in concentrations that are significantly higher than any of the sediment samples tested. This suggests that compound A is not only bioavailable, but also bioaccumulative. This also suggests that compound A is lipophilic.

Compound B, on the other hand, was only found in two (of fifteen) fish samples and it was found at very low concentrations, relative to compound A [18]. This suggests that compound B may be less bioavailable than compound A. But it could also suggest that compound B is preferentially metabolized and therefore less likely to bioaccumulate.

Octanol/water partition coefficients are correlated to: the partitioning between water and sediment [20], bioconcentration [21], and aqueous solubility [22]. Compounds are expected to bioaccumulate in an aquatic species if they possess a $LogK_{ow}$ value that is between 5.0 and 7.5 [21]. Based on the molecular structure of compounds A and B, their $LogK_{ow}$ values can be estimated through an atom/fragment contribution method [23, 24]. Compound A is estimated to have a $LogK_{ow}$ value of 6.46, and compound B has an estimated $LogK_{ow}$ value of 5.40 [25].

Based on these values, it can be seen that compound A is more lipophilic than compound B. It should have a higher affinity for sediments, and will be more likely to bioaccumulate. This is in agreement with experimental data.

Compound B is also expected to have higher aqueous solubility than compound A, based on its $LogK_{ow}$. The aqueous solubility of compound A is estimated to be 0.02mg/L (at 25°C) and the aqueous solubility of compound B is estimated to be 0.23mg/L (at 25°C) [26]. Based on this higher aqueous solubility and lower lipophilicity, compound B will have lower affinity for sediments. This probably contributes to the lower concentrations of compound B found in Lake Ontario sediments, relative to compound A.

Extraction

There are various methods used for the extraction of semivolatile organic compounds from solid matrices. These include: soxhlet extraction, ultrasonic extraction (solid-liquid extraction with sonication or shake flask method), supercritical fluid extraction (SFE), accelerated solvent extraction (ASE), and microwave-assisted extraction (MAE).

The mechanism for extraction involves the desorption of solutes from the solid surface, diffusion into the layer of organic material surrounding the solid,

and partitioning from the organic material and into the extracting solvent [27]. Extraction efficiency is governed by three factors:

i) Solubility

The solubility of an analyte in a solvent depends mostly on the type of solvent chosen for extraction. A solvent with Henry's Law Constant larger than the Henry's Law constant of the analyte should be chosen. In this way, the analyte will not escape the solvent, and will concentrate in the solvent as the solvent evaporates [P]. The dimensionless Henry's Law constant can be determined from equation (1) below.

$$H' = \frac{P_{vp}\,(MW)}{0.062\;ST} \qquad (1)$$

P_{vp} = vapour pressure (mmHg), MW = molecular weight,
S = aqueous solubility (mg/L), T = temperature (K)

For a given solvent, the solubility of the analyte in the solvent is directly affected by temperature and pressure.

ii) Mass Transfer

Mass transfer includes the penetration of the solvent into the crevasses of the matrix, and the extraction of analytes from the surface of the solid. These processes depend on the diffusion coefficient of the analyte in the solvent, and on matrix characteristics such as particle size. Mass transfer is promoted by agitation, increased temperature and pressure, reduced particle size, and low solvent viscosity [28].

iii) Matrix Effects

Matrix effects account for the removability of analytes from the sample. It is more difficult to remove analytes from a matrix which they have occupied for a longer period of time. Over time, analytes can diffuse into tiny pores present in a sample, or bind very strongly to organic matter surrounding the solid matrix. As kinetics (of diffusion), of the solvent, to get into the pores is very slow, the converse is also true: extraction is a slow process.

Extraction Methods

Extraction techniques for extracting semivolatile organic compounds from solid matrices should ideally be exhaustive [29]. These methods should also be able to perform fast extractions and be easy to use. If the extractions are performed routinely, then automation is also essential.

The common goal of extraction methods, for solid samples, is to achieve better interaction between the extracting solvent and the solid matrix. Increased interaction will lead to increased extraction efficiency. Since extraction kinetics are governed strongly by temperature and pressure, extraction techniques for analytes in solid matrices can be grouped into one of two categories:

i) Classical Methods

These extraction techniques are performed at atmospheric pressure. Heat and/or ultrasonic vibrations are employed to facilitate the removal of analytes from the matrix. These extractions are often time consuming, and involve the use of large volumes of high-purity organic solvents. This results in higher costs, and lower throughput of samples. Classical extraction methods include Soxhlet and ultrasonic extraction.

ii) High Temperature/Pressure Methods

Extraction techniques that involve increased temperature and pressure are more efficient than the Classical Methods. There is usually a high initial cost (for the purchase of equipment) but, all things considered, these techniques are more cost effective in the end. High Temperature/Pressure Methods are more environmentally friendly, and yield a higher throughput of samples. Supercritical fluid extraction, ASE, and MAE fall under this category of extraction techniques.

Soxhlet Extraction

In Soxhlet extraction, a mass of solid sample is placed in a porous thimble. The solvent, located in a flask below the thimble, is heated to reflux. As the solvent evaporates, the vapour travels from the flask up a side arm to a condenser. The solvent vapour is then cooled and condenses to reform liquid solvent. The condensed solvent then runs down the condenser and falls into the sample thimble. Since the thimble is porous, when enough solvent has accumulated, it will be siphoned back down into the solvent flask. As the solvent passes through the sample, it extracts the organic compounds. Because the organic compounds are less volatile than the solvent, when the extract is heated in the flask, only the solvent evaporates. The organic compounds therefore become concentrated in the flask. As the sample is repeatedly extracted with fresh solvent, Soxhlet is an effective and exhaustive extraction technique. A Soxhlet system can be set up and left to run independently. The extractions are allowed to run unsupervised for set periods of time – usually 12-24 hours. Unfortunately, since the condensed solvent that performs the extraction is cool, the extraction is time consuming. This technique requires a relatively large volume of solvent.

The Soxhlet extractor was designed by Baron Von Soxhlet in the mid-nineteenth century [28]. Until the 1980s, Soxhlet extraction was the most widely used extraction technique for removing semivolatile analytes from solid matrices.

It is still considered as a benchmark technique against which other extraction techniques are often compared. Soxhlet has since been replaced by newer, more efficient, extraction techniques such as MAE and ASE.

Accelerated Solvent Extraction

Accelerated Solvent Extraction (ASE), or Pressurized Fluid Extraction, is performed at elevated temperatures (100-180°C) and pressures (1500-2000psi). A known mass of solid sample is loaded into an extraction cell between two filters. The cell is placed in the ASE instrument, and solvent is added. The cell is then heated and pressurized. The sample undergoes static extraction for a selected time period (usually 5 minutes). Extraction can be performed up to 5 times. Following each extraction, fresh solvent is used to flush the extract into a collection vial.

When the last extraction is complete, and the solvent has been flushed into the collection vial, the solvent lines are purged with nitrogen gas to push any remaining solvent into the collection vial.

The ASE system is completely automated, and can extract up to 24 samples independently. The analyst must load the samples and collection vials into the instrument, but can then leave the instrument unattended and return hours later to collect the extracts. Since the extraction cells have built-in filters, filtration of the extract is automatic and not required post extraction. The extracts will however, require clean up and concentration prior to analysis.

Under high pressure (as in the ASE system), the boiling point of the solvent is increased, and so it can be used for extraction at temperatures above its normal boiling point and still remain in the liquid phase [28]. The increased pressure helps the solvent to penetrate into the smallest pores in the sample matrix. Analyte solubility increases, and mass transfer occurs more rapidly at elevated temperatures. Van der Waals forces, hydrogen bonding, and dipole interactions are overcome at high temperatures [28].

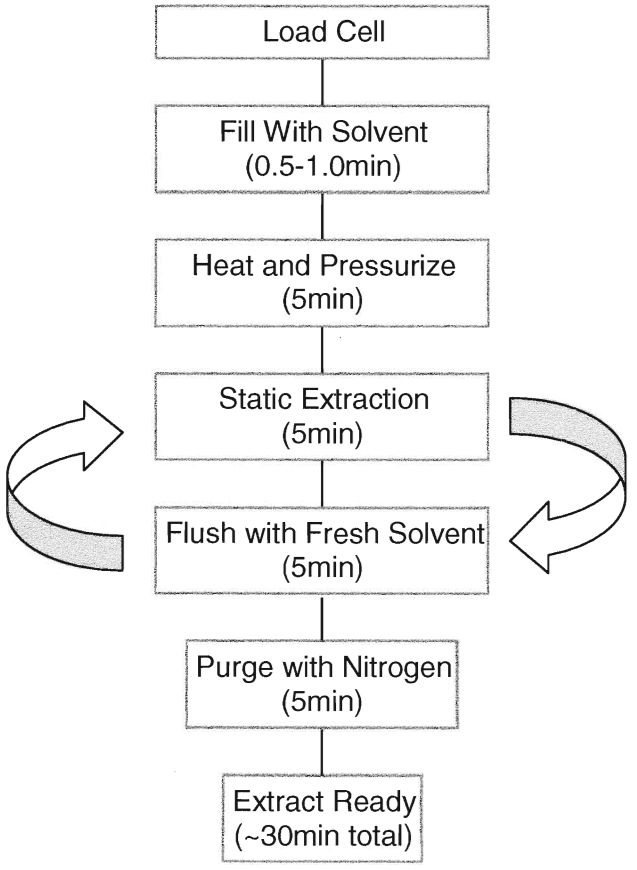

Figure 3 – Steps involved in a typical accelerated solvent extraction. Extract ready time assumes 1 static extraction. Several static extractions are usually performed.

The increased temperature also decreases solvent viscosity and surface tension, which facilitates diffusion into the matrix. These factors make ASE a faster and more efficient extraction method. The reproducibility of ASE is also better than classical extraction techniques – possibly due to its automation [30].

As with other extraction techniques, there are many parameters that must be optimized in an extraction in order for ASE to yield optimum results. These parameters include: extracting solvent, extraction temperature, static extraction time, and number of static extraction cycles [30]. Several authors report the use of Factorial Designs for the purposes of method optimization [31, 32].

Solvents

There is no universal solvent capable of extracting all types of analytes, and so a solvent, or solvent system, of similar polarity to the analytes should be chosen [33]. The solvent must yield optimum recovery, with high reproducibility. In general, a solvent in which the analytes are highly soluble, and the sample matrix has low solubility should be chosen [28]. Solvents that are effective in classical extraction techniques can usually be employed in ASE unless the matrix becomes soluble in the solvent at high temperatures.

Mixed solvent systems are suggested for the extraction of wet samples. The system is usually composed of two solvents: a water-miscible solvent (such as acetone), and a hydrophobic solvent. The water-miscible solvent is chosen to extract analytes from the layer of water on the solid particles of the matrix. A hydrophobic solvent of similar polarity to the analytes is then chosen to promote solubility of the analytes in the extracting solvent system [33].

Gan *et al.* experimented with several solvents/solvent systems in the extraction of atrazine and alachlor from soils [34]. Solvents used were dichloromethane/acetone (1:1, v/v), methanol, and hexane. When extracting relatively fresh samples (soil spiked with analytes two weeks before extraction), no difference was observed between the various solvents. However, when extracting aged samples (samples spiked with analytes 8-26 weeks prior to extraction), 1:1 dichloromethane: acetone and methanol were both found to be similar in extracting ability, and both were found to be significantly more affective than hexane [34]. US EPA method 3545A recommends the use of dichloromethane/acetone (1:1, v/v) for the extraction of organochlorine pesticides [33].

Popp *et al.* also experimented with the use of different extraction solvents/solvent systems in ASE [35]. In extracting PAHs from solid wastes, dichloromethane/acetone (1:1, v/v), acetone/hexane (1:1, v/v), and toluene were tested. It was demonstrated that, under the same extraction conditions, toluene

was the best extraction solvent by far. Recoveries of PAHs with toluene were found to be 30% higher than with dichloromethane/acetone. US EPA method 3545A recommends the use of dichloromethane/acetone (1:1, v/v) for the extraction of PAHs from soils [33]. This shows that the choice of solvent for extraction in ASE is significant, and should be optimized.

Extraction Time

It has been shown that multiple short extractions are more effective than longer single extractions. Popp *et al.* experimented with static extraction times of 5, 10, and 15 minutes for the extraction of PAHs, chlorinated pesticides, polychlorinated dibenzo-*p*-dioxins, and dibenzofurans in solid wastes [35]. It was found that when samples were extracted for 10 or 15 minutes, the recoveries were nearly the same but higher than those achieved for 5 minute extractions. Popp *et al.* also demonstrated that the yield of two successive 5 minute extractions were higher than the single 10 or 15 minute single extractions [35].

Accelerated solvent extraction has become popular in recent years, and has come to replace older, classical extraction techniques in many labs since its approval as a standard method by the United States Environmental Protection Agency (US EPA) in 1996 [33]. It was initially approved as a standard method for the extraction of organochlorine and organophosphorus pesticides, chlorinated herbicides, and polychlorinated biphenyls in sediments. It has since been applied to a wide range of compounds, and matrices. Accelerated solvent extraction has been shown to be useful in extracting: fatty acids in plasma [36], dioxins and furans in mineral matrices [37], terpenes in tree leaves [38], DDT metabolites in fish [31], bisphenol A in meat [39], antioxidants in microalga [32], and even organometallics in biological samples [40]. These topics only scratch the surface of potential for this extraction technique.

Accelerated Solvent Extraction vs. Soxhlet Extraction

Many authors have reported on the extraction efficiency of ASE vs. traditional Soxhlet extraction [29, 30, 41-43]. Most authors have found that ASE has the potential to be equal to, and in many cases superior to Soxhlet. However, optimization is essential, and choice of solvent is paramount. Even with the increased efficiency and potential automation of the Soxtec extractor, ASE is still a preferred extraction technique [41].

GC/MS Technique

Gas chromatography/mass spectrometry combines the high resolving power of GC with the very sensitive and selective detection and identification of MS. The two techniques combined yield a powerful analytical tool that can be used for the analysis of complex mixtures. It has evolved since the 1970s to become a versatile technique that can be used for a broad variety of applications [44]. Some of the areas in which GC/MS can be applicable include: chemistry, forensic science, biochemistry, medicine, food chemistry, environmental science, geochemistry, and gas analysis [45].

How it Works

Gas chromatography is a means of separating volatile, or semi-volatile, thermally-stable compounds. Mass spectrometry is a powerful detection technique.

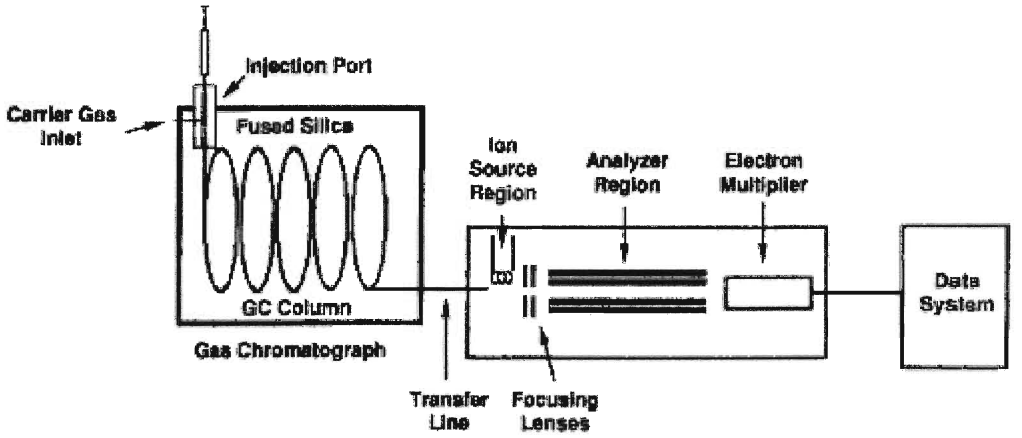

Figure 4 - Schematic of gas chromatograph/mass spectrometer [44].

A sample is injected into the hot injector of the GC, where it evaporates. The vapour is pushed onto the column by the flow of carrier gas (inert gas). The column is coated with a stationary phase which is chosen based on the analytes. Once on the column, solutes will be separated based on their differing affinities for the stationary phase of the column. Those solutes having a higher affinity for the stationary phase will be retained longer than those solutes that have a low affinity for the stationary phase. Solutes will elute from the column directly into the ion source of the mass spectrometer. Here, the analytes will be ionized. After ionization, the ions are drawn into the mass analyzer where only selected ions will be allowed to pass through. These selected ions are accelerated to the detector. The detector sends a signal to the computer, which translates the result into a chromatogram.

Sample Preparation

Sample preparation for trace analysis in gas chromatography is very important. Sample preparation involves any work that is done to the sample from the time of sample collection to the time of analysis and may include: extraction, clean up, solvent exchange, concentration, and sometimes derivatization. It must be considered that essentially all of what is injected into the GC will be deposited

in the mass spectrometer except for some sample components that do not escape the liner, or are retained by the column. Semivolatile, and non-volatile materials can contaminate the column, and the mass spectrometer. Volatiles are easily pumped away by the vacuum system, but less volatile compounds can deposit in the ion source and will result in a decrease in sensitivity and increased maintenance, amongst other unfavourable effects [44]. Sample clean up should be performed, whenever possible, to minimize the introduction of contamination (in the form of non-volatiles) to the GC and MS.

Solvent selection for GC/MS is also significant. A solvent should not yield ions in the mass range of interest [44]. This will prevent one source of interference. Low molecular weight solvents, such as methanol, are often favoured as they will not produce ions in the range monitored for analytes. This is especially important when the analytes are of low molecular weight, and elute close to the solvent peak [44]. The significance of injection solvent selection will be discussed later.

Analytes that are not sufficiently volatile for gas chromatographic separation can sometimes be volatilized through derivatization. Derivatization can also enhance thermal stability, improve peak symmetry, provide selectivity, and allow for more sensitive detection [44].

Injection

There are three different injection techniques used in gas chromatography. *Split injections* are used for samples in which the compounds of interest compose >0.1% of the sample being injected. *Splitless injections* are used for trace analysis – when analytes constitute 0.01% of the sample. *On-column injections* are usually reserved for analytes that will decompose at temperatures above their boiling point [46]. As this project is concerned with trace analysis, splitless injections will be considered.

In a splitless injection, about 2μL of dilute sample is injected into the quartz liner of the injector. High injector temperatures (relative to the boiling point of analytes) are preferred as they promote more efficient transfer of solutes from the injector to the column [47]. During injection, the split vent remains closed. It will be opened after a predetermined amount of time has passed. Nearly complete transfer of the sample from the injector to the column is accomplished [48].

In splitless injections, refocusing techniques are often required because the sample is transferred from the injector to the column slowly - which results in band-broadening. Two common refocusing techniques are: solvent trapping, and cold trapping. In solvent trapping, the initial column temperature is set to be about 40°C below the boiling point of the solvent [46]. This will result in the condensation of the solvent at the head of the column and will hold up the analytes. The analytes will be focused into discreet bands which will result in sharp peaks.

Alternatively, in cold trapping, the initial column temperature can be chosen to be 150°C below the boiling point of the analytes of interest [46]. In doing this, the solvent and volatile compounds will migrate down the column whereas the compounds of interest will be condensed and focused at the head of the column until the column temperature increases and chromatography begins.

Chromatography

Chromatography was fist described by Russian botanist, Mikhail Tswett in the early 1900s. Tswett applied the technique to the separation of plant pigments [49].

Chromatography is a process which separates the components of a mixture through the distribution of the components between a stationary phase and a mobile phase [50]. The mobile phase provides transport for the mixture components as it is forced through the miscible stationary phase. The stationary

phase is chosen with respect to the analytes. It is chosen such that the analytes will variably distribute themselves between the mobile and stationary phases [51]. Analytes that are more strongly retained by the stationary phase will move more slowly through the mobile phase, whereas the analytes that are weakly retained will travel quickly through the mobile phase. This differential mobility provides a basis for separation of the components into discreet bands [51].

Analytes will distribute themselves between the stationary and mobile phases according to their partition coefficient, K.

$$K = \frac{c_s}{c_m} \qquad (2)$$

Where, c_s = concentration of solute in stationary phase

c_m = concentration of solute in mobile phase

The solutes will then be present in the mobile phase as local concentrations, and will be eluted in order of increasing partition coefficients [50].

Interfaces

In the past, wide-bore columns required higher flow rates than an MS vacuum could withstand [44]. An interface was required to reduce the flow for the MS. The use of capillary columns provides flow rates that are acceptably low for the MS vacuum, and direct coupling of the column in the ion source is possible. Also, since the gas chromatograph releases the separated components of a mixture in the gas phase, they are ready for gas phase ionization methods such as electron impact or chemical ionization.

There are three major advantages to direct coupling. They include: i) low detection limits because all of sample is transferred into the ion source; ii) decomposition is avoided as solutes do not contact any surface other than the stationary phase; iii) resolution is not degraded by a dead volume [45].

.

Ion Sources

Ion sources provide a place and a mechanism for ionization to occur. The ion source yields the energy required to ionize the analytes as they elute from the column, into the source. For GC/MS, ionization occurs either via electron impact (EI) or chemical ionization (CI), which will be discussed in detail later. Both EI and CI can occur from the same ion source.

Ionization Techniques

A variety of ionization techniques exist – two of which will be discussed here. Both ionization techniques described here involve ionization of analytes in the gas phase.

Electron Impact Ionization

Electron impact, or electron ionization (EI), is a hard (or high-energy) ionization technique in which electrons, typically between 50 and 100eV, collide with analyte molecules resulting in ionization.

Analyte molecules enter the ion source, of the MS, in the gas phase where they encounter an electron beam. The electrons are produced by a heated filament and are accelerated towards an anode resulting in a beam [52]. Ionization occurs due to interactions between the field of the analyte molecule, and the electron [53]. These interactions occur as electrons come close enough to the analyte molecules as they pass by, or as they pass through the molecules. The result of these interactions can be expressed according to equations 3-5 shown below. The first possible result, of the interaction between analyte and electron, is electronic excitation of the analyte. In this scenario, one of the electrons in the analyte is promoted to a higher orbital (equation 3).

$$e_b + M \rightarrow M^* + e_b' \quad (3)$$

The second possible result involves the ejection of a molecular electron from the analyte. This will cause the formation of a radical cation (equation 4).

$$e_b + M \rightarrow M^{+\bullet} + e_m + e_b' \quad (4)$$

The third possible result, of the interaction between an electron from the electron beam and the analyte molecule, is the direct capture of the electron by the analyte. This interaction results in the formation of a radical anion (equation 5).

$$e_b' + M \rightarrow M^{-\bullet} \quad (5)$$

Where, e_b: bombarding electron before collision
M: analyte molecule
$M^{+\bullet}$: molecular cation of analyte
$M^{-\bullet}$: molecular anion of analyte
e_m: emitted molecular electron
e_b': bombarding electron after collision

This scenario is of the lowest probability of the three. The radical cations formed in this process are unstable and the radical anion will fragment [45]. The negative ion mass spectrum is not usually informative in terms of structural information and consists of few fragment ions [53]. Due to the lower incidence of electron capture (to be discussed later) in EI, negative ion EI is characteristically less sensitive than positive ion EI.

Electron ejection is the most likely outcome, and the desired outcome for mass spectrometry. Electrons have high kinetic energy and low mass, and

therefore cause little increase in the translational energy of analyte molecules. Molecules, after collision, are however left in highly excited rotational and vibrational states. As the molecules relax, they will disintegrate into many fragments [53]. This results in a complex mass spectrum. Since only about 10eV is necessary to ionize most organic molecules, but typically 70eV is applied, extensive fragmentation results from this excess energy [52]. The electron energy must be greater than the ionization potential of the analyte molecule for ionization to occur in EI. 70eV is usually chosen because good reproducibility and a high ion yield are achieved at this energy [45]. Structural information can be obtained from the fragmentation patterns of molecules. Also, since a molecule, when exposed to an electron beam of the same energy, will always yield the same fragments, the mass spectrum is characteristic of that molecule, and can be used for identification.

Chemical Ionization (Positive Ion Chemical Ionization)

Softer ionization techniques are desired (over EI) when the determination of molecular weight is essential for structure elucidation. Chemical ionization (CI) is a softer ionization technique, than EI, as analyte ions are generated by bimolecular processes. That is, analyte molecules are not ionized by primary electrons. A reagent gas such as methane, isobutane, or ammonia is pumped directly into the ion source (typically at 10^2 Pa) [54]. This excess of reagent gas results in the preferential ionization of reagent gas molecules via electron impact. Ions formed of the reagent gas in turn ionize the analytes.

Negative Ion Chemical Ionization (NICI)

Although in EI, the formation of negative ions is inefficient, at the increased pressure observed in CI, there is a substantial increase in the yield of negative ions.

Electron capture is the most important mechanism in negative ion chemical ionization. Although it is not technically a CI process, it does occur under similar conditions to CI, and forms negative ions via soft ionization methods, and is therefore considered an NICI process [54].

Electron capture is of specific interest because of its selectivity, and superior sensitivity for many compounds of environmental concern due to their toxicity and/or ubiquity.

Neutral molecules are susceptible to electron capture if they have the ability to accommodate an extra electron. To do this, the molecule must have an empty orbital of low energy. Halogenated molecules, or molecules containing phosphorus, sulphur, nitro groups, or conjugated double bonds can house the extra electron [45]. This makes NICI a selective ionization process.

Analyte molecules that respond well under electron capture detection (ECD), typically will also respond well in electron capture negative ion mass spectrometry [55]. NICI offers an additional dimension of selectivity from the potential of selective ion monitoring (SIM) in mass spectrometry. The use of SIM mode can often eliminate co-elution of analytes with interferences, or other analytes.

Alkanes do not have a vacant orbital of low energy, and so are not amenable to chemical ionization. They are however, good candidates for buffer (reagent) gases - especially methane. Buffer gases, in NICI, absorb excess energy that results in the formation of the negative ions [45]. Buffer gases are used in place of reagent gases in NICI. Methane is the most common choice for a buffer gas. Other possible choices for buffer gases include ammonia and carbon dioxide [56]. Similarly to CI (positive ion chemical ionization), the choice of buffer gas can affect the degree of fragmentation.

The buffer gas plasma, resulting from electron impact ionization of the buffer gas and subsequent reactions with other gas molecules, will contain low energy electrons. These electrons are called thermal electrons. Thermal electrons

result from ionization reactions within the plasma, or from primary electrons that lost much of their energy in a previous ionization. Thermal electrons will yield negative ions from molecules by electron capture [52]. Electron capture is technically a non-CI process because the electrons involved are freely moving through the plasma, and are not acquired from a reacting ion.

Ions formed through electron capture result from one of three possible mechanisms, as seen in equations 18-20. The first two possible mechanisms, shown in equations 18 and 19, are *associative resonance capture* and *dissociative resonance capture,* respectively.

$$MA + e_b \rightarrow MA^{-\bullet} \quad (18)$$

$$MA + e_b \rightarrow [M\text{-}A]^- + A^{\bullet} \quad (19)$$

$$MB + e_b \rightarrow [M\text{-}B]^- + B^+ + e_m \quad (20)$$

Where: A, B = possible fragments

As seen in the reactions above, in the associative resonance capture an electron is captured by the analyte molecule to yield the negative molecular ion. Electrons that result in the formation of the molecular ion are typically of lower energy (0-2eV) than those that result in the dissociative mechanism (0-15eV) [52]. In dissociative resonance capture, once the analyte molecule captures an electron from the plasma, it fragments due to excess energy. Associative resonance capture is more likely for analyte molecules that contain several electronegative atoms, or for those capable of resonance. The choice of buffer gas can also influence which reaction takes place. The use of ammonia, instead of methane, decreases the occurrence of the dissociation reaction, and the associative mechanism dominates [56]. This could mean that ammonia is a more efficient buffer gas in that it offers

more collisional stabilization. Lower incidence of the dissociative resonance results in a more abundant molecular ion peak, which can enhance sensitivity.

Thermal electrons having energies greater than about 15eV, can result in *ion pair production* upon capture – as in equation 20 above. This type of reaction is similar to a typical EI mechanism, but yields fragments of the molecule that are not structurally significant. Ion pair production is not an important electron capture process.

Mass spectra generated by electron capture processes are extremely sensitive to changes in conditions. The reproducibility of these spectra is highly dependent on the temperature, pressure, and cleanliness of the ion source, the purity of the buffer gas, and the tuning conditions of the instrument [45]. These factors are responsible for the reputation of irreproducibility electron capture has obtained.

Ions, in NICI, can also be made through ion-molecule reactions, as in traditional chemical ionization. The most common bimolecular reaction in NICI is proton abstraction (equation 21).

$$M + A^- \rightarrow [M\text{-}H]^- + AH \qquad (21)$$

This type of reaction will yield a quasi-molecular ion, $[M\text{-}H]^-$. Most of the excess energy given off in a proton abstraction will be carried off by the new AH molecule as vibrational energy [45]. This leaves a relatively stable quasi-molecular ion behind.

As NICI processes have a means for disposing of excess energy resulting from ionization, the quasi-molecular ions tend to be more stable than those formed in classical CI, and less fragmentation is usually observed.

Electron capture is more likely to occur than bimolecular processes, in NICI, because electrons have higher mobility than ions. Electrons will be involved in many more collisions with analyte molecules than ions produced from the ionization of buffer gas molecules. Electron capture reactions may also be the

fastest two-body processes that occur in the gas phase [57]. This increased rate of reaction is responsible for the high sensitivity associated with this process.

Electron Impact vs. Chemical Ionization

Chemical ionization results in a simplified spectrum (in comparison to EI) in which the molecular ion (or quasi-molecular ion) peak is usually present, from which the molecular weight can be determined. In EI, there is more fragmentation, but the fragments can be used to obtain structural information about the analyte. Fragmentation can be too extensive though, which can make identification complicated. EI and CI techniques are complimentary in analyte identification.

Chemical ionization can occur in an EI source that is able to withstand the increased pressure required for CI. Many mass spectrometers on the market today are able to perform both CI and EI ionization and can easily be switched between the two ionization modes. Electron impact and CI both are limited to analytes that are sufficiently volatile, and thermally stable, to be ionized in the gas phase.

Chemical ionization, unlike EI, can provide the ability to differentiate between isomers. Small structural differences between isomers can be mirrored through the CI mass spectra. Ketones, for example, typically lose a water molecule in mass spectrometry. But, for steroidal ketones ionized using chemical ionization, this reaction is shown to be selective. 5,β,3-ketosteroids show a marked loss of water molecules in the CI spectra, whereas 5,α,3-ketosteroids do not [45]. This is only one example of the extra selectivity offered by CI processes. Electron capture, an NICI process, is an ionization process that is selective towards electronegative moieties (similar to an Electron Capture Detector). This type of ionization not only provides additional selectivity, but also enhanced sensitivity. For the appropriate types of compounds, namely electrophilic compounds, electron capture NICI can yield sensitivity that is 100-1000 times better than traditional electron impact [58].

Fragmentation can be controlled, to varying degrees, in both EI and CI. In CI, the degree of fragmentation can be controlled by the use of different reagent gases, source temperatures, and source pressures. The effect of temperature on fragmentation will be discussed in the next section.

Methane and ammonia, as reagent gases in CI will both yield a quasi-molecular ion. However, protonation by NH_4^+ is significantly less exothermic than protonation with CH_5^+ due to the higher acidity (lower proton affinity) of CH_5^+ [52]. As a result, the quasi-molecular ion formed using ammonia as a reagent gas will be more stable, whereas the quasi-molecular ion formed using methane as a reagent gas will be more likely to fragment. Differences in fragmentation by the use of different reagent gases can also be useful for structure elucidation. Increasing the pressure of the ion source in CI will increase the rate and number of collisions. This will lead to increased efficiency of plasma formation, and increased ionization efficiency.

In EI, altering the electron energy can control fragmentation. However, spectra obtained through ionization carried out at electron energies different from 70eV cannot be compared to spectral libraries for identification. These spectral databases are composed of spectra obtained for compounds ionized by EI with electron energy of 70eV.

Although the mass spectra of many compounds ionized via CI mechanisms have been published [59], spectral databases for EI are much more extensive and widely available. Most GC/MS systems are sold with a subscription to an EI spectral database that can search based on comparison of a spectra obtained by the instrument.

Effect of Source Temperature in NICI

Fragmentation in electron capture NICI, is highly temperature dependent. Increasing the temperature in the ion source imparts additional thermal energy on the sample. This thermal energy can cause the analytes to contain an excess of

vibrational and rotational energy before the ionization reaction [45]. If the analyte molecule has excess energy before capturing an electron, the molecular ion will have more energy, and will therefore be less stable. This will increase the likelihood of a dissociative resonance mechanism, or ion pair production. The abundance of the molecular ion peak will be decreased, as the occurrence of the associative resonance mechanism will diminish. The abundance of fragment ions will increase at higher source temperatures. In the case of polyhalogenated molecules, the fragments will often be due to the loss of a halogen atom [58].

Jaffe *et al.* reported significantly different mass spectra were obtained for fluorobiphenyls with source temperatures of 100°C and 250°C. A marked increase in sensitivity was also noted for these compounds when the ion source was kept at 100°C during analysis [14].

Mass Analyzers

Mass analyzers act as a mass filter. They separate ions according to their mass to charge (m/z) ratio [44]. The specified mass range is scanned, and ions are separated in space or in time.

The two most common mass analyzers are the magnetic sector, and the quadrupole. The magnetic sector is not typically the mass analyzer of choice for chromatography because chromatographic bands are too narrow and the magnetic field cannot be varied fast enough to record their spectra [46].

An alternative to magnetic sector instruments are time-of-flight (TOF) mass analyzers. TOF has become increasingly popular because of its mass accuracy and scan speed [44]. The TOF mass analyzer can store around 500 spectra per second, and therefore complex mixtures can be analyzed (by GC/MS with TOF mass filter) in a few seconds [44].

Quadrupole mass spectrometers are the most favoured for GC/MS applications because of their low cost and fast scanning rate. The quadrupole

separator is composed of four parallel cylindrical metal rods which are positioned in a square arrangement [44]. A constant voltage, and a radio-frequency oscillating voltage are applied to the rods. This allows ions with a specific m/z a stable trajectory, and they are able to pass through the filter [44]. Ions of different m/z, or non-resonant ions, will collide with the rods and will not be allowed to pass through to the detector. The applied voltages can be varied rapidly to allow ions of different m/z to pass though the analyzer [46].

Detectors

Detectors for mass spectrometry must be able to convert small ion currents into recordable signals [44]. In order to do this, they must have large gain. Mass spectrometric detectors must also have a fast response in order to detect sharp chromatographic peaks. The two most common detectors in mass spectrometers are the electron multiplier, and the photomultiplier tube (PMT). The PMT will be considered here.

In a PMT, the mass-resolved ions, from the mass analyzer, collide with a phosphor-coated target [44]. This results in the conversion of ions to photons which are then amplified and detected. PMT detectors are typically longer lasting than electron multipliers because they are sealed units and are therefore resistant to contamination.

Limitations of GC/MS

For years, gas chromatography has been the key technique to most analytical puzzles. In recent years high performance liquid chromatography (HPLC) has gained much popularity. This is most likely due to the limitations of gas chromatography, many of which do not apply to HPLC.

Only volatile and semi-volatile compounds that are thermally stable are amenable to GC separation. Unfortunately, this only accounts for about ten

percent of all organic compounds [44]. There are techniques, such as chemical derivatization, that can be used to make solutes suitable for GC/MS analysis. Compounds that are not sufficiently volatile or thermally stable for GC/MS analysis can usually be determined by HPLC/MS.

When GC is coupled to MS, only certain flow rates can be tolerated by the MS while being able to maintain vacuum. The flow rates that can be tolerated limit the inner diameter (ID) of the column that may be used to 0.25mm-0.32mm ID [44]. This is not necessarily a large drawback. Smaller ID columns have increased efficiency and therefore greater resolving power. They also have lower bleed. The sample capacity will be lower for smaller ID columns, but MS is a sufficiently sensitive detector, and this should not be a problem [60]. Since these columns can be directly coupled to the MS, there is complete transfer of sample components from the GC column to the ion source of the MS.

One of the largest problems associated with GC/MS is contamination. Non-volatile components of the sample can contaminate the analytical column and the ion source. Columns continuously bleed into the MS, especially if they are not conditioned or used properly (according to manufacture's instructions). Non-volatiles in the sample can be prevented, to some degree, from entering the GC/MS system by packing the inlet liner with glass wool. A guard column can also be installed ahead of the GC column to help prevent the transfer of non-volatile material to the analytical column and the MS ion source. There is nothing to stop the bleed of column material into the ion source. This will continuously decrease sensitivity and eventually require maintenance.

Objective of the Study

It has now been over 10 years since Hites *et al.* last looked into fluorinated compounds migrating from the Hyde Park landfill and into the Niagara River – Lake Ontario. It would be interesting to see what the current status of these

compounds is given that the remediation at the Hyde Park landfill was considered to be completed, according to the US EPA, in 2003 [12].

In this study, a method was developed to extract, concentrate, and determine the concentration of some fluorinated compounds in sediment samples. A dated sediment core from the Mississauga basin of Lake Ontario was extracted using accelerated solvent extraction (ASE), and then analyzed by gas chromatography/ electron capture negative ionization/mass spectrometry (GC/ECNI/MS) for fluorinated compounds to yield a temporal trend of these compounds in the lake. The temporal trend of these compounds will be reflective of the activity of the Hyde Park landfill and the elution of these and other toxic chemicals from the landfill.

Part II – Polynuclear Aromatic Hydrocarbons

What are PAHs?

Polynuclear aromatic hydrocarbons, also known as polycyclic aromatic hydrocarbons, are a structurally diverse class of large, non-polar, organic molecules that form as the result of incomplete combustion of organic matter [61]. PAH structures are composed of multiple fused benzene rings and exist in a vast array of molecular sizes. They are highly unsaturated carbonaceous solids that generally have high boiling points (about 220°C to well over 500°C), low vapour pressure (10^{-5} to 10^{-13} kPa at 25°C), and have low (1mg/L), to extremely low (< 1μg/L), solubility in water [62]. PAHs are soluble in aromatic and non-aqueous solvents [63]. The vapour pressure and aqueous solubility generally tend to decrease with increasing molecular weight of the PAHs, but there is no specific relationship to govern the changes in these characteristics with respect to molecular weight because these properties are highly influenced by geometric orientation of the aromatic rings [62]. As a result of their hydrophobicity, PAHs have a high affinity for particulate surfaces.

Sources of PAHs and Exposure

PAHs are derived through both natural and anthropogenic sources. They are formed in the incomplete combustion of organic matter. The most prevalent natural sources of PAHs include forest fires and volcanic eruptions, although they may possibly be formed through biosynthesis, and the decay of organic matter [61].

Anthropogenic sources are, not surprisingly, the most significant sources of PAHs. These sources include (but are not limited to): the burning of fossil fuels, municipal and commercial incineration, heat and power generation, and vehicular emissions (especially motorcycles, snowmobiles, and lawnmowers) [62].

Fuels produced from crude oil, coal, and oil shale are the most significant sources of energy for the industrial nations of the world. These raw materials are also used to produce the petrochemicals which are the foundation of the synthetic fibers and plastics industries [64].

The primary sources of human exposure to PAHs are through cigarette smoke (1^{st} and 2^{nd} hand), particulate emissions from the industrial production of metallurgical coke [61], and food ingestion [65].

Toxicity

British surgeon Sir Percival Pott first reported a high incidence of scrotal cancer in chimney sweeps in 1775 [66]. This raised awareness of the potential dangers of soot, tar, and pitch, but it took over 150 years before the carcinogenic compounds were identified as PAHs [66]. It has since been known that long term exposure to mixtures of PAHs can lead to various kinds of cancer. Based on animal experiments, Benzo[a]pyrene is one of the most potent carcinogens of the PAH family, although a number of other PAHs are also known carcinogens [61].

Polycyclic aromatic hydrocarbons can only be biologically active if they can bind to proteins, nucleic acids, and especially DNA [61]. Binding will not occur unless the PAHs are activated. Activation occurs through enzymatic mechanisms within the body that chemically modify the PAH.

The known carcinogenicity of PAHs has shadowed other toxic effects of the compounds. They are also known to cause endocrine disruption [67], enzyme induction, and immunosuppression, in addition to respiratory and skin disorders [61].

There is potential for PAHs to bioaccumulate in fatty tissues. They have been found to possess $\log K_{ow}$ values of 4-6 [68]. Due to this lipophilicity, fats and oils represent a major source of PAHs in the diet [69].

The US EPA had identified 16 PAHs as "priority pollutants" due to their carcinogenicity and ubiquity [70]. See Figure 5.

PAHs, and Their Fate, in the Environment

Benzo[a]pyrene has been found in vegetables, grown for human consumption, at 10-20μg/kg (dry weight), and other PAHs have been found in plants in concentrations ranging from 5-110μg/kg (dry weight) [71]. It has been suggested that PAHs may be a product of plant biochemical synthesis [72]. Polycyclic aromatic hydrocarbons were also shown to be formed during the growth and germination of lentils, rye, and wheat [71]. A number of plants showed an increased growth rate when fed carcinogenic PAHs, and rye's grain output increased three-fold [73]. It was thus suggested by Harrison *et al.* that PAHs are present as a natural background in plants and soils and that humans have always been exposed to PAHs in the natural environment [74].

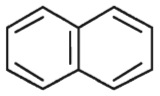

Naphthalene
91-20-3

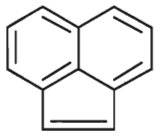

Acenaphthylene
208-96-8

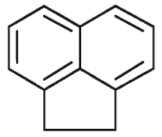

Acenaphthene
83-32-9

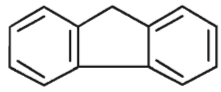

Fluorene
86-73-7

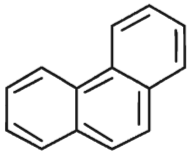

Phenanthrene
85-01-8

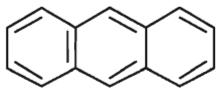

Anthracene
120-12-7

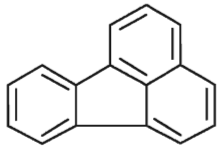

Fluoranthene
206-44-0

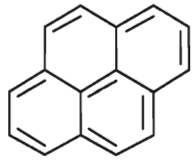

Pyrene
129-00-0

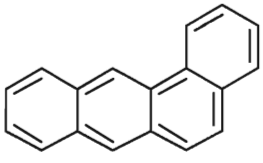

Benzo[*a*]anthracene
56-55-3

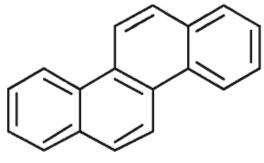

Chrysene
218-01-9

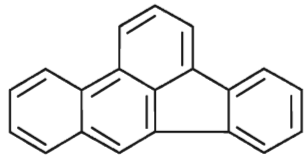

Benzo[*b*]fluoranthene
205-99-2

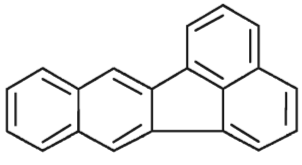

Benzo[*k*]fluoranthene
207-08-9

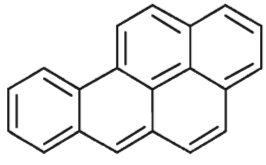

Benzo[*a*]pyrene
50-32-8

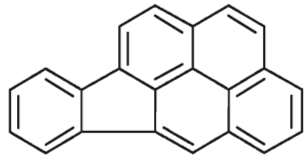

Indeno[1,2,3-*cd*]pyrene
193-39-5

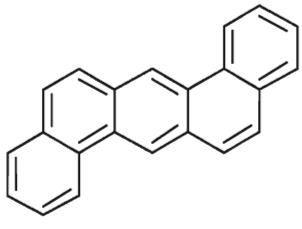

Dibenzo[*a,h*]anthracene
53-70-3

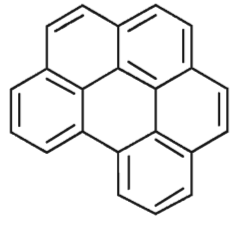

Benzo[*ghi*]perylene
191-24-2

Figure 5 – 16 Priority PAHs as outlined by US EPA [70] and CAS numbers

Owing to their volatility and low aqueous solubility, PAHs in the environment are most often found adsorbed to particles. Not surprisingly, their highest concentrations are found in sediments. In sediments, PAHs are found in higher concentrations where there is more organic matter [75].

Polycyclic aromatic hydrocarbons can sublime into the atmospheric environment, and have also been found adsorbed to respirable fraction of airborne particulate matter [61]. Similarly, PAHs in natural waters are most often found adsorbed to suspended particles, or in sediments [62]. The contamination of natural waters with organic solvents [74], and surfactants [61], has been shown to enhance the solubility of PAHs. Surfactants, however, must be present in excess of their critical micelle concentration in order to affect PAH solubility.

Atmospheric PAHs can be degraded through reactions with ozone, hydroxyl radicals, nitrogen oxides, sulfur dioxides, and through photo oxidation [61]. When exposed to the above mentioned processes, PAHs are expected to have a half-life of a few hours to a maximum of a few days. Aggregates of particulate matter can protect the PAHs from exposure, prolonging the half-life.

Photo oxidation is also the most likely course of degradation for PAHs in natural waters. Most PAHs are expected to be quite stable in dark, deep, cold waters adsorbed to particles in anaerobic conditions [61].

Polycyclic aromatic hydrocarbons in soils will likely be degraded through photo oxidation, and biodegradation. Microorganisms in soil may be an effective degradation tool, but only in surface layers. PAHs in sediments that are not exposed to natural light will persist for extended periods of time [61].

Reactions of PAHs

In General, PAHs are more reactive than benzene. They can undergo all reactions characteristic of aromatic compounds including: substitutions, additions, and eliminations [61].

Methods for the Determination of PAHs

Polycyclic aromatic hydrocarbons are ubiquitous throughout the environment. Due to their mutagenic and carcinogenic properties, their detection at very low levels in a variety of matrices is paramount. The concentration of PAHs is often determined from air, water, soil and sediment, food, and tissue samples [61, 62, 65, 77]. PAHs are often present in extremely complex mixtures containing isomeric structures and alkylated derivatives, in addition to PAHs with heteroatoms such as nitrogen, sulfur, and oxygen [78], which can be difficult to separate. This is especially true in environmental samples. Ideally, the best analytical technique should yield high resolution separation, with high sensitivity and reproducibility, and have low detection limits [77]. This technique must also have the ability to separate and quantify a mixture of compounds that cover a wide range of polarities, volatilities, and molecular sizes and shapes [78].

The United States Environmental Protection Agency (US EPA) has established test methods for the determination of PAHs in a variety of matrices including (but not limited to): ambient air [79], drinking water [80, 81], groundwater [82], municipal and industrial wastewater [83], soils/sludges and solid wastes [84], and shellfish tissue [85].

The analytical techniques most often suggested for the determination of PAHs are high performance liquid chromatography with UV/VIS (HPLC/UV/VIS) or Fluorescence (HPLC/FL) detection, and gas chromatography with flame ionization (GC/FID) or mass spectrometric (GC/MS) detection.

Chen *et al.* [76] outlined three reasons why the determination of PAHs can be problematic: i) PAHs, in environmental and food samples, are present in very low concentrations (ppb or ppt); ii) oftentimes when PAHs are extracted from the matrix in which they are found, interferences are extracted with them; iii) some PAHs are structurally very similar - which makes chromatographic separation, and differentiation difficult. There is no perfect method for the determination of

PAHs. Due to the complex nature of samples containing PAHs, the resolution of coeluting peaks can be difficult and oftentimes impossible to obtain. Each method has its advantages, and its drawbacks. Methods using HPLC and GC will be considered here.

HPLC Methods

High performance liquid chromatography separation of PAHs is typically faster than GC. All sixteen US EPA priority PAHs can be fully resolved in 23 minutes [86].

In addition to separating and detecting PAHs, LC can also provide a means of fractionating PAHs for subsequent separation and detection by other chromatographic and spectrometric techniques [70].

Normal Phase HPLC

Normal phase (NP) HPLC utilizes a polar stationary phase to separate analytes. The mobile phase is non-polar. A solvent is said to have a higher eluent strength, the more polar it is. Analytes are eluted in order of increasing polarity.

Normal phase HPLC is not commonly employed in the determination of PAHs as PAHs are non-polar, and would not have a very strong affinity for the polar stationary phase. Polar stationary phases typically contain Amino, (-$(CH_2)_3NH_2$), Cyano (-$(CH_2)_3CN$), or Diol (-$(CH_2)_2OCH_2CH(OH)CH_2OH$) moieties [46]. A low affinity for the stationary phase will result is poor separation. High resolving power is required in the separation of PAHs.

Normal Phase HPLC is not as common (as Reverse Phase HPLC see below) in general because chromatographic problems are common. The polar stationary phase can have active sites that strongly adsorb solute molecules, which results in peak tailing [46]. Peak tailing will be discussed in a later section.

Reverse Phase HPLC

In Reverse Phase (RP) HPLC, a non-polar stationary phase is used to separate solutes that are eluted through the column by a polar mobile phase. A less polar solvent will have a higher eluting strength. Solutes are eluted in order of decreasing polarity.

The most common column used, for RP-HPLC determination of PAHs, is a C_{18} column and mobile phases are usually composed of varying proportions of H_2O:CH_3OH or H_2O:CH_3CN [69].

Reverse phase HPLC is more common than NP-HPLC as it is less sensitive to polar impurities, such as water, that may present in the sample or mobile phase.

In recent years, RP-HPLC has gained much popularity in the area of PAH determination, and has become one of the dominant types of separation used for this purpose. The US EPA has named RP-HPLC as the method of choice for the analysis of PAHs in aqueous effluents [83], and drinking water [80, 81].

Detection

The most common types of detectors for PAH analyses by HPLC are fluorescence (Fl), and UV/VIS detectors [87, 76].

Fluorescence detection is the most popular, and most sensitive [86] of the two detection techniques because PAHs are naturally fluorescent [88], and they can be detected by this method with high sensitivity. As PAHs are fluorescent, but the matrix and most interferences are not, the PAHs can be selectively seen by the detector. There is one problem with fluorescence detection (with respect to PAHs), namely Acenaphthylene. Acenaphthylene is only very weakly fluorescent and is not as amenable to this type of detection. This problem can be somewhat overcome, however, with a carefully developed method in which the PAHs are adequately resolved to allow automatic wavelength changes [77]. Benzo[*ghi*]perylene also has low fluorescence sensitivity [78].

Fluorescence detection is well suited to the determination of Benzo[*a*]pyrene, which is one of the most carcinogenic PAHs and has received the most attention. Benzo[*a*]pyrene is the only PAH listed in the European Union's regulated pollutant list, and is the only PAH listed as a "Level 1 substance" by the Great Lakes Binational Toxics Strategy between Canada and the US [78].

Probably the biggest advantage to the use of fluorescence detection is the selectivity it offers. When other detection methods are employed, extra sample preparation may be necessary to separate the compounds of interest from matrix interferences [76]. If these matrix interferences do not produce fluorescence, the extra preparation can be avoided with the use of fluorescence detection. The more sample preparation required, the more opportunity for the loss of analytes.

Due to the low sensitivity of a couple of PAHs, as described above, Fluorescence detection is often paired with UV/VIS detection [86, 87]. With the use of UV/VIS, all 16 PAHs can be detected at multiple wavelengths. 254nm is the wavelength that yields the highest sensitivity, but is less sensitive that fluorescence detection [76]. The UV spectra of PAHs are characteristic, and are different for isomers. This helps in the differentiation of the many PAH isomers.

Conclusions about HPLC

High performance liquid chromatography methods are losing popularity for the determination of PAHs. It is becoming increasingly common for LC to be used only for fractionation or clean up prior to GC analysis [78].

Gas Chromatographic Determination of PAHs

Gas Chromatography is usually the preferred technique for the separation of PAHs. GC offers the desired balance of sensitivity, resolution, and selectivity that HPLC cannot match [78]. PAH samples are of a complex nature, and it is not uncommon for them to contain hundreds of components that cover a wide range of

concentrations and volatilities [89]. Gas chromatography has the resolving power required to separate this number of compounds, within a reasonably short period of time. Liquid chromatography columns have a limited peak capacity, and can only resolve a few dozen components [78].

One of the major advantages to using gas chromatography, for the determination of PAHs, is its compatibility to mass spectrometers [78]. Mass spectrometric detection allows for the positive identification of analytes in a sample, and their selective determination.

Polynuclear aromatic hydrocarbons fit within the narrow margin of compounds that have physical properties that make them amenable to GC.

There are a large number of factors that can affect the retention and separation of PAHs. These include, but are not limited to: injection solvents, injection volume, solvent effects, injection conditions (speed, liner volume, temperature) and temperature programming [78, 90, 91].

The two most common methods for the determination of PAHs involving gas chromatography are GC/MS and GC/FID [87]. Both of these techniques will be considered here.

GC Stationary Phases

Selecting an appropriate stationary phase is the single most important aspect in method development. The most common stationary phases for PAH determination are non-polar methyl polysiloxanes, or slightly polar phenyl methyl polysiloxanes [89]. These phases have high thermal stability, and are low-bleed - contributing to a low background. Methyl polysiloxanes are available with varying degrees of phenyl substitution (0, 5, 50, and 60%) [CM].

Most standard test methods for PAH determination recommend the use of a 5% phenyl methyl polysiloxane (DB-5) column [78]. However, this column has some difficulty resolving several pairs of closely eluting PAHs including:

Benzo[*b*]fluoranthene and Benzo[*k*]fluoranthene, and Indeno[1,2,3-*cd*]pyrene and Dibenz[*ah*]anthracene [92].

Recently, authors have reported the use of liquid crystalline phases [65, 78, 92]. Berset and Holzer [92] describe these smectic phases as layered structures. The layers are composed of rigid, planar molecules that are arranged parallel to each other, but perpendicular to the surface of the column. Each layer is one or, at most, a few molecules thick. Solutes, traveling through the capillary, are separated based on their vapour pressures in addition to dispersion, dipole, and induced-dipole interactions with the stationary phase [92]. Intermolecular interactions with the stationary phase add an additional element of selectivity to the chromatography.

These liquid crystal phases have been shown [78, 92] to provide adequate separation of the three above-mentioned pairs of PAHs. However, these columns have their drawbacks. As the analytes experience increased interaction with the stationary phase, analysis time is considerably longer. The elution order of compounds may change, among different liquid crystal columns, due to poor column-to-column reproducibility [65]. These columns are also not as thermally stable as the methyl polysiloxane columns, and limited temperatures can be used during analysis [78, 92].

Mid-polarity columns, 50% phenyl-substituted methyl polysiloxane (DB-17), have also been applied to the separation of PAHs. These columns have also been found to provide adequate resolution to the commonly coeluting peaks of the DB-5 column, but they do not share the drawbacks of the liquid crystal columns. This makes the DB-17 column a new popular choice for the separation of PAHs.

Despite the maturity of the technique, new stationary phases are constantly being developed for GC [78].

GC Column Dimensions

Traditionally, columns ranging from 30-60m in length are used for PAH analysis in GC. Long columns are often needed to acquire adequate separation of some groups of PAHs. The shortest column that will provide the resolution required for a given application should be used. Longer columns will have higher resolving power, but it comes with a price. Analysis time, and band-broadening increase with increasing column length.

Since a 30m DB-17 column was shown to provide excellent resolution of PAHs, Bordajandi *et al.* [65] applied the same PAH mixture to a 60m column, of the same phase, under a fast temperature ramp (25°C/min). Under these conditions, Dibenz[ah]anthracene and Indeno[1,2,3-*cd*]pyrene were not completely resolved, but more importantly, the response of late-eluting PAHs were reduced significantly, and the analysis time was increased by nearly 30 minutes.

The response of late-eluting compounds is often affected by the amount of time spent on the column. These compounds can benefit from the use of thin-film columns as the analysis time would be decreased.

Bordajandi *et al.* [65] experimented with different film thicknesses of the DB-17 stationary phase. A 30m (column A) and a 60m (column B) long column both with 0.25mmID × 0.25μm d_f (film thickness) were compared to three other columns (all DB-17): a 20m × 0.18mmID × 0.18μm d_f (column C), a 30m × 0.32mmID × 0.15μm d_f (column D), and a 10m × 0.10mmID × 0.10μm d_f (column E).

It was found that the yield of late-eluting PAHs was maximized by using shorter columns, and thinner-film columns [65].

GC Injection Techniques

Split Injection

Split injections are not commonly used in the determination of PAHs in environmental samples because the concentration of PAHs is too low. Split injections are also notorious for mass discrimination amongst compounds of different volatilities within the sample.

Splitless Injection

Splitless injections have been most commonly reported in the literature, in the determination of PAHs, despite discrimination incurred against high-boiling compounds [65]. A pressure pulse can be used, during splitless injections, to transfer the sample vapours from the injector to the column faster, and with higher efficiency [93]. This type of injection is known as Pulsed Splitless, and it involves an increase in column head pressure during sample injection. The split vent is kept closed during splitless injection. In Pulsed splitless injection, the column head pressure is increased while the split vent is closed. As a result of faster transport of solutes from the injector to the column, there are significant reductions in analyte discrimination, adsorption, and degradation [93]. The high column head pressure also allows for larger injection volumes to be used, which can increase the sensitivity of the determination.

Glass Wool in Split/Splitless Injector Liners

Grob *et al.* [48] described three reasons why an injector liner should be packed with glass wool when performing splitless injections. First, it increases the reproducibility of measurements. This increased precision results in lower standard deviations, and higher certainty in experimental values. Secondly, sample droplets that are injected are prevented from falling to the dirty bottom of

the injector because they get trapped by the glass wool. If the droplets were to fall to the bottom of the injector, most of this material would not find its way to the column. Third, due to the larger volume of sample injected in splitless injection, the sample will tend to form droplets upon leaving the syringe in the injector. The wool will break up droplets of sample, which will result in more complete transfer of solutes to the analytical column which yields reduced random errors.

There is one condition in which glass wool can have a negative effect on sample transfer. Glass wool, in splitless injection, helps to retain non-volatile material in the liner, to prevent it from reaching the analytical column. While this is beneficial, because it helps to preserve the column, it can also result in decreased transfer of high-boiling solutes that are of interest [48].

Itoh *et al.* discovered something very interesting about the injector liner in PAH analysis [67]. Since PAH recovery is often strongly dependent on matrix effects, Itoh *et al.* performed an isotope dilution method. In doing this, an isotope-labeled internal standard is used, which is the same molecule as the analyte, except that it has a different mass isotope for some of the atoms in the molecule. This labeled internal standard, will behave very much like the original analyte, and in using it for quantification, matrix effects are negated. As the labeled internal standard will behaving so similarly to the actual analyte, the two usually cannot be chromatographically separated, and mass spectrometry must be used for detection.

Itoh *et al.* used not only deuterated versions of their PAH analytes as internal standards, but also ^{13}C-labeled versions as well in order to determine the response ratios of the original PAHs to both of the different labeled versions [67].

It was found that the deuterated PAHs were considerably less sensitive to accumulated residue (from previous injections) in the glass wool of the injector liner than both the actual PAHs and the ^{13}C-labeled PAHs [67]. As a result, the response ratio of PAH to its deuterated counterpart decreased significantly with increasing liner residue. This difference would result in significant underestimation of PAHs determined [67].

The above example shows that a dirty injection liner can not only cause a decrease in response of analytes, but data can also be skewed to an unexpected bias.

Programmed Temperature Vapourizing (PTV) Injection

The use of Programmed Temperature Vapourizing (PTV) injector has also been reported [65]. A PTV injector is similar to a conventional split/splitless injector except that it is temperature programmable from temperatures well below 0°C (with the use of cryogenic cooling) [94], and uses liners that are more narrow [65]. The sample is introduced into a cold injector, and a temperature program is then applied. The analytes are transported to the column in a controlled manner, which improves the transfer of high-boiling compounds, and reduces the effects of mass discrimination. This type of injection is suitable trace analysis of late-eluting compounds that have boiling points well above the boiling point (at least 100°C) of the solvent [94].

The main drawback of PTV injection is the time required for optimization. The efficiency and performance of the injection is affected by liner type, injection volume, initial temperature of the injector, and temperature programming of the inlet [94].

On-Column Injection

On-column injections are often performed in the determination of PAHs. In this type of injection, an aliquot of the sample is injected directly onto the analytical column. The initial column temperature is usually kept well below (at least 20°C) the boiling point of the solvent to invoke solvent effects (to be discussed later). Cold on-column injections have been shown to improve the resolution of early-eluting PAHs, and to reduce the discrimination against late-

eluting PAHs [89]. This makes on-column injections the preferred injection technique for PAHs.

Gas Chromatography/Flame Ionization Detection (GC/FID)

The response from a flame ionization detector is proportional to the number of carbon atoms in the molecule. In light of this, compounds in the same isomer group can be quantified even in the absence of a matching calibrant [78]. This is one major advantage in using flame ionization detection. For example, samples contaminated with mineral oils are very complex, and are rich in alkylated species. GC/MS cannot identify the many unresolved components, and FID is the only way to quantify unknown hydrocarbons [69].

Polycyclic aromatic hydrocarbons are usually present, in environmental samples, as complex mixtures. When mass spectrometric detection is available, it is usually used for the determination of PAHs, while FID is reserved for the detection of aliphatic compounds and alkanes [95].

Although flame ionization detection (FID) was widely used for the determination of PAHs in the 1980s, with the decreasing cost of GC/MS instruments, GC/FID has lost much of its popularity as a method for the determination of PAHs [89]. In GC/FID, interferences can coelute with PAH peaks, which would result in inaccurate results.

Gas Chromatography/Mass Spectrometry (GC/MS)

Mass spectrometry is the most common method of detection for PAHs because of the sensitivity and selectivity it offers. For some PAH isomers resolution is difficult, but with the use of selective ion monitoring (SIM), coeluting compounds can be separated in ion chromatograms.

Utilizing mass spectrometric detection, in gas chromatography, allows for the use of an isotope dilution method for quantification. Deuterated analogues, or

^{13}C-labelled analogues, of several PAHs can be added to samples prior to sample preparation and analysis. The deuterated PAHs can be differentiated from the originals, as their mass spectra will be different. These compounds can be added to samples as surrogates, prior to sample preparation, to judge the recovery of the analytes from the extraction/clean up procedure and from the matrix. The deuterated analogues can also be added immediately prior to analysis, as internal standards, to help negate errors that arise due to volatility or discrimination resulting from injection technique [89].

Quadrupole (EI/CI) Mass Spectrometry

Mass spectrometric detection of PAHs is most commonly performed using a quadrupole mass analyzer, in electron impact ionization mode. When ionized, PAHs tend to have very abundant molecular ion peaks, and little fragmentation, which allows for sensitive detection in both electron impact and chemical ionization [89].

Chemical ionization in the determination of PAHs has also been reported. When methane is used as a reagent gas, a mass spectrum very similar to that of EI is observed [78]. Due to the low abundance of negative ions obtained in CI, NICI is less sensitive that CI and EI, and is therefore not a very useful tool for the determination of PAHs.

Ion-Trap Mass Spectrometry

Mass spectrometers equipped with an ion-trap is especially well suited to the determination of PAHs. Unlike quadrupole instruments, sensitivity is not gained through the limitation of ions detected, and so the entire spectrum can be collected with greater sensitivity than quadrupole-SIM [77]. In this way, all samples can be run in full scan mode, with high sensitivity. Sample spectra can be archived, and then reviewed at a later time for newly emerging compounds of

interest [78]. Also, newly emerged compounds of interest can be traced back to their time of onset if samples are run and archived regularly for extended periods of time [89].

Ion-trap MS does have limitations. Due to the capacity of the ion-trap, linearity can be a problem [79].

Ion-trap mass spectrometers have been shown to be more sensitive that GC/MS (quadrupole) and HPLC/FL in the determination of PAHs [78, 96].

Conclusions

HPLC does have some advantages over GC analysis of PAHs: it offers better separation of some PAHs, and does not result in the discrimination of high-boiling PAHs [65]. GC, however, is more compatible with mass spectrometric detection and offers enhanced selectivity and sensitivity, which cannot be matched by HPLC methods.

For the best possible resolution of PAHs, LC-GC combination can be used. The sample is fractionated by LC and then subsequently analyzed by GC/MS [78].

Analysis Based on Peak Area/Height

Peak heights are more easily, and more accurately determined that peak areas. Peak heights are, however, inversely proportional to peak widths [51]. Small changes in column conditions such as eluent flow rate, column temperature, and sample injection can result in band-broadening, and results obtained through peak height may be inaccurate [51]. In particular, sample injection speed is critical for early-eluting peaks. With syringe injection, relative errors of 5-10% are not uncommon. As peak areas are independent of these broadening effects, they represent a more acceptable analytical variable than peak heights.

Injection Solvents in GC

Standard solutions are often prepared in different solvents depending on the requirements of the analytical technique with which the analytes will be determined. The 16 US EPA PAHs, for example, are most commonly determined by RP-HPLC and GC/MS. For RP-HPLC, the standards are usually prepared in polar solvents, such as methanol and acetonitrile. Standards for GC are usually prepared in aliphatic or aromatic non-polar solvents [97]. Clean-up procedures will often result in sample extracts being produced in a solvent different from the calibration standards [97].

Injection solvents in GC can have a dramatic effect on analyte response, and chromatographic behaviour. The ideal solvent chosen for GC analysis should: i) not degrade the analytes; ii) have a low vapour pressure to avoid changes in concentration due to evaporation of solvent; iii) not interfere with the analysis of the compound; iv) not degrade the analytical column [98].

Gebhart *et al.* [DG] reported an interesting phenomenon in the GC/MS determination of polychlorinated biphenyls (PCBs). It was found that on-column injection of PCBs in hexane resulted in the transfer of about three times more PCBs than on-column injections in decane [99]. No explanation was offered for this discrepancy.

Trotter [98] also reported on injection solvent having an effect on the response on analytes. A mixture of organophosphorus pesticides, determined by gas chromatography/flame photometric detection (GC/FPD), was injected using five different solvents (isooctane, methanol, acetone, acetone:isooctane = 1:9, and ethyl acetate). Significant differences between the response of the pesticides were not found in the use of different injection solvents. The acetone:isooctane solvent mixture resulted in the highest responses for the pesticides, and methanol resulted in the lowest [98].

Lee *et al.* [97] compared the response factors of the 16 US EPA priority PAHs in five different solvents (acetonitrile, methanol, toluene, isooctane, and cyclohexane) and found that solvents of similar polarity (i.e. MeOH and acetonitrile) could give significantly different responses. This suggests that the difference in response is due to the boiling point of the solvent, or possibly the interaction of the solvent with the analytical column, and not necessarily the polarity of the solvent. Lee *et al.* attributed the differences in response factors, for the PAHs in different solvents, to the ability of the solvent to transfer the PAHs from the injector to the GC column. Isooctane was found to be the most efficient solvent for the 16 US EPA priority PAHs [97].

Grob [100] was quick to write a rebuttal to the explanations offered by Lee *et al.* Grob wrote that the phenomenon observed by Lee *et al.* was "not compatible with the basic concept of splitless injection" and that "peak sizes must be independent of the solvent used" [100]. Grob then went on to explain how the injections employed by Lee *et al.* were much too large for the design of injector used, and how only various fractions of the injected standards would actually reach the column, which accounts for the different response factors obtained using solvents of different volatility and polarity [100].

Brindle *et al.* [90] sought to determine the best injection solvent for the determination 16 US EPA priority PAHs by GC/MS. A mixture of the PAHs was injected using seven different solvents (dichloromethane, hexane, benzene, cyclohexane, acetonitrile, isooctane, and toluene) [90]. These solvents were chosen to represent a range of volatilities and polarities. Of the seven solvents, toluene was found to yield the largest peak areas and peak heights of the PAHs. It was rationalized that toluene was the best solvent because it had the highest boiling point. And in accordance with Grob and Grob's model of the solvent effect, solvents with a higher boiling point will show increased solvent effect [90].

Trevelin *et al.* [101] set out to determine not only the best solvent, but the optimum conditions for the determination of the 16 US EPA priority PAHs by

GC/FID. Solvent type, initial column temperature, injection volume, splitless hold time, and the injector temperature were optimized using factorial design and Simplex optimization. The results indicated that the variable with the largest effect on the determination was the injection volume. The choice of solvent was second only to this parameter. It was found that xylene was the best solvent under the conditions of the experiment, however, only two solvents were attempted, xylene and benzene [101]. Trevelin *et al.* showed that the appropriate solvent, under the optimized conditions, had a significant effect on the response of late-eluting PAHs.

The results of Brindle [90] and Trevelin [101] draw a similar conclusion. In both cases, the least volatile solvent was found to yield the best response especially from late-eluting PAHs. This result is significant because in GC determinations, the high-boiling PAHs often give significantly reduced response in comparison to the other early-eluting PAHs. These authors have shown that the use of a higher-boiling solvent can maximize the response of these late-eluting PAHs, some of which are known carcinogens. The development of analytical techniques with the sensitivity to detect threshold limits of PAHs from complex matrices, as outlined by the European Union (EU), World Health Organization (WHO), and the US EPA is of high importance.

Grob and Grob [102] outlined the role of the solvent in splitless injection. It was shown that a solvent of the right volatility, under optimum conditions, will yield a "solvent effect" which promotes improved separation, sharpened peaks, and increased response of analytes [102]. This emphasizes the need to develop an optimized method.

High-Boiling Alcohols

The use of high-boiling alcohols as injection solvents for PAHs was reported by Brindle *et al.* [103]. Following experiments involving typically used injection solvents for PAHs [90], it was found that high-boiling solvents were able

to increase the response of late-eluting PAHs. Since high-boiling aromatic solvents were found to be effective injection solvents for the determination of PAHs by GC, it is wondered whether it is solely the boiling point of the solvent that determines its applicability, or the type of solvent. There are a number of high-boiling alcohols that may make ideal injection solvents for PAHs.

Problems Associated with GC Determination of PAHs

Resolution

As previously discussed, it can very difficult to achieve the required separation of some PAHs in gas chromatography. Increased column length, alternative stationary phases, and thinner-filmed columns can help with this matter. However, oftentimes attempted solutions only result in new problems.

Mass Discrimination

Mass Discrimination refers to the problem of decreased response of late-eluting (high-boiling) analytes, respective to early-eluting solutes, in gas chromatography. This is a very common problem, and is characteristic in PAH determinations in GC.

Many factors can contribute to mass discrimination. The most significant source of discrimination comes from the injection technique. Discrimination can result from the selective elution of more volatile compounds from the syringe into the hot injector [47]. In actuality, the problem is that too much of the volatile species are entering the injector, when higher-boiling components are staying behind (in the syringe). When a sample is injected into the hot injection port of the GC using a syringe, once the plunger is depressed, some sample is left behind in the needle. As the needle is in the hot injector, and metal is good conductor of

heat, the needle quickly becomes hot and the volatile contents evaporate, and expand into the injector [47].

Grob has described three ways in which discrimination, due to selective elution, can be reduced or eliminated [47]: i) fast injections; ii) the use of high-boiling injection solvents; and iii) injection through a short needle.

The temperature of the injector port may also contribute to discrimination effect. Typical injector temperatures in GC analyses, for samples containing high-boiling constituents, range from 250°C-300°C. If high-boiling solutes have boiling points in excess of 450°C, they will not volatilize to the same degree as compounds whose boiling points are close to, or below, the injector temperature. In splitless injection, the split vent is closed during injection, but then is set to open, some time thereafter. Splitless hold times are typically 0.5-1 minute in length. This means that after one minute, most (fraction depends on split ratio) of the sample left behind in the injector will be lost through the split vent. Low boiling components of the sample will quickly volatilize and flow into the column while some of the high-boiling components are left behind.

These sources of discrimination described above are typical of splitless injection, and are more likely to occur in samples that contain solutes with a wide range of boiling points [47], like PAHs.

In GC determinations of the 16 US EPA priority PAHs, the high-boiling PAHs elute late in the analytical run. The final temperature in the temperature program for PAHs can range from (260°C-315°C) [69, 77, 78, 92, 96, 104]. Therefore, these compounds also elute at high temperatures. At high temperatures, column bleed is more significant, and can contribute to a noisier baseline, which will lead to decreased sensitivity. Also, since the compounds stay on the column for longer periods of time (relative to early-eluting PAHs), band-broadening will occur – which will also contribute to decreased sensitivity.

It was shown by Bordajandi *et al.* [65], that the response of late-eluting PAHs decreased significantly from the use of a 30m column to at 60m column. It

has also been suggested that the late-eluting PAHs are susceptible to thermal decomposition at the high final temperatures of the GC run [69].

The response of late-eluting PAHs can be enhanced through the use of shorter columns, and columns with thinner films [65].

Peak Fronting/Peak Tailing

During method optimization, Brindle and Li [90] found that the choice of initial column temperature could significantly affect the shape of PAH peaks. It was observed that symmetrical peaks could only be obtained within a certain range of initial column temperatures. At temperatures below the optimum range, peak fronting was observed, and above the range peak tailing was observed. It was also found that the peak fronting and tailing were intensified the further the initial column temperature was from the optimum values [90]. Peak fronting occurred at initial column temperatures that were below the boiling point of the solvent, and peak tailing occurred when the initial column temperature was more than 20°C above the boiling point of the solvent. This behaviour was not solvent dependent [90]. The effect of fronting and tailing was found to be more significant for the early-eluting peaks than the late-eluting peaks.

Scope of the Study

Many authors have reported the effects of different injection solvents in GC determinations [97-100, 103, 104]. And Grob has well-addressed the effect of solvent on hydrocarbon response, and identified the solvent, and its effect, as an important factor in splitless injections [91, 102, 105]. In this study, high-boiling alcohols will be used as injection solvents for the 16 US EPA priority PAHs. The chromatographic conditions will be optimized, and the effect of the high-boiling alcohols on chromatographic behaviour of the PAHs will be studied. Also the effects of solvent trapping, and cold trapping will be observed.

The 16 US EPA priority PAHs are appropriate for this study, as they are priority persistent organic pollutants (POP), they cover a wide range of boiling points and volatilities, and are readily available. These PAHs, and their order of elution, are shown in Table 1.

Order of Elution	PAH Name	Boiling Point (°C)
1	Naphthalene	218
2	Acenaphthylene	280
3	Acenaphthene	279
4	Fluorene	295
5	Phenanthrene	340
6	Anthracene	340
7	Fluoranthene	384
8	Pyrene	404
9	Benzo[*a*]anthracene	438
10	Chrysene	448
11	Benzo[*b*]fluoranthene	481
12	Benzo[*k*]fluoranthene	480
13	Benzo[*a*]pyrene	495
14	Indeno[1,2,3-*cd*]pyrene	>500
15	Dibenzo[*a,h*]anthracene	>500
16	Benzo[*ghi*]perylene	>500

Table 1 – Elution order and boiling points of 16 PAHs.

Chapter 2 – Experimental

Part I – Fluorinated Compounds

Solvents

Hexane, Dichloromethane, Methanol, Isooctane, and Toluene - all of distilled-in-glass grade - were purchased from Caledon Laboratories Ltd. (Georgetown, ON).

Reagents

The following standards were purchased from ABCR Chemicals (Karlsruhe, Germany): Benzotrifluoride 99%, 3-Chlorobenzotrifluoride 98%, 3-Aminobenzotrifluoride 99%, 2,4-Dichlorobenzotrifluoride 98%, and N-[3-(trifluoromethyl)phenyl]benzamide 97%.

Some of the fluorinated standards required for this project were not available for purchase, and so they were synthesized, in house, by an organic chemist – Bradford Sullivan. The compounds required for the synthesis of the chlorinated benzamides (6-8) were ordered from Sigma-Aldrich (Oakville, Ontario) and include: 3-(trifluoromethyl)-aniline 99+%, 4-Chlorobenzoyl chloride 99%, 2,4-Dichlorobenzoyl chloride 98%, and 2,4,6-Trichlorobenzoyl chloride 97%.

For the synthesis of compounds 9 and 10, the following chemicals were ordered from Alfa Aesar (Ward Hill, Massachusetts): 2-Chloro-5-(trifluoromethyl)benzoyl chloride 97%, trifluoromethanesulfonic acid 98%, chlorobenzene 98+%, ethane-1,2-dithiol 98+%, $BF_3{\cdot}Et_2O$ 98+%, SelectFluor® fluorinating reagent {1-Chloromethyl-4-fluoro-1,4-diazoniabicyclo[2.2.2]-octane bis(tetrafluoroborate)} 98+%, and hydrogen fluoride pyridine complex ca. 70% HF.

Synthesis

Although Hites *et al.* were able to synthesize compounds 9 and 10 via the proposed mechanism in Figure 1 (see Introduction), this reaction scheme results in very poor yield. Hites *et al.* synthesized these compounds solely for the purposes of mass spectral comparison (identification). Yield was not important as the study was not of a quantitative nature.

For a description of the synthetic pathways used to make all compounds for this study, please see Appendix 1. For related spectra, see Appendix 2.

Standards

For the liquid compounds (1-4), 10μL of each compound was transferred to a 100mL flask and filled to volume with toluene to make solutions of ca. 100ppm. 5ppm solutions, for method development, were prepared by transferring 500μL of the 100ppm solution to a 10mL flask and filling to volume with toluene.

For the solid compounds (5-10), a known mass was dissolved in 100mL volumetric flasks, and filled to volume with toluene to make approximately 500mg/L mother solutions. These solutions were then used to make further dilutions, with isooctane, of 5mg/L (for method development), and of 500, 100, 50, 25, 12.5, 6.2μg/L (for calibration purposes).

Sampling

A sediment core from Lake Ontario, station 1034 (43°35'32''N, 78°13'53''W) – in the Mississauga Basin, was withdrawn on July 10, 2006 by the Canada Centre for Inland Waters [106]. The core was sliced into samples, at 1cm intervals, to a depth of 15cm. This depth corresponds to approximately 100 years of sedimentation. Core dating and the sedimentation rate were determined by ^{210}Pb-dating [106]. Samples were frozen until used.

Extraction and Sample Preparation

As with most sample preparation, the general steps followed include homogenization and size reduction, extraction, concentration, clean up, and analysis [28].

Prior to extraction, the sediment samples were allowed to thaw and air dry for one week in a fume hood. Once dry, the sediments were ground, using a mortar and pestle, to a fine powder. After grinding, the samples were thoroughly mixed to ensure a homogeneous mixture. Approximately 2g masses of ground, dried sediments were then transferred to an ASE extraction cell where they were sandwiched between two layers of 20-30 mesh Ottawa Sand – to eliminate void volume in the cell.

Samples were extracted in the Dionex Accelerated Solvent Extractor® with 100% dichloromethane as the extraction solvent. The ASE was operated in the preheat method. In this mode, the sample cell was heated to the extraction temperature of 100°C and then filled with solvent. The cell was then pressurized to 2000psi. The samples underwent static extraction for 10 minutes. Following extraction, the extract was flushed into the amber collection vial with fresh dichloromethane. The flush volume of solvent was 70% of the cell volume. Each sample was extracted three times, and the extracts of each sample were combined in the respective collection vials. The final solvent flush was purged into the collection vial with nitrogen gas.

Once removed from the ASE, the extracts were exchanged into isooctane and reduced to 1mL under a gentle stream of nitrogen gas on the Meyer N-EVAP (Organomation Associates, Inc. – South Berlin, MA, USA) at 30-35°C. The 1mL extracts were then cleaned up on a silica gel column. The column was composed of 100% activated silica gel sandwiched between two layers of anhydrous sodium sulfate. A thin layer of pesticide-grade glass wool (Supelco – Oakville, Ontario)

was used at the bottom of each column to prevent the transfer of solids from the column into the extracts.

Extracts were applied to the silica gel column, and the column was eluted with 30mL of 100% hexane, 60mL of dichloromethane/hexane (1:1, v/v), 40mL of methanol/dichloromethane (1:20, v/v), and 40mL of 100% methanol. This operation resulted in the separation of the original extract into four fractions; A, B, C, and D. Fractions A and D and fractions B and C were collected together. These fractions were collected in a round-bottom flasks containing 3mL of isooctane, and rotary-evaporated on a Büchi Rotovapor (Switzerland), powered by a Büchi B-169 vacuum system, at 30-35°C. The fractions were each reduced to 1-2mL in isooctane and then transferred with three washings (totaling 10mL) of dichloromethane into calibrated glassware. Each fraction was further reduced to exactly 1mL under nitrogen on the N-EVAP at 30-35°C. As the fluorinated compounds were not found to elute in fractions A or D, this combined fraction was not included in the analysis. Sulfur clean up was not required, as elemental sulfur elutes in fraction A.

Special care was taken, throughout all reductions, to ensure that extracts were not allowed to reduce to dryness.

Instrumentation

Determination of the fluorinated compounds, in core sediment sample extracts, was performed on an Agilent 6890N gas chromatograph coupled to an Agilent 5973 Inert mass spectrometer. The GC was equipped with a DB5-MS column, from Agilent Technologies Canada Inc. (Mississauga, ON), approximately 30m in length, having an internal diameter of 0.25mm and a film thickness of 0.10μm (30m × 0.25mm × 0.10μm). This thin film column is essentially non-polar consisting of 5% diphenyl and 95% dimethyl polysiloxane. The carrier gas, ultra high purity helium from Air Liquide Canada Inc. (Hamilton,

Ontario) was connected to the GC gas line via a stainless steel dual stage regulator.

Experimental Conditions

The temperature program used in the analysis of fluorinated compounds is shown below in Table 2.

Ramp (°C/min)	Temperature (°C)	Hold Time (min)
-	$T_0 = 85$	3
10	300	15

Table 2 – Temperature program chosen for separation of fluorinated compounds

1μL of the sample extracts in isooctane were injected in pulsed splitless mode into the heated injector at 250°C. The pulse pressure was set at 30psi with a pulse time of 1.5min. The helium flow rate was set at 1.3mL/min. The transfer line to the MS was held at 290°C throughout the analysis.

The MS was operated in negative ion chemical ionization (NICI) mode with methane gas from Air Liquide Canada Inc. (Hamilton, Ontario) serving as the buffer gas. Source and quadrupole temperatures were maintained at 150°C and 106°C, respectively. The fluorinated standard was first run in full scan mode, with a mass range of (m/z) 50-400, to determine the retention times of the analytes. A selected ion monitoring (SIM) method was then designed with appropriately timed windows for the analysis. The extracts were run in SIM mode according to the method shown below in Table 2.

SIM Window	Compound(s)	Ions Monitored (m/z)	Respective Dwell Times (ms)	Start Time (m)
1	A	284, 304, 306	50	4.00
2	B	282, 284, 318	50	12.30
3	MC DC	299, 300, 301 297, 261, 299	30	15.00
4	TC	295, 331, 333	50	17.05

Table 3 – Ions monitored, for respective dwell times, in the SIM window for each compound (MC, DC, and TC refer to mono, di, and tri-chlorinated benzamides, respectively. See page 73.)

Sample extracts were run on the GC/MS under continuing calibration to ensure instrumental reproducibility and performance. Quantitation was performed on ion chromatograms, of the most abundant ion (m/z) available, for each analyte.

Part II – Polynuclear Aromatic Hydrocarbons

Solvents

HPLC grade 1-butanol, 1-pentanol, 1-hexanol, and cyclopentanol were purchased from Sigma-Aldrich (Oakville, Ontario). Toluene, also of HPLC grade, was purchased from Caledon Laboratories Ltd. (Georgetown, ON).

Reagents

A mixture of 16 PAHs (2000µg/mL of each in a solution of 1:1 benzene in dichloromethane) was obtained from Sigma-Aldrich (Oakville, Ontario). The contents of the 1mL ampule were quantitatively transferred to a 50mL flask and filled to volume to make a solution of 40ppm PAHs in toluene. The 40ppm standard was diluted 10-fold in the various injection solvents to make working solutions of 4ppm.

Instrumentation

Experiments involving the PAHs were performed on a Perkin Elmer Autosystem XL gas chromatograph coupled to a Turbomass Gold mass spectrometer. The GC was equipped with an Rtx-50 column, from Chromatographic Specialties Inc. (Brockville, ON), approximately 30m in length, having an inner diameter of 0.25mm, and a film thickness of 0.25µm (30m × 0.25mm × 0.25µm) with a 5m × 0.53mm ID guard column also from Chromatographic Specialties (Brockville, ON). This column is of intermediate polarity with its stationary phase consisting of 50% diphenyl and 50% dimethyl polysiloxane. A DB-17MS column from Agilent Technologies Canada Inc. (Mississauga, ON) was also used for some preliminary experiments. Helium, Trace Analytical 5.5 from Praxair (Mississauga, Ontario), was used as the carrier

gas. The helium tank was connected to the GC gas line via a stainless steel dual stage regulator.

Experimental Conditions

The temperature program used for PAH experiments is shown below in Table 4.

Ramp (°C/min)	Temperature (°C)	Hold Time (min)
-	T_o = variable	4
10	195	5.5
25	275	19
20	310	5

Table 4 – General temperature program for the PAH study. Initial column temperature varied over 100°C range about the boiling point of the solvent.

Specialty septa and o-rings were required for high injector temperatures used in PAH experiments, and the optimum injector temperature study. A Kalrez o-ring was purchased from Perkin Elmer (Woodbridge, Ontario), and BTO septa were ordered from Chromatographic Specialties Inc. (Brockville, Ontario).

2μL of the 4ppm PAH working solutions were injected in splitless mode into the pulsed split/splitless injector at 285°C. The split vent was set to open 60 seconds after injection with a split flow of 50mL/min. The carrier flow rate was set at 4mL/min until the split vent opened, and was then reduced to 1.4mL/min. This high initial flow rate was chosen to help increase the pressure in the inlet, and thus to maximize the amount of analyte that reaches the column.

The TurboMass Gold was operated in electron impact (EI) ionization mode with electron energy set to 70eV. The source and transfer line temperatures were maintained at 150°C and 300°C, respectively. The PAH mixtures in various solvents were run in both selective ion monitoring (SIM), and full scan modes. In full scan, ions with a mass to charge ratio (m/z) of 76-305 were monitored. In

SIM, some of the PAHs were grouped together according to their characteristic ions. Table 5 below displays the ions monitored in each SIM window.

SIM Window	PAHs	Ions Monitored (m/z)	Respective Dwell Times (ms)
1	Full Scan	76 - 305	N/A
2	Acenaphthylene	151, 152	10, 10
3	Acenaphthene	153, 154	10, 10
4	Fluorene	165, 166	10, 10
5	Phenanthrene, Anthracene	76, 178	10, 10
6	Fluoranthene, Pyrene	202, 203	70, 70
7	Benzo[*a*]anthracene, Chrysene	226, 228	10, 10
8	Benzo[*b*]fluoranthene, Benzo[*k*]fluoranthene, Benzo[a]pyrene	126, 252	50, 50
9	Indeno[1,2,3-*cd*]pyrene, Benzo[*ghi*]perylene	276, 277	70, 70
10	Dibenzo[*a,h*]anthracene	278, 279	70, 70

Table 5 – Ions monitored, for respective dwell times, in the SIM window for each PAH, or group of PAHs.

The SIM windows were set up such that they did not overlap unless absolutely necessary. Only windows 9 and 10 overlapped each other. In order to determine the varying retention times of the PAHs (resulting from different initial column temperatures), prior to each experiment, the PAH working solution in the desired solvent was run once at each initial column temperature prior each

experiment. The SIM windows for each PAH, or group of PAHs, were then adjusted to the correct retention times.

The TurboMass Gold has the ability, without sacrificing sensitivity, to perform SIM and full scan runs simultaneously. For this reason, a full scan method was always run parallel to the SIM methods. The two parallel scans provided confirmation, both by retention time and mass spectral comparison, of the identity of each peak.

Quantitation of PAHs was performed on the TIC (total ion current) chromatogram (two ions) for each peak. Peak areas and peak heights were used in the comparison of the different high-boiling alcohols as injection solvents.

Chapter 3 – Results and Discussion

Part I – Fluorinated Compounds

Method Development

In a preliminary study, extracts from a dated sediment core from Lake Ontario, were screened for the fluorinated compounds. The sediment samples had been previously prepared in accordance with SOP 03-3751 [107] (a method developed by the National Laboratory for Environmental Testing, in Burlington, ON) and screened for other compound classes. The core samples chosen for the determination corresponded (by date) to the years when the Hyde Park landfill was at the height of its operation. Those years should also have been the years of maximum deposition for the fluorinated compounds in sediments. These extracts were screened, by mass spectrometry, for masses that correspond to the ten fluorinated compounds using electron impact ionization, but no matches were found. Since the compounds were not found, the methodology had to be rethought.

The two most obvious reasons why these compounds were not detected in the sediments are: i) MS using EI ionization is still not sensitive enough to detect these compounds; or ii) the sample preparation procedure is not viable for the compounds of interest.

It was found that the method for the sample preparation, that had been used on the core samples, called for ultrasonic extraction with 1:1 acetone in hexane, partitioning into water, and back-extraction with dichloromethane. This was followed by clean-up on a silica gel column and fractionation via two solvent systems: 100% hexane, and dichloromethane in hexane (1:1, v/v) [107]. In the work of Hites *et al.*, sample extracts had been fractionated from the silica gel clean up column into 100% hexane, 80% dichloromethane in hexane, and 100% dichloromethane [10]. The latter two fractions were found to contain the fluorinated compounds. This information supported suspicions that SOP 03-3751 was not a viable method for the fluorinated compounds.

A recovery study was performed on seven of the ten fluorinated compounds that, at that time, were available. These compounds included: 4-chlorobenzotrifluoride (CBTF), 2,4-dichlorobenzotrifluoride (DCBTF), 3-amino-benzotrifluoride (ABTF), N-(3-trifluoromethyl)-phenylbenzamide (TFMPB), 4-chloro-N-[3-(trifluoromethyl)-phenyl]benzamide (MC), 2,4-dichloro-N-[3-(trifluoromethyl)phenyl]benzamide (DC), and 2,4,6-trichloro-N-[3-(trifluoromethyl)phenyl]benzamide (TC). These compounds will be referred to as compounds 2-8, respectively. Benzotrifluoride (BTF) was not included in the recovery study as it elutes in the peak of toluene, which is the injection solvent that was used during method development.

A 1mL aliquot of a 5ppm solution of these compounds was applied to a column of 100% activated silica gel in a column between two layers of anhydrous sodium sulfate. The column was eluded with four solvent systems: 100% hexane, (1:1, v/v) dichloromethane in hexane, 5% methanol in dichloromethane (1:20, v/v), and 100% methanol. The fluorinated compounds were found to elute in the (1:1, v/v) dichloromethane in the hexane fraction and the 5% methanol in dichloromethane (1:20, v/v) fraction. Although this experiment did not include fluorinated compounds A and B, the work of Hites *et al.* showed that these two compounds elute in the same fractions as the others involved in the study.

Once all ten fluorinated compounds were available, a method was developed for their determination. A 5ppm standard of all ten compounds was run on the Agilent GC/MS in full scan mode and the retention times of all the compounds were determined (except BTF, as described above). Once adequate separation of the analytes was achieved, and the retention times determined, a SIM method was developed which included a retention window for each compound in which the 3 most abundant ions per compound from the EI mass spectrum were monitored. This method was then tested by running a 50ppb standard in the SIM program.

A method was developed in the same way on an instrument set up for negative ion chemical ionization (NICI). When the concentrated standard was

run in full scan mode on the NICI instrument, something interesting was noted. Even though NICI is expected to be especially sensitive to halogenated molecules, it was found that the fluorinated compounds did not respond to this ionization technique. Only compounds that were chlorinated (in addition to fluorinated) responded and even then, not all of them. Therefore, the method developed in NICI did not apply to BTF, CBTF, DCBTF, ABT, and TFMPB.

In NICI, the fluorinated standards were run at two different source temperatures: a high source/quadrupole temperature (230°C/150°C) and a low source/quadrupole temperature (150°C/107°C). It was found that compounds A and B responded differently to these temperatures – see Figure 1. A better response was noted for compound A at the low source temperature, and a better response for B was noted at the high source temperature. For this reason, it was decided that any samples would have to be run at both source temperatures.

Since only compounds A and B were found in the samples analyzed for this project, much of the discussion hereafter will focus on these analytes.

Figure 6 shows an overlay of two chromatograms. The black chromatogram was determined with the source/quadrupole temperature set to 150°C/106°C, respectively. The green chromatograph was obtained with a high source/quadrupole temperature of 230°C/150°C, respectively.

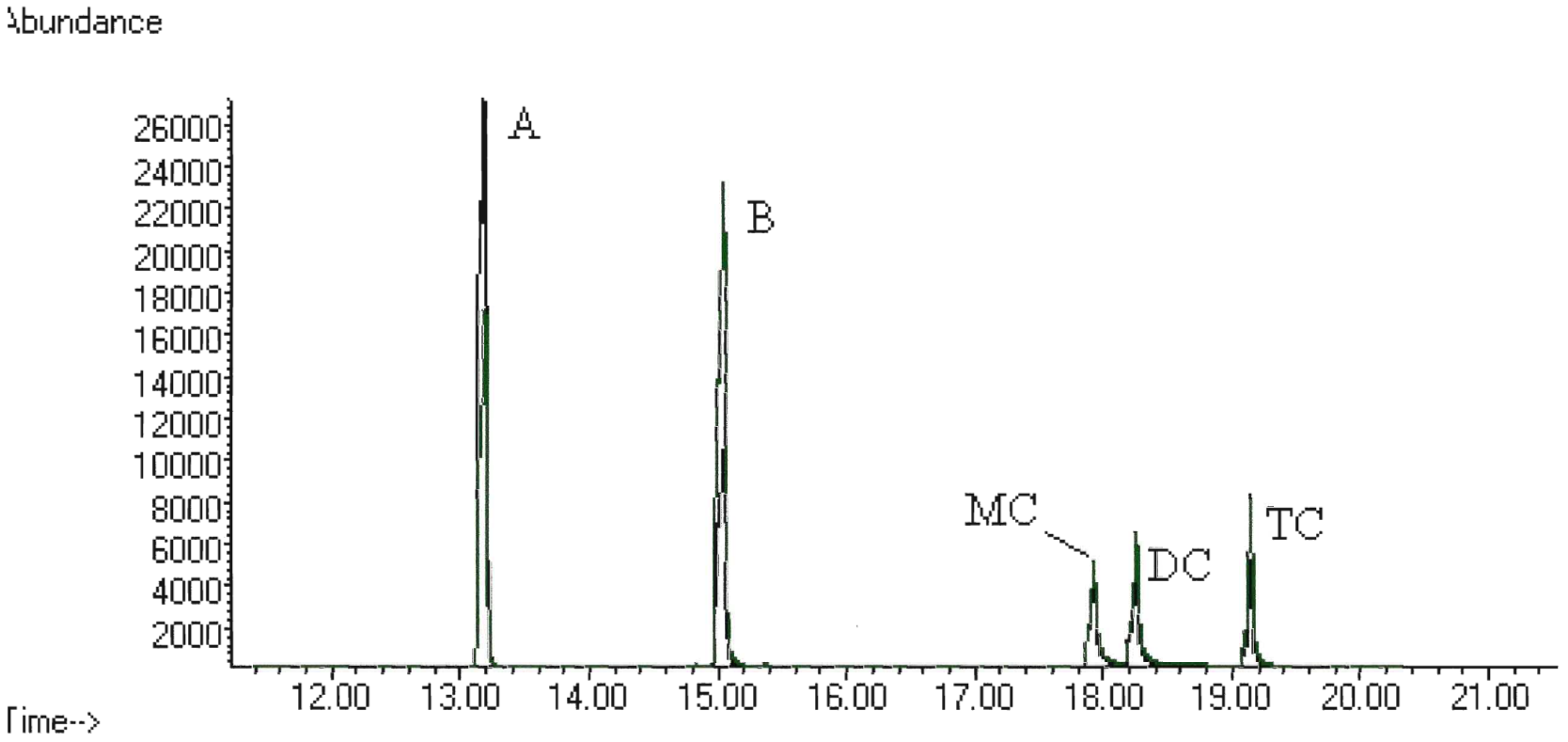

Figure 6 – ECNI chromatogram of A, B, MC, DC, and TC with a high (green) and low (black) source/quadrupole temperature

It can be seen that the black chromatogram yields a larger peak for compound A (t_R=13.19min) and the green chromatogram yields larger peaks for compounds B (t_R=15.01min), MC (t_R=17.92min), DC (t_R=18.25min), and TC (t_R=19.15min).

In addition to the response change observed in compounds A and B, their mass spectra also changed with changing source temperature as well.

Interpretation of Spectra

Compound A

The ECNI mass spectrum for compound A (MW=340amu) at a low source temperature (150°C/106°C) contains only one cluster of ions – see Figure 7. The distribution of ions in this cluster is typical of a compound containing one chlorine atom. The base peak of this spectrum is of m/z=304, which represents the $[M\text{-}HCl]^-$ ion. This ion is most likely formed through a dissociative resonance electron capture reaction. The $[M\text{-}HCl]^-$ ion is a pseudo-molecular ion peak in this cluster and is present in lieu of a molecular ion peak.

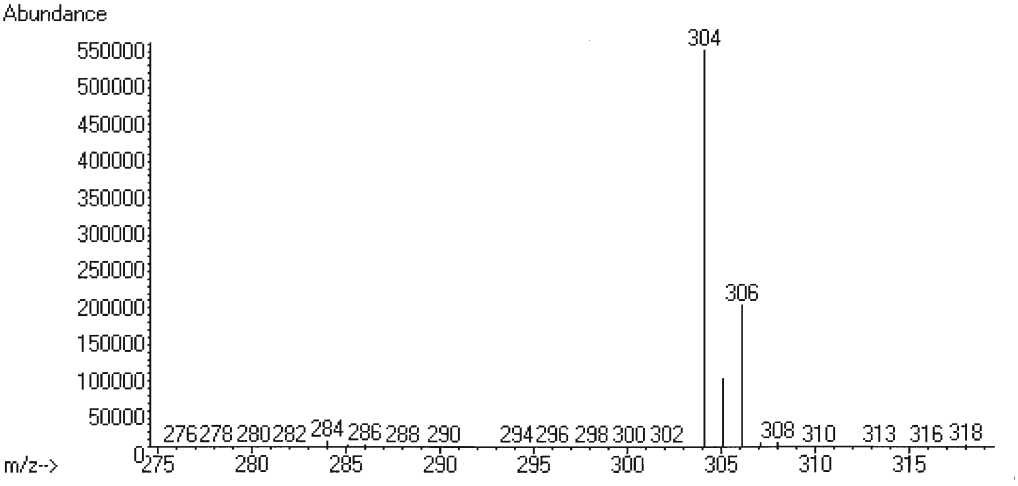

Figure 7 – ECNI mass spectrum of compound A (source/quad = 150°C /106°C)

When the temperature of the source/quadrupole is increased to 230°C/150°C, a new cluster of ions appear centered about m/z=284 – see

Figure 8. This mass-to-charge ratio corresponds to an $[M\text{-}HCl\text{-}HF]^-$ ion. This fragment must have one chlorine atom based on the characteristic peak, located 2 mass units higher and one third in abundance. The higher source temperature will result in more energy for the ions in the ion source. The $[M\text{-}HCl]^-$ ion, resulting from dissociative resonance capture, will also have some extra internal energy after ionization. Due to the reduced stability of this ion, some additional fragmentation is observed.

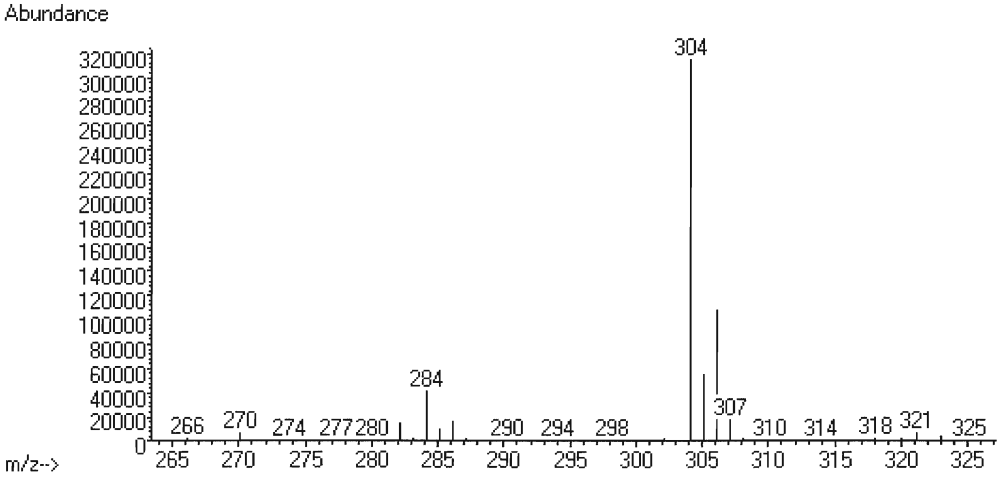

Figure 8 – ECNI mass spectrum of compound A (source/quad = 230°C/150°C)

As seen, the above ECNI spectra are quite different than the EI spectrum shown below (Figure 9). The ECNI spectra show less fragmentation, and have a more abundant molecular ion peak (pseudo-molecular ion), than the EI spectrum, even at high source/quadrupole temperatures.

In the EI spectrum, the molecular ion peak, although small, is present (m/z=340), and the corresponding peak two mass units higher that is two thirds the height. The most abundant ion though is the m/z=161 ion which corresponds to a $[M\text{-}CF_3\text{-}Cl\text{-}C_6H_3]^-$ ion.

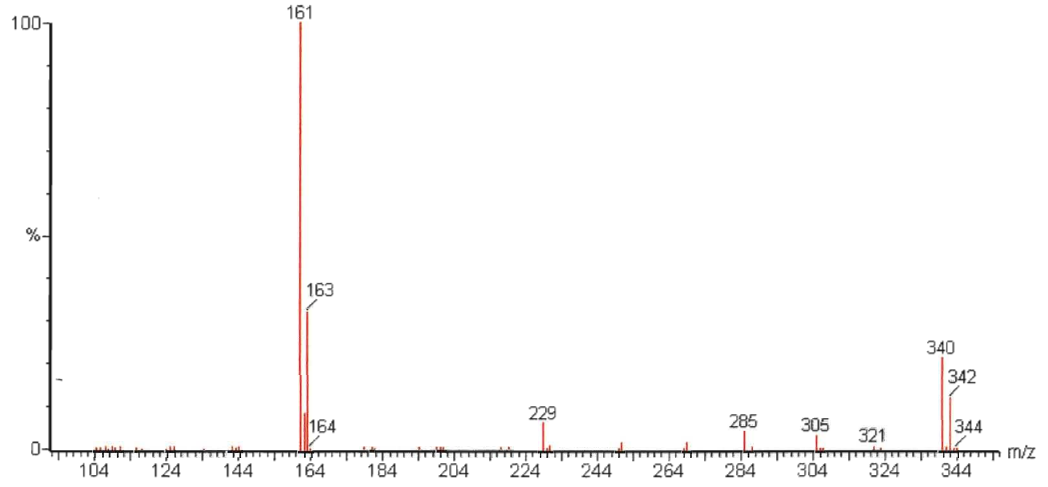

Figure 9 – EI mass spectrum of compound A

Compound B

The ECNI mass spectrum of compound B (MW=318amu) at a low source temperature (source/quad = 150°C/106°) contains two clusters of ions – see Figure 10. The distribution of the cluster of ions at m/z=318 is characteristic of a compound containing two chlorine atoms. The base peak of this spectrum, at m/z=318, is the $[M]^{-\bullet}$ ion. This ion is formed through an associative resonance capture reaction, and is the negative molecular ion.

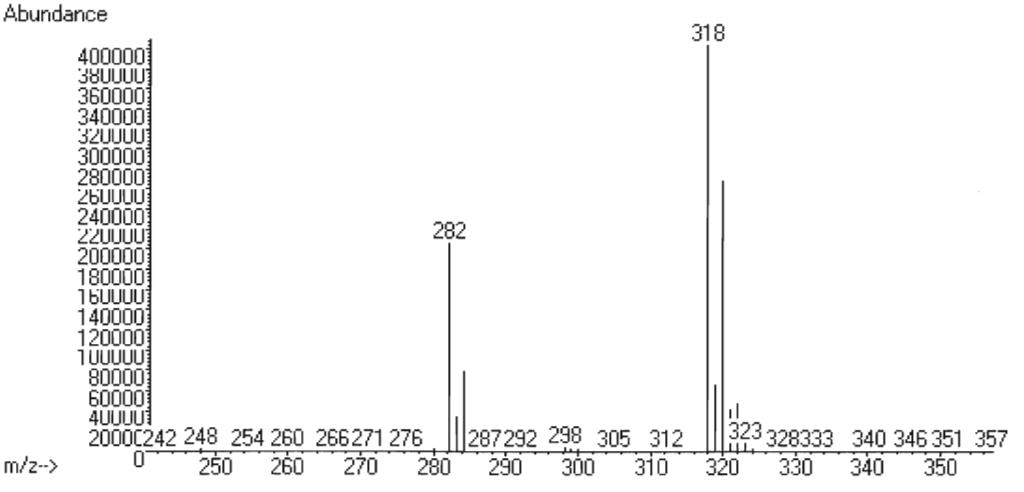

Figure 10 – ECNI mass spectrum of compound B (source/quad =150°C/106°C)

The second cluster of ions, the smaller of the two, is at m/z=282. The distribution of this cluster is characteristic of a molecule containing one chlorine atom and the base peak (m/z=282) is likely the $[M-HCl]^-$ ion.

When the source temperature is increased (source/quad = 230°C/150°C), the distribution of the ion clusters changes – see Figure 11. The $[M-HCl]^-$ cluster at m/z=282 is now larger than the cluster at m/z=318. At this higher source temperature, the thermal electrons are of higher energy and therefore, dissociative resonance capture dominates.

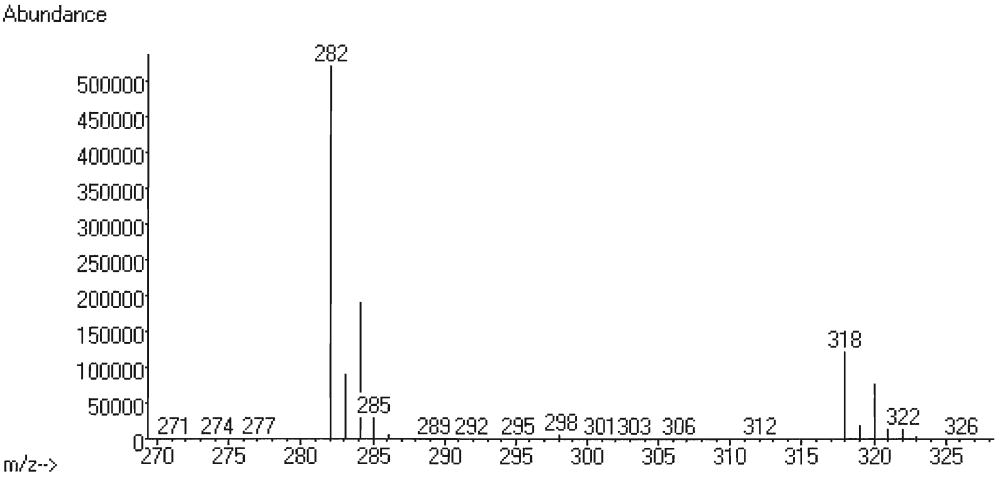

Figure 11 – ECNI mass spectrum of compound B (source/quad =230°C/150°C)

The EI mass spectrum (Figure 12) for compound B also shows more fragmentation than both of the ECNI mass spectra (low and high source/quadrupole) for this compound. It also possesses a much smaller molecular ion peak. The most abundant peak in the EI mass spectrum is m/z=139, which corresponds to the $[M-CO-C_6H_4-Cl]^-$ ion.

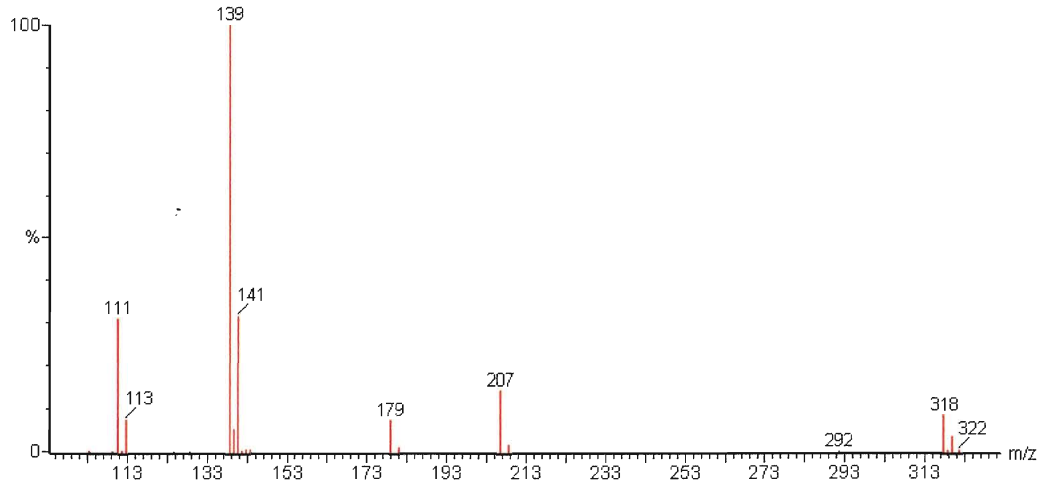

Figure 12 – EI mass spectrum of compound B

Quality Control

With every set of 10-12 samples, one lab blank, two lab spikes, and one lab duplicate were carried through the entire sample preparation procedure including: ASE extraction, reductions (Rotavapor and N-Evap), clean-up and fractionation on silica gel column, and GC/MS determination.

The lab spikes comprised Ottawa sand spiked with 100µL of a 5ppm standard containing all of the fluorinated compounds and 100µL of a 1ppm PAH standard containing deuterated PAHs (d-fluorene, d-pyrene, d-benzo[a]pyrene, and d-naphthalene). All samples in each set were also spiked with 100µL of the same deuterated PAH standard.

In the GC/MS analysis of the sample extracts, the extracts were run in a specified order: 1) isooctane blank, 2) the calibration standards run from least to most concentrated, 3) isooctane blank, 4) samples run in order from least to most concentrated. After every 6 samples, an intermediate concentration standard was run (for continuing calibration), and an isooctane blank.

In all blanks, the concentration of compounds A and B were found to be below the detection limit.

Quantification

Quantification was performed by the comparison of peak areas, from ion chromatograms, to external standard calibration curves produced using the same respective ions. All standards and samples were determined with a high source/quadrupole temperature despite the fact that some compounds showed a better response to the low source/quadrupole temperature (see Problems and Sources of Error). Standards used in calibration are listed below.

Compound	Mass (mg)	V Toluene (L)	Concentration (mg/L)	5ppm Std.	500ppb Std.	100ppb Std.	50ppb Std.	25ppb Std.	12ppb Std.	6ppb Std.
A	76.4	0.1	764.00	7.64	764.00	152.80	76.40	38.20	19.10	9.55
B	48.9	0.1	489.00	4.89	489.00	97.80	48.90	24.45	12.23	6.11

Table 6 – Actual concentrations of standards used in calibration curves for compounds A and B

Compound A

As seen in the ECNI mass spectrum at the high source/quadrupole temperature, shown in Figure 8, the three most abundant ions are m/z=284, 304, and 306. These three ions were used in SIM determination of the extracts, to yield a TIC (total ion current) chromatogram of the three ions. In this way, compound A could be determined, not only by retention time, but also by the relative distribution of these three ions at the corresponding retention time. Quantitation was then performed by extracting an ion chromatogram of m/z=306 (the most abundant ion). The peak area at the observed retention time for A in the mass chromatogram was integrated and the area compared to a calibration curve for A.

The calibration curve for A was obtained by running the standards listed in Table 1 in the SIM method, and extracting the mass chromatogram for m/z=306. The peak corresponding to compound A was then integrated and the calibration graph was plotted as peak area vs. known concentration in the standard, for each standard.

In the quantification of compound A only the standard of lowest concentration could be used for calibration purposes. When standards of higher concentration were included, the resulting calibration curve skewed the data. Although only the standard of lowest concentration was used, a calibration plot for all of the standards (except 500ppb), and a calibration for only the standards used in quantification are shown (Figures 13 and 14).

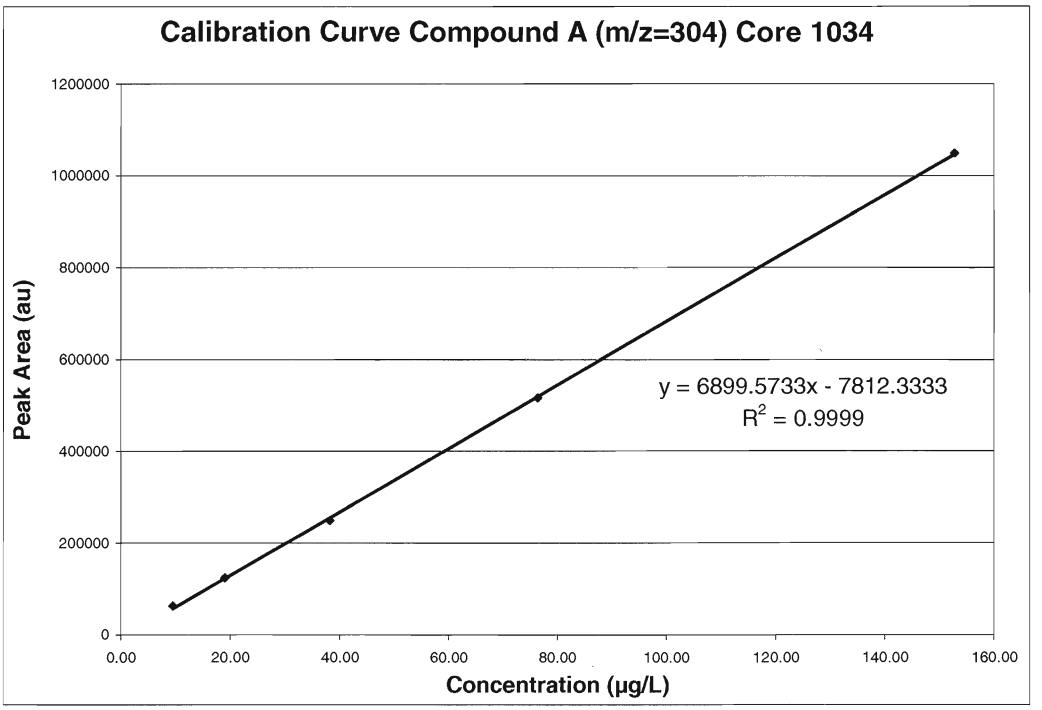

Figure 13 – Calibration curve for 6, 12, 25, 50, 100ppb standards for compound A (m/z=304)

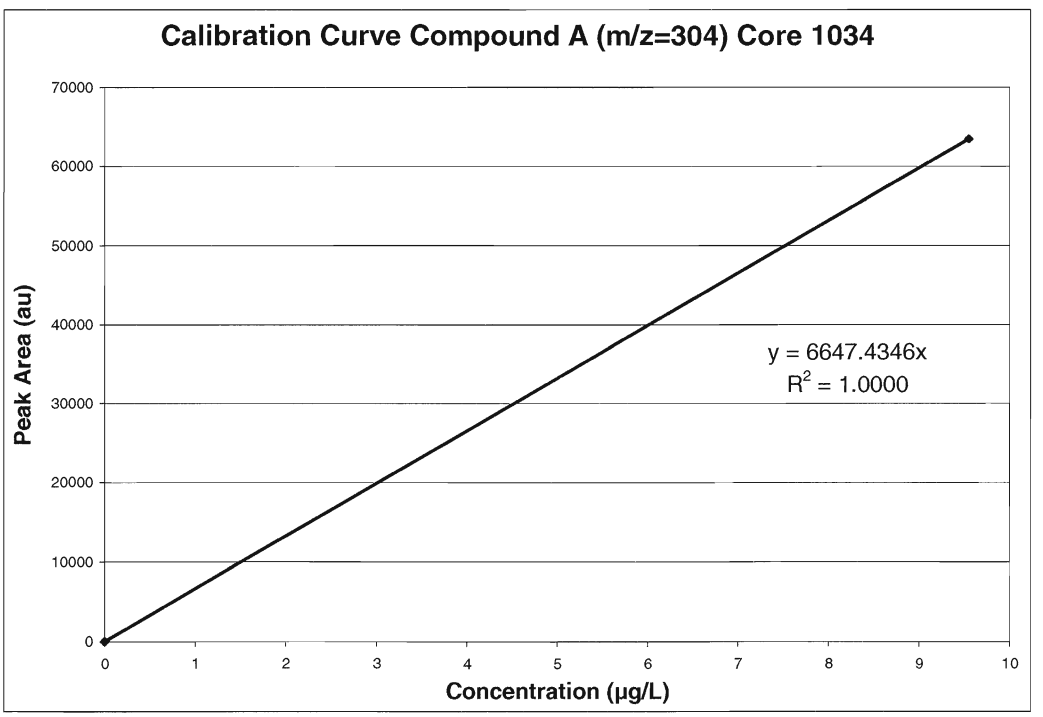

Figure 14 – Calibration curve for calibration range of compound A (m/z=304)

Compound B

In the case of compound B, things were done a little differently. Looking at the ECNI mass spectrum for compound B at a high source/quadrupole temperature, the most abundant ions are m/z=282, 284, and 318. The two most abundant ions, for this compound, are m/z=282 and m/z=284. In this case, neither of these ions were used for quantitative purposes as they were both present in an interfering peak. Compound B eluted as a coelution with this interference. The resolution between compound B and the interference was poor, at best, and because the interference also contained the two most abundant ions, quantification of compound B was performed using m/z=318. Utilizing this ion, quantification was then done in the same manner as described for compound A.

Compound B was quantified based only on the calibration standard of lowest concentration as well. A calibration plot including all of the calibration standards, except 500ppb, is shown in Figure 15 and a calibration plot for the single-point calibration is shown in Figure 16.

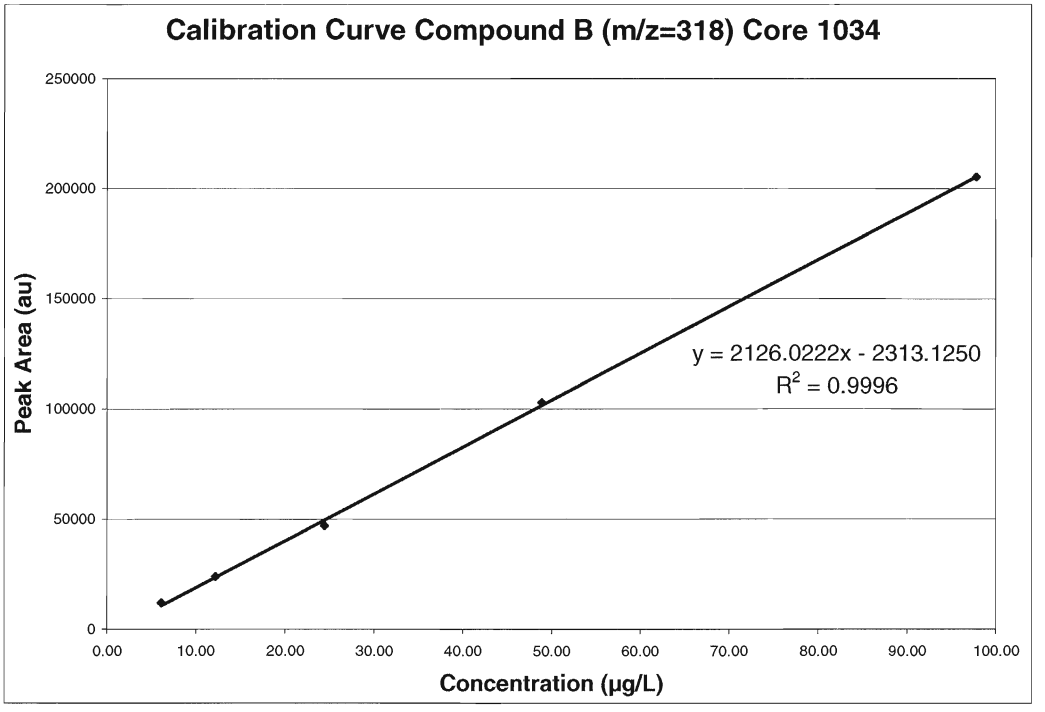

Figure 15 – Calibration curve for 6, 12, 25, 50, 100ppb standards for compound B (m/z=318)

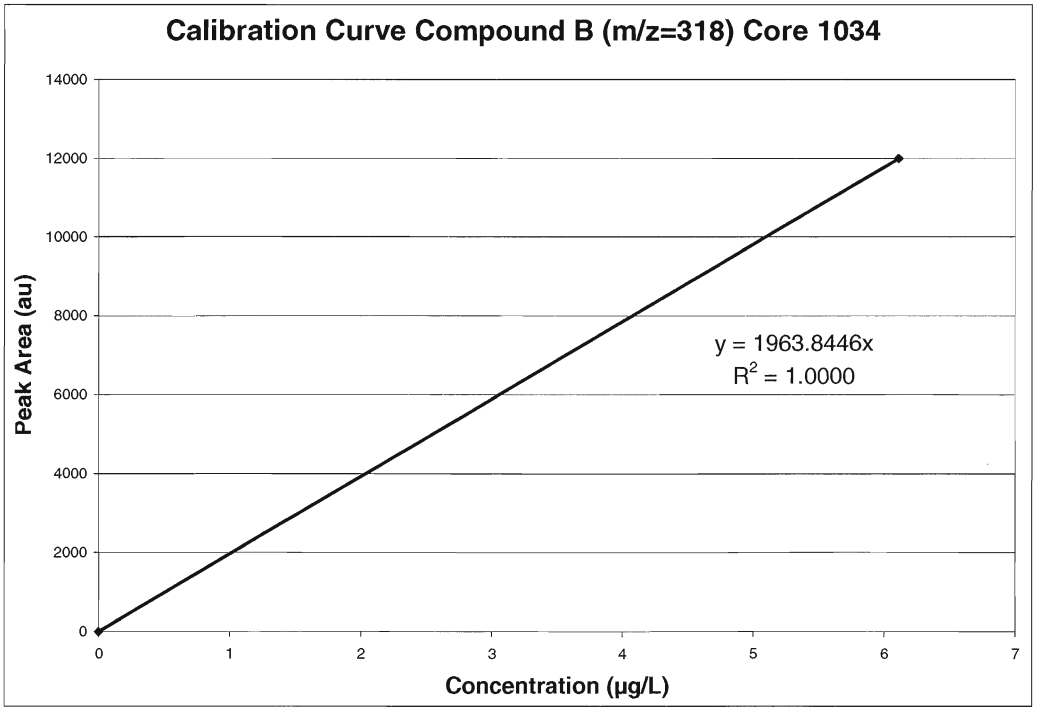

Figure 16 – Calibration curve for calibration range of compound B (m/z=318)

Results

The concentrations of compounds A and B in the core samples were plotted against the respective depth of the samples (within the core), to obtain a depositional trend of the compounds in Lake Ontario (see Figures 17 and 18).

The trend observed for compound A is very strange, but it is also meaningless. From the two lab spikes that were prepared and run alongside the samples, it was determined that the average recovery of compound A is 19%. This poor recovery likely means that the results of the determination are skewed in some way. These skewed recoveries are undoubtedly responsible for the unexpected shape of the profile shown in Figure 17.

The resulting profile for compound B, however, is quite interesting. It is interesting because it closely resembles the results published by Hites *et al.* [10, 18] for compounds A and B. This profile is also interesting as it is similar in shape to the profiles obtained of other industrial chemicals which are contaminants in Lake Ontario, such as dioxin-like polychlorinated biphenyls [108], and polychlorinated naphthalenes [109].

Looking at the profile obtained for compound B in Lake Ontario, there are five interesting regions on the graph – see Figure 18. In region 1 the concentration of compound B is below the detection limit. This is the preindustrial era. In region 2, the concentration of compound B starts to increase as OCC's manufacture of 4-chloro-benzotrifluoride is underway. Region 3 represents the time of maximum deposition of compound B. In region 4, the concentration of compound B is quickly declining. The Hyde Park Landfill would have been closed at this time, and remediation commenced. Region 5 represents the present, and is especially interesting in the case of compound B. It would be expected that levels of compound B should have returned to background levels (below the detection limit), if it is no longer entering Lake Ontario. But compound B has not returned to background levels. This could imply that it is still escaping from the Hyde Park Landfill and accumulating in the lake. It is also possible that increased levels of compound

B (from background levels) are being detected due to physical perturbation of the sediments in Lake Ontario. It is most probable that non-background levels of compound B are detected at present due to a combination of physical disturbance of sediments, and continued migration of the compound from the dumpsite.

This profile for compound B is a depositional history of this compound that originates from the Hyde Park Landfill. Compound B has no other known sources. Therefore, this profile reflects the history of the operation of the dump.

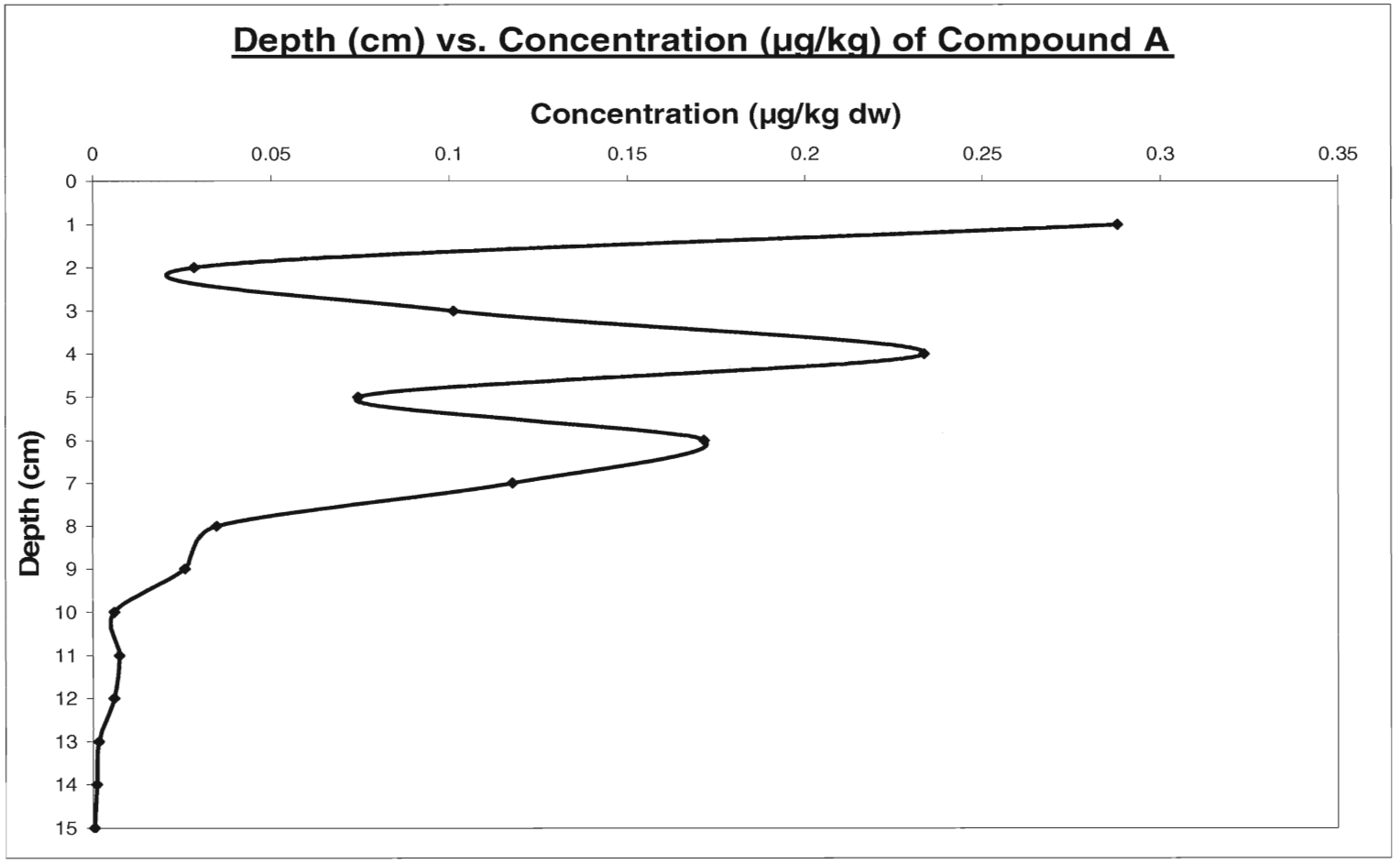

Figure 17 – Concentration profile for compound A at station 1034

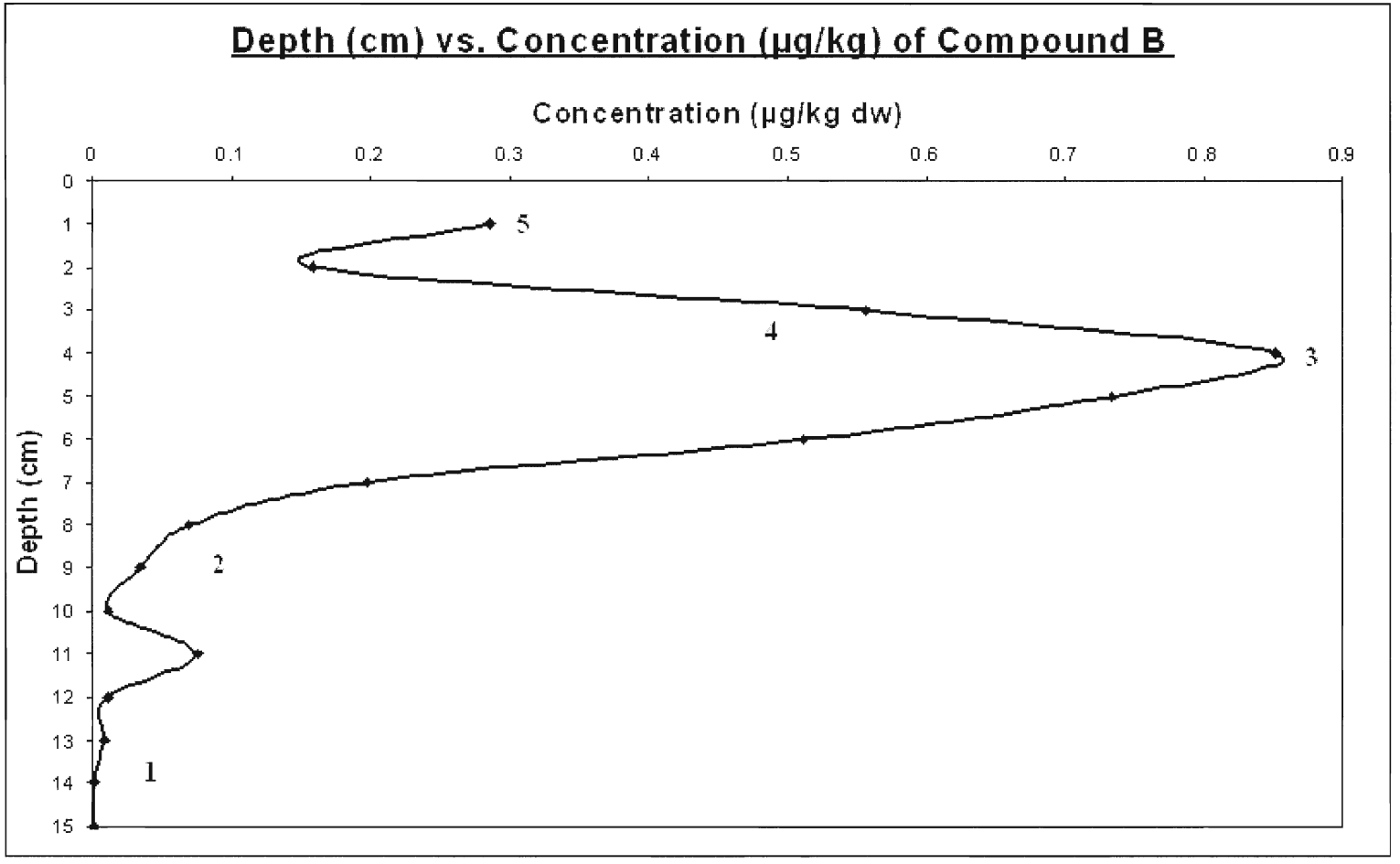

Figure 18 – Concentration profile for compound B at station 1043

Problems and Sources of Error

Source/Quadrupole Temperature

Although compound A responded better at a low source/quadrupole temperature, the samples were all run at the high source/quadrupole temperature. It was found, through continuing calibration, that the reproducibility of the determination was poor at the low source/quadrupole temperature.

Electron capture negative ion chemical ionization does have a reputation for being irreproducible. Small discrepancies in the ion source temperature, buffer gas, sample volume, as well as source contamination, can all contribute to decreased reproducibility [45].

Poor Recovery of Compound A

There are not many potential explanations for the poor recovery observed for compound A. This is mainly because most of the potential causes should have affected the recovery of both compounds – not just compound A.

Cross-contamination of samples is not likely. Compound A is not expected to be volatile enough to transfer between samples when left open in the fume hood to thaw and dry over a week. Also, instruments that came into direct contact with the samples for crushing, mixing, transferring, and measuring were well cleaned between uses. It is possible that some loss of compound A could be attributed to adsorption to glassware. But it is more likely that this would also have affected the recovery of compound B as well.

The most likely cause of the selective loss of compound A is something that relies on a difference in properties between compounds A and B. Compound A is more volatile than compound B and, as a result, a loss attributed to reduction of extracts on the Rotavapor or N-Evap is possible, although care was taken to ensure that none of the extracts were reduced to dryness. The reductions could take place with the water bath set to a lower temperature.

As Hites *et al.* found compound A (and B) eluted from a silica gel clean-up column with 100% dichloromethane, it is doubtful that it would not have eluted with 5% methanol in dichloromethane. However, with all of the compounds now available, a new recovery study should be conducted to be sure in which fractions these compounds do elute.

The most likely cause for the loss of compound A is in the extraction procedure – the ASE. The ASE was operated in the "preheat" method. In this way, the sample cell containing the contaminated sediment is heated to the extraction temperature of 100°C prior to the addition of solvent, and pressurization. There is a definite potential for the loss of volatile and semivolatile analytes by heating the extraction cell to 100° without any solvent present. If the analytes were to volatilize prior to the addition of solvent, they would most likely be lost. It is for this reason, that the "prefill" procedure of ASE is preferred. In this procedure, the sample cell is filled with solvent and pressurized prior to heating. It is also possible that a different extraction solvent may have a higher extraction efficiency for compound A.

Compound B Coelution

Compound B coeluted with another compound in the sample extract, and so for quantification purposes, an ion had to be chosen such that it was not common between compound B and the coeluting peak. Unfortunately, ions m/z=282 and 284, both of which are more abundant than m/z=318, were both characteristic of the unknown coeluting compound.

A better temperature program should have been developed, if possible, to eliminate the coelution between compound B, and the interference. Then compound B could have been quantified through its most abundant ion.

Choice of Surrogates

Deuterated PAHs were added as surrogates to the sample extracts prior to analysis. PAHs are expected to be amenable to ECNI because of their

conjugated double bonds. However, the deuterated PAHs were not seen in the standards and surrogates. Fluorinated compounds are also expected to respond well in ECNI but, again, this was not seen. Fluorinated compounds only responded in ECNI if they also contained chlorine atoms.

Limited Sample Set

Data obtained in this study was limited to one core from Lake Ontario. In order to draw any diffinitive conclusion regarding the potential migration of chemicals from the Hyde Park Landfill, data from more cores that cover a wider spread of the lake are necessary. Suspended sediments from the entry point of the Niagara River to Lake Ontario would be very useful for this purpose.

Choice of Mass Range

In NICI, dissociative electron capture typically results in the loss of halogen atoms from polyhalogenated molecules [58]. At a high source/quadrupole, temperature, the dissociative reaction becomes more likely than associative electron capture. The analysis of compounds A and B was performed at a high source/quadrupole temperature, and the resulting mass spectra of these compounds show the increased fragmentation due to dissociative electron capture. It can also be seen, from the spectra, that the resulting fragments correspond to the loss of HCl or HF from the parent molecule.

The determination of compound A was found to be more sensitive at a low source temperature. This is because, the ions monitored corresponded to the molecular ion less HCl, or the molecular ion less HCl and HF. m/z=35 was not monitored. The author neglected to observe a substantially wide mass range in intial method development, and even though the chloride ion must be present in the spectrum, it was not observed. Although the chloride ion is not structually significant, if monitored in addition to a structually significant ion

such as the $[M\text{-}HCl]^-$ ion, it could enhance the sensitivity of the determination for both compounds A and B. The fluoride ion is not exepected to be significant based on the ECNI mass spectra of the compounds.

Use of an Internal Standard

Internal standard calibration should have been used for quantification. An internal standard similar to compound A (such as a deuterated or ^{13}C-labelled version), would have been especially useful, if added prior to extraction, as it would have negated any matrix effects or losses during sample preparation. As compounds A and B were shown to behave differently through sample preparations and analysis, a different internal standard should be chosen for the quantification of compound B.

Part II – Polycyclic Aromatic Hydrocarbons

Factors Affecting Performance and Chromatographic Behaviour in Gas Chromatographic Determination of PAHs

Injector Temperature

The optimum injector temperature for PAH analysis was determined. A 4ppm solution of 16 PAHs in toluene was used for experimentation. Injector temperatures ranging from 250°C to 400°C were tested. An upper bound for the injector temperature was defined by the thermal stability of the septa. Ideally, the injector temperature is chosen to be about 50°C above the boiling point of the highest boiling component to ensure flash volatilization in the injection port. In the case of PAHs, this is not possible. The late-eluting PAHs have boiling points well over 500°C. Even with the use of specialty, high temperature septa and o-rings, the injector temperature is limited to a maximum temperature of 400°C. Peak areas and peak heights of selected PAHs were plotted against the varying injector temperatures.

It is expected that, as the injector temperature increases, the peak areas and peak heights of the PAHs will increase (especially the high-boiling PAHs), as more of each analyte will volatilize and reach the column and detector. This trend was observed for injector temperatures of 250°C through 390°C. The response of all PAHs was reduced at 400°C, however the optimum injector temperature was chosen to be 360°C. Response increase for PAHs was far more significant for injector temperatures between 250°C and 360°C than the increase observed for injector temperatures between 360°C and 390°C.

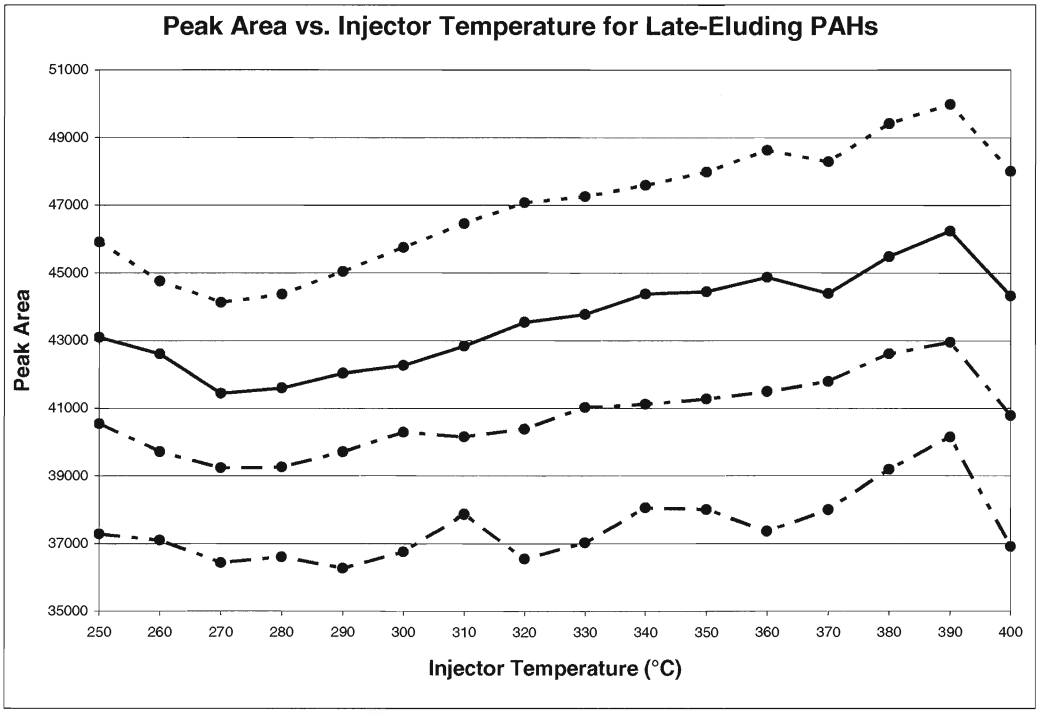

Figure 19 – Effect of injector temperature on peak area of late-eluting PAHs (from top to bottom: Benzo[*a*]pyrene, Benzo[*ghi*]perylene, Dibenzo[*a,h*]anthracene, Indeno[1,2,3-*cd*]pyrene)

With the use of specialty high thermal stability septa and o-rings, it was thought that 360°C would be an ideal injector temperature. However, the author neglected to consider the thermal stability of the column. As a portion of the column resides in bottom of the inlet, it is therefore exposed to these same high temperatures as the septa and o-rings. An injector temperature of 285°C was chosen for all PAH analysis. This temperature was chosen prior to the attachment of a guard column. Although a guard column was used afterwards, the injector temperature of 285°C was maintained.

Splitless Hold Time

Another parameter requiring optimization, in splitless injection, is the splitless hold time. In splitless injections, the split vent is kept closed during injection, for a predetermined period of time, and is then opened after injection for the rest of the analytical run. The time period, during which the split vent is

kept closed, is known as the splitless hold time. If the split vent is opened too soon after injection, analytes can be lost through the split vent and not make it to the analytical column. This loss would result in decreased response and therefore decreased sensitivity. Solvent tailing may be observed, if the split vent is left closed for too long after injection [110].

The splitless hold time was optimized by running a PAH standard in toluene at various splitless hold times ranging from 0-120 seconds. The response of naphthalene (low-boiling) and benzo[*ghi*]perylene (high-boiling) were plotted against the corresponding splitless hold times. The point at which the resultant curves level off is the optimum splitless hold time. From this experiment, the optimum splitless hold time was chosen to be 45s – see Figure 2 below.

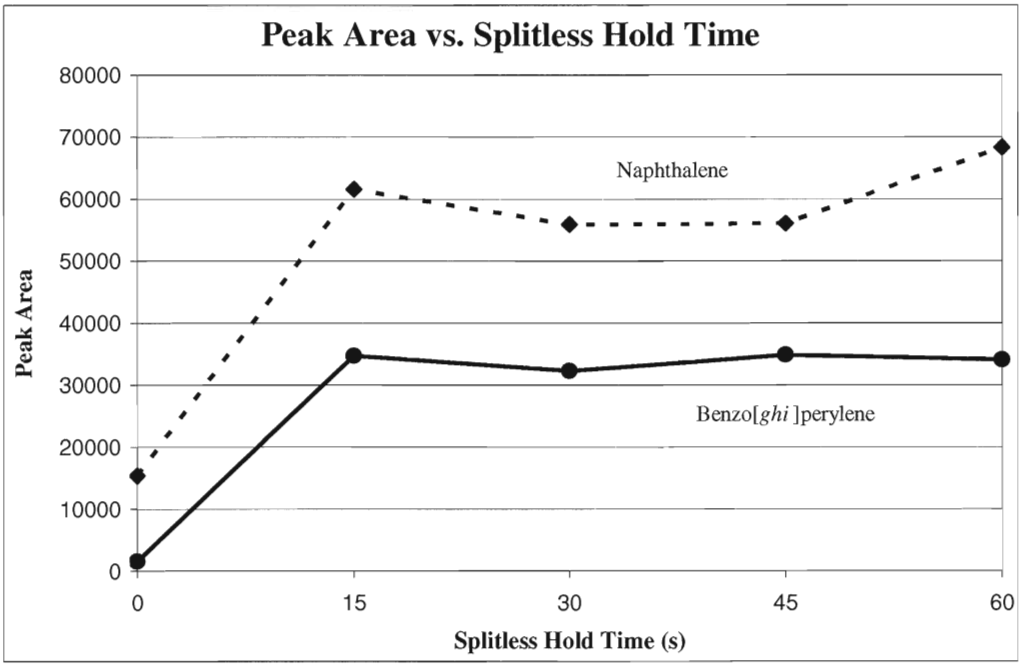

Figure 20 – Peak Area vs. Splitless Hold Time for Naphthalene and Benzo[ghi]perylene

At a splitless hold time of 0 seconds (i.e. split vent opened immediately after injection), the responses of both naphthalene and benzo[*ghi*]perylene were very low. At splitless hold times over 60 seconds, the solvent peak tailed excessively. The response of both compounds was stabilized at 45 seconds

which is why this was chosen as the optimum splitless hold time. Naphthalene actually had an increased response at 60 seconds, but at this splitless hold time, the peak corresponding to benzo[*ghi*]perylene was slightly reduced. Increasing the response of the late-eluding compounds is of higher priority than increasing the response of naphthalene. The naphthalene peak is lost with the solvent peak for higher-boiling solvents and is therefore not significant to this project.

Temperature Program

The temperature program is one of the most important factors to consider during method development. A temperature program was developed that offered the best possible separation, of all 16 PAHs in the shortest period of time. There are 3 pairs of PAHs that are notoriously problematic in terms of coelution: phenanthrene and anthracene, benzo[*b*]fluoranthene and benzo[*k*]fluoranthene, and indeno[1,2,3-*cd*]pyrene and dibenz[*a,h*]anthracene Special attention was paid to these groups, during temperature program development, to ensure the best resolution possible. In Figure 21 below, it can be seen that these problematic PAH pairs elute on isotherms. It can also be seen that of the three problematic PAH pairs, only benzo[*b*]fluoranthene and benzo[*k*]fluoranthene are not completely resolved. These compounds are 80% resolved.

During method development, it was found that the peak height of late-eluting PAHs, indeno[1,2,3-*cd*]pyrene and dibenz[*a,h*]anthracene, could be maximized by having them elute sooner, on a temperature ramp (see Figure 22). As they spent less time on the column, they showed much less band-broadening effects. However, since their area response was the same whether they eluted on an isotherm or a ramp the temperature program that elutes them on an isotherm was chosen. When these two compounds elute on a ramp, resolution is lost. It was decided that resolution is more important that peak height, and so the temperature program in which this PAH pair elutes on an isotherm was chosen (as shown in Figure 3).

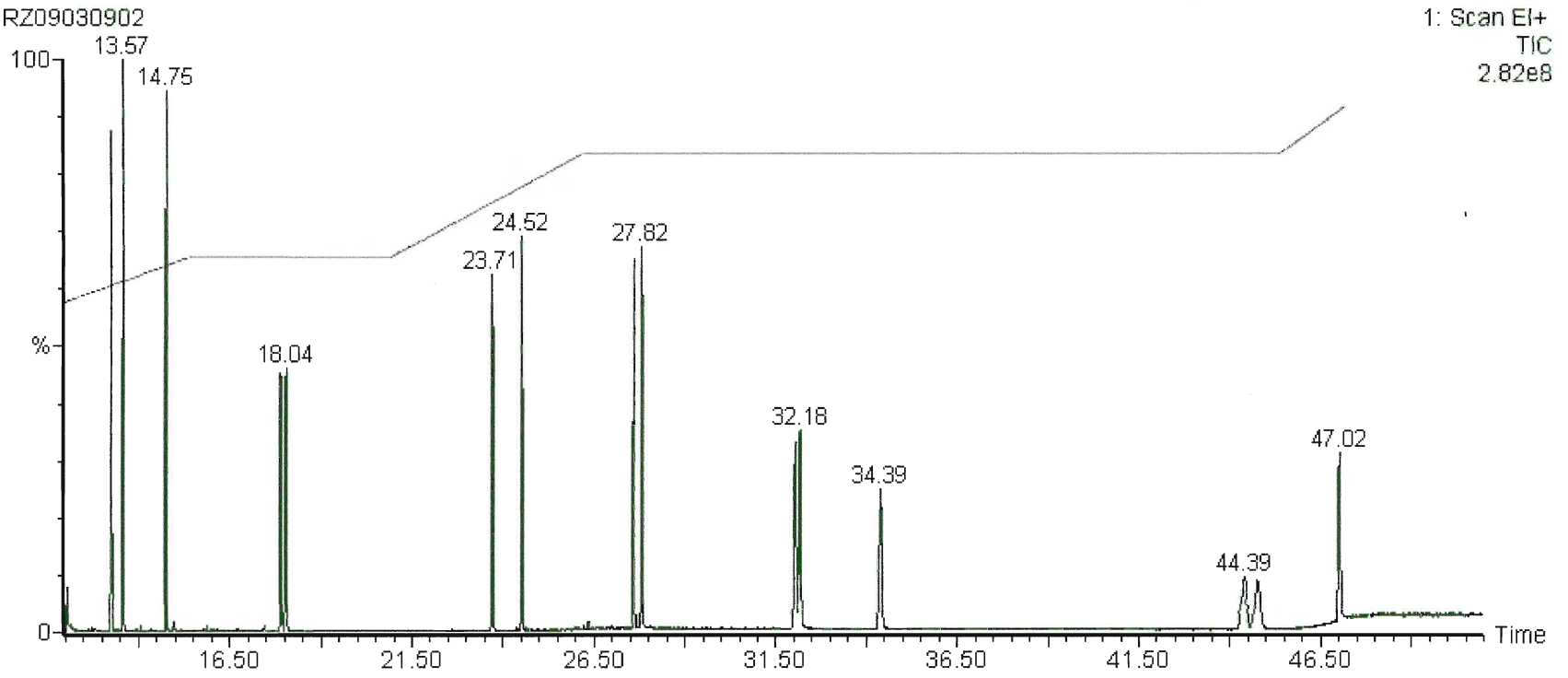

Figure 21 – Temperature program (used in all PAH experiments) overlaying chromatogram of PAHs in cyclopentanol (T_0=81°C)

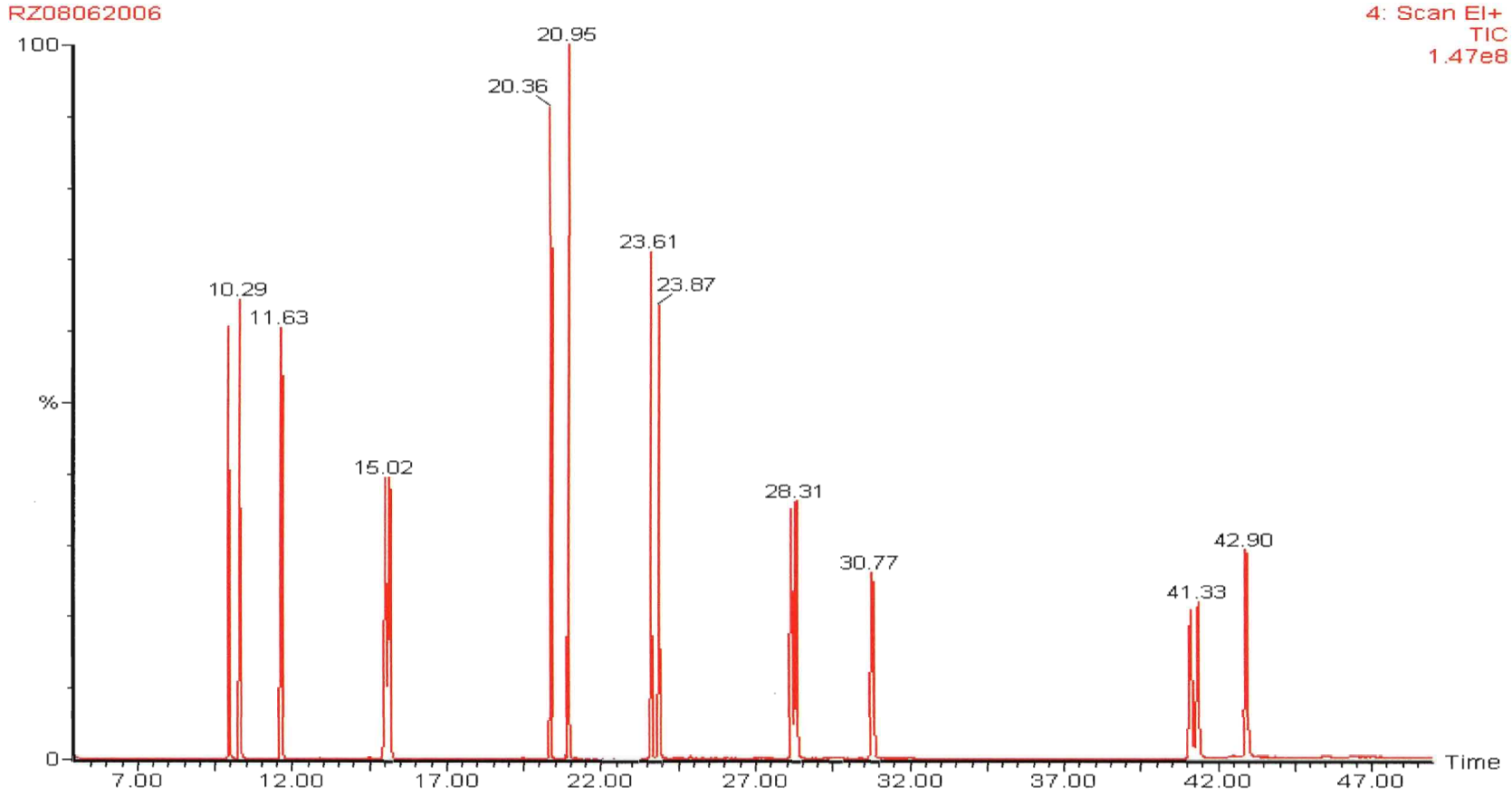

Figure 22 – Old temperature program in which the peak height of late-eluting PAHs was maximized (This temperature program was not used for experiments in the determination of PAHs.)

Initial Column Temperature

It has been shown that the initial column temperature can have dramatic effects on resolution and peak symmetry [90]. In addition to peak symmetry, the author wished to investigate which parameter (solvent trapping, or cold trapping) had significant impact on PAH response, particularly for the late-eluting PAHs, which are notoriously susceptible to mass discrimination. Initial column temperature was varied, for each solvent (see Table 7), by 100°C range about the boiling point of the solvent. The initial column temperature for each solvent, that resulted in the largest cumulative peak areas for the late-eluting PAHs (last 6 PAHs), was chosen as the optimum initial column temperature for that solvent. Herein, PAHs referred to as "early-eluting" corresponds to PAHs 2-10, and PAHs termed "late-eluting" corresponds to PAHs 11-16 (see table 1), unless otherwise stated. Naphthalene is not included, as it elutes with the solvent peak for most of the solvents tested here. The solvents, their respective boiling points, and the initial column temperatures tested for each, are shown in Table 7.

Solvent	**Boiling Point of Solvent (°C)**	**Column T_o Range (°C)**
Toluene	110.6	50-150
1-Butanol	117.7	57-157
1-Penanol	134.0	77-177
Cyclopentanol	140.4	81-181
1-Hexanol	157.6	98-188
n-Octane	125.7	65-165

Table 7 – Solvents used in comparison study with PAHs

Effect on Response

Tables 8a-19a show the effect of initial column temperature on PAH peak area and peak height. A 4ppm solution of the 16 US EPA priority PAHs, in each of the 6 solvents shown in Table 1, was run at initial column temperatures ranging 100°C about the boiling point of the solvent (in 10°C increments). At each initial column temperature, the peak areas and peak heights of PAHs 2-16 were determined through their respective ion chromatograms. The results of these experiments are shown in Tables 8a-19a. The results are tabulated as relative average peak areas and heights (relative to the optimum initial column temperature). The initial column temperature residing at the boiling point of the solvent is shaded in each table. The reproducibility for three successive injections for each solvent at each initial column temperature was measured for peak areas and heights. These results are tabulated below each table of peak areas and peak heights (Tables 8b-19b).

The results in Tables 8a-19a are given as a percent and are relative to the initial column temperature which was chosen to be the optimum value.

For 1-hexanol, the maximum initial column temperature attempted was limited to 188°C by the temperature program, however, initial column temperatures of 168°C and above were omitted from results due to excessive splitting of early-eluting PAHs. 1-pentanol and cyclopentanol had initial column temperatures of 177°C and 181°C, respectively, omitted also due to excessive splitting of early-eluting peaks. This will be discussed further in the appropriate section.

	PAH														
Column T_o (°C)	2	3	4	5	6	7	8	9	10	11	12	13	14	15	16
57	100	100	100	100	100	100	100	100	100	100	100	100	100	100	100
67	100	101	95	97	96	100	98	98	99	97	96	97	94	93	99
77	99	98	94	94	93	98	96	97	98	98	95	95	91	89	95
87	103	102	97	96	93	96	96	94	96	95	95	93	87	83	93
97	104	102	95	97	93	94	95	95	95	96	93	91	85	80	90
107	101	100	92	100	96	97	96	92	94	94	91	90	82	76	89
117	102	100	95	94	91	99	99	91	92	90	91	88	80	73	88
127	105	104	98	91	89	96	93	89	91	90	89	85	76	70	85
137	105	103	95	95	93	95	94	88	89	88	87	82	74	66	83
147	107	104	95	91	87	97	97	84	85	87	84	80	71	63	81
157	111	104	97	95	99	93	93	86	87	84	84	78	68	58	79

Table 8a – Relative average peak areas of PAHs (n=3) in 1-butanol at varying initial column Temperatures

	PAH														
Column T_o (°C)	2	3	4	5	6	7	8	9	10	11	12	13	14	15	16
57	1	2	3	2	2	0	1	1	1	3	1	2	3	4	3
67	2	0	1	2	2	1	3	1	0	2	1	1	1	1	1
77	1	1	0	1	0	1	2	1	1	2	1	1	2	2	0
87	1	1	1	1	1	1	1	1	1	1	1	0	1	1	0
97	1	0	2	1	1	2	2	2	0	1	1	1	1	1	1
107	0	1	1	1	1	2	2	1	1	1	1	0	2	1	1
117	1	0	1	1	0	0	2	1	0	1	1	0	1	2	1
127	1	0	0	1	1	1	2	1	1	1	0	1	2	1	2
137	1	1	1	0	1	1	1	0	1	1	2	1	1	1	1
147	1	1	0	2	0	2	2	0	2	1	2	1	2	1	1
157	0	1	1	1	1	2	3	2	1	2	1	2	2	2	0

Table 8b – %RSD for average peak areas of PAHs (n=3) in 1-butanol at varying initial column temperatures

	PAH														
Column T_o (°C)	2	3	4	5	6	7	8	9	10	11	12	13	14	15	16
57	100	100	100	100	100	100	100	100	100	100	100	100	100	100	100
67	112	105	95	96	101	96	97	98	102	99	94	96	101	90	99
77	108	109	101	99	95	96	102	93	96	99	96	96	93	85	97
87	108	114	102	98	99	98	97	96	96	95	93	92	91	79	88
97	121	108	97	101	95	92	91	90	92	93	94	90	87	82	91
107	111	108	86	105	99	96	95	89	91	99	89	90	84	74	88
117	93	102	93	89	95	91	94	98	93	91	86	86	82	71	88
127	91	102	85	86	93	102	91	88	94	90	88	87	78	69	83
137	81	83	83	93	93	94	87	87	95	89	84	83	74	64	81
147	91	79	81	83	87	85	83	84	88	89	82	79	72	59	78
157	49	46	53	76	79	88	81	87	86	87	82	79	69	55	81

Table 9a – Relative average peak heights of PAHs (n=3) in 1-butanol at varying initial column temperatures

	PAH														
Column T_o (°C)	2	3	4	5	6	7	8	9	10	11	12	13	14	15	16
57	12	13	4	2	2	7	3	4	9	3	7	1	6	4	3
67	1	12	10	1	4	14	5	5	6	4	7	3	4	5	9
77	10	10	3	2	4	11	4	3	5	3	1	0	3	1	2
87	13	8	9	6	3	9	4	5	2	2	2	4	4	3	6
97	2	10	7	4	2	5	10	6	7	3	1	3	1	2	2
107	5	7	6	3	4	6	11	9	6	1	4	2	3	7	2
117	8	3	3	2	2	6	2	2	2	1	2	6	5	2	4
127	5	3	9	3	1	2	1	3	3	3	3	4	5	5	6
137	0	1	6	1	3	7	6	6	5	5	6	3	5	6	4
147	5	7	0	7	1	9	11	8	3	4	2	2	3	4	3
157	7	5	3	1	5	1	8	4	6	8	6	5	4	7	3

Table 9b – %RSD for average peak height of PAHs (n=3) in 1-butanol at varying initial column temperatures

	PAH														
Column T_o (°C)	**2**	**3**	**4**	**5**	**6**	**7**	**8**	**9**	**10**	**11**	**12**	**13**	**14**	**15**	**16**
77	100	100	100	100	100	100	100	100	100	100	100	100	100	100	100
87	102	103	103	100	99	101	100	100	100	101	98	98	96	95	97
97	104	105	105	102	101	99	97	98	99	97	98	96	90	85	94
107	108	109	108	106	103	101	100	98	97	97	94	94	86	78	90
117	96	97	97	103	104	103	101	94	94	95	91	91	82	74	88
127	100	101	102	100	99	97	98	94	93	93	88	89	78	69	86
137	100	100	103	101	102	104	102	93	94	90	87	88	76	66	83
147	84	87	92	100	101	103	104	94	93	92	88	87	75	65	83
157	72	69	75	101	110	108	106	95	95	93	89	87	72	62	82
167	68	64	64	98	101	112	111	100	99	96	89	87	70	59	81

Table 10a – Relative average peak areas of PAHs (n=3) in 1-pentanol at varying initial column Temperatures

	PAH														
Column T_o (°C)	**2**	**3**	**4**	**5**	**6**	**7**	**8**	**9**	**10**	**11**	**12**	**13**	**14**	**15**	**16**
77	2	1	1	1	1	1	2	3	2	1	1	1	1	1	1
87	1	1	1	1	0	1	1	1	0	1	1	1	1	2	0
97	1	0	1	1	1	1	1	0	1	1	0	0	1	1	1
107	1	2	1	0	1	1	1	1	1	1	0	0	1	1	1
117	0	1	1	1	0	2	1	1	1	1	1	0	0	1	0
127	1	0	0	0	0	2	1	1	0	1	1	1	0	3	1
137	1	2	0	1	2	2	0	0	1	1	2	1	2	3	1
147	1	1	1	0	1	2	2	1	1	1	2	0	1	2	0
157	1	2	1	1	0	0	1	1	0	1	1	1	1	2	2
167	1	0	1	1	2	3	2	1	1	2	1	1	2	1	1

Table 10b – %RSD for average peak areas of PAHs (n=3) in 1-pentanol at varying initial column temperatures

	PAH														
Column T_o (°C)	**2**	**3**	**4**	**5**	**6**	**7**	**8**	**9**	**10**	**11**	**12**	**13**	**14**	**15**	**16**
77	100	100	100	100	100	100	100	100	100	100	100	100	100	100	100
87	99	108	95	99	98	110	110	104	94	95	97	99	95	89	101
97	98	114	103	100	99	102	106	95	98	94	92	95	89	81	95
107	100	107	114	108	99	107	102	92	102	95	95	96	88	78	86
117	90	101	99	106	101	115	110	94	95	93	89	91	80	69	86
127	94	108	98	105	98	112	114	86	98	90	88	86	77	68	87
137	92	93	102	101	103	107	112	97	89	88	86	88	73	66	85
147	68	67	80	92	89	98	117	90	94	88	90	86	74	63	86
157	53	60	68	80	81	102	100	89	99	90	94	87	71	57	85
167	53	55	57	75	78	101	111	95	103	94	91	85	68	56	85

Table 11a – Relative average peak heights of PAHs (n=3) in 1-pentanol at varying initial column temperatures

	PAH														
Column T_o (°C)	**2**	**3**	**4**	**5**	**6**	**7**	**8**	**9**	**10**	**11**	**12**	**13**	**14**	**15**	**16**
77	13	2	11	5	3	13	5	10	6	2	4	4	2	2	2
87	10	7	3	1	2	3	7	0	2	1	4	3	3	6	2
97	14	5	9	6	2	7	6	8	5	1	1	2	2	1	1
107	8	14	4	5	3	6	15	5	1	2	2	0	2	1	1
117	11	7	5	4	7	5	10	7	10	2	2	3	2	2	6
127	6	3	11	1	1	2	4	8	3	5	2	1	3	3	4
137	2	2	3	2	4	7	1	1	3	2	2	2	4	6	3
147	4	5	3	5	4	8	4	10	9	3	2	0	5	3	2
157	1	2	1	5	3	9	11	6	9	3	3	2	5	1	3
167	2	5	7	3	2	7	4	4	5	2	4	3	1	1	3

Table 11b – %RSD for average peak height of PAHs (n=3) in 1-pentanol at varying initial column temperatures

	PAH														
Column T_o (°C)	2	3	4	5	6	7	8	9	10	11	12	13	14	15	16
81	100	100	100	100	100	100	100	100	100	100	100	100	100	100	100
91	92	92	95	93	97	97	95	97	95	96	94	96	96	95	95
101	94	94	96	95	96	95	94	96	95	93	95	94	93	92	93
111	104	102	99	96	98	97	97	94	93	94	92	93	90	90	91
121	104	103	98	98	101	99	98	92	91	91	91	90	87	84	88
131	100	97	92	92	94	91	96	94	92	90	89	90	84	82	87
141	102	99	95	95	98	101	96	99	96	92	90	90	83	81	86
151	102	99	96	97	99	104	103	99	96	94	93	92	82	79	84
161	99	97	97	98	100	107	108	103	99	97	96	94	81	77	83
171	100	98	100	95	98	108	108	104	104	96	96	92	78	74	81

Table 12a – Relative average peak areas of PAHs (n=3) in cyclopentanol at varying initial column Temperatures

	PAH														
Column T_o (°C)	2	3	4	5	6	7	8	9	10	11	12	13	14	15	16
81	3	3	3	1	3	1	5	2	2	0	4	1	2	2	2
91	4	3	1	1	1	1	1	1	1	0	1	0	0	0	1
101	1	1	1	1	1	2	2	1	1	0	1	0	1	1	2
111	1	1	1	1	1	2	3	0	0	1	1	1	1	1	1
121	1	2	1	0	0	2	3	1	1	2	0	0	1	1	0
131	0	1	0	1	0	1	2	1	1	1	0	1	1	1	1
141	1	1	1	1	1	1	2	1	1	1	1	0	1	1	1
151	0	1	0	1	1	1	2	1	1	1	0	2	2	2	2
161	1	0	1	1	0	2	2	0	1	0	1	0	1	1	1
171	1	0	0	0	1	2	2	1	2	4	1	2	2	4	2

Table 12b – %RSD for average peak areas of PAHs (n=3) in cyclopentanol at varying initial column temperatures

	PAH														
Column T_o (°C)	2	3	4	5	6	7	8	9	10	11	12	13	14	15	16
81	100	100	100	100	100	100	100	100	100	100	100	100	100	100	100
91	101	90	95	93	98	105	88	94	90	94	92	93	98	97	101
101	101	91	102	98	100	96	96	91	90	94	94	95	91	96	97
111	109	97	91	98	99	103	91	92	92	90	86	93	93	91	95
121	93	87	101	101	104	102	94	90	88	91	87	91	85	86	90
131	101	77	97	96	99	101	103	89	89	88	87	93	83	79	90
141	100	85	91	97	107	105	100	94	93	88	86	90	84	80	88
151	99	88	82	101	106	106	108	98	96	91	89	95	82	75	89
161	86	83	92	97	106	101	112	107	96	98	96	95	83	78	86
171	81	71	80	99	102	103	96	105	94	98	92	93	79	71	82

Table 13a – Relative average peak heights of PAHs (n=3) in cyclopentanol at varying initial column temperatures

	PAH														
Column T_o (°C)	2	3	4	5	6	7	8	9	10	11	12	13	14	15	16
81	10	4	10	3	5	10	3	8	5	4	6	4	4	4	6
91	1	5	8	5	4	6	13	5	12	4	2	1	3	5	3
101	5	2	6	7	5	10	7	4	5	5	4	6	2	3	5
111	4	7	7	4	7	4	11	6	7	3	3	0	3	2	4
121	11	13	5	5	7	12	7	2	3	3	2	1	1	3	2
131	5	3	4	3	4	4	3	8	4	0	3	2	1	2	2
141	5	11	5	5	8	11	3	6	6	1	3	5	2	4	7
151	1	2	6	4	4	7	4	10	6	4	4	2	9	4	8
161	6	2	2	6	4	6	4	3	5	6	1	1	1	2	4
171	8	4	6	2	3	8	13	5	3	2	2	4	5	3	5

Table 13b – %RSD for average peak height of PAHs (n=3) in cyclopentanol at varying initial column temperatures

	PAH														
Column T_o (°C)	2	3	4	5	6	7	8	9	10	11	12	13	14	15	16
98	100	100	100	100	100	100	100	100	100	100	100	100	100	100	100
108	108	108	103	100	99	97	96	95	96	95	97	96	94	92	95
118	115	115	104	102	101	101	99	95	94	94	94	93	89	85	92
128	117	117	107	103	101	102	101	93	92	91	93	91	86	80	89
138	107	106	96	96	95	97	97	96	96	92	92	90	82	76	87
148	100	100	89	97	97	102	100	94	95	92	92	88	79	69	84
158	98	97	87	81	82	103	102	93	93	90	93	88	75	65	82

Table 14a – Relative average peak areas of PAHs (n=3) in 1-hexanol at varying initial column Temperatures

	PAH														
Column T_o (°C)	2	3	4	5	6	7	8	9	10	11	12	13	14	15	16
98	1	2	1	2	3	1	2	2	2	2	2	2	1	2	1
108	1	0	0	1	2	1	2	1	1	1	1	1	2	2	2
118	1	1	0	1	1	0	1	1	2	1	1	2	2	3	1
128	1	1	2	0	1	1	2	1	1	1	1	1	2	3	1
138	1	0	1	1	1	1	2	0	1	1	1	0	1	2	0
148	1	1	2	0	0	3	1	3	0	2	2	1	1	3	2
158	1	1	2	1	1	1	2	0	1	0	0	1	1	2	2

Table 14b – %RSD for average peak areas of PAHs (n=3) in 1-hexanol at varying initial column temperatures

	PAH														
Column T_o (°C)	2	3	4	5	6	7	8	9	10	11	12	13	14	15	16
98	100	100	100	100	100	100	100	100	100	100	100	100	100	100	100
108	112	106	107	105	97	98	89	97	91	96	92	96	97	88	92
118	113	119	109	107	95	100	103	96	88	94	90	89	93	82	83
128	119	109	98	104	99	102	98	96	91	93	87	87	86	72	84
138	109	102	102	104	89	105	102	105	86	93	88	87	82	73	86
148	103	92	91	101	91	101	99	94	92	96	86	83	80	64	79
158	95	76	84	89	83	95	99	90	87	92	88	85	76	59	76

Table 15a – Relative average peak heights of PAHs (n=3) in 1-hexanol at varying initial column temperatures

	PAH														
Column T_o (°C)	2	3	4	5	6	7	8	9	10	11	12	13	14	15	16
98	10	9	1	1	5	5	5	4	4	4	4	3	4	6	1
108	13	0	6	7	3	8	11	4	8	2	4	4	1	5	7
118	12	4	10	5	6	8	1	7	5	4	1	4	4	1	4
128	5	6	7	1	4	4	3	2	3	1	1	5	2	1	3
138	6	7	3	2	8	4	4	3	6	2	1	2	5	5	5
148	2	8	3	5	4	13	6	2	5	4	4	3	3	2	4
158	2	3	4	3	5	9	2	5	7	1	2	2	4	5	6

Table 15b – %RSD for average peak height of PAHs (n=3) in 1-hexanol at varying initial column temperatures

	PAH														
Column T_o (°C)	2	3	4	5	6	7	8	9	10	11	12	13	14	15	16
50	100	100	100	100	100	100	100	100	100	100	100	100	100	100	100
60	96	95	96	97	96	97	97	96	96	97	95	100	98	97	96
70	97	95	96	96	95	97	97	94	95	95	94	98	95	94	95
80	98	97	98	97	97	97	99	95	94	94	98	98	93	93	94
90	98	99	101	101	100	95	99	96	95	96	98	98	93	92	93
100	97	96	98	102	103	98	99	96	96	97	98	98	92	91	92
110	98	97	100	100	99	99	99	95	96	97	95	97	91	90	91
120	101	101	102	100	101	95	97	93	94	96	97	97	90	89	90
130	103	102	105	102	103	98	96	94	95	94	97	96	89	88	90
140	106	104	105	104	105	101	101	96	96	95	95	95	90	88	91
150	108	106	107	102	103	102	102	94	93	95	95	95	87	87	89

Table 16a – Relative average peak areas of PAHs (n=3) in toluene at varying initial column Temperatures

	PAH														
Column T_o (°C)	2	3	4	5	6	7	8	9	10	11	12	13	14	15	16
50	5	5	3	1	1	4	3	2	2	3	2	5	1	0	2
60	1	1	1	0	1	2	1	1	0	1	2	1	1	1	1
70	0	2	1	1	0	1	2	1	0	1	1	1	0	0	1
80	2	0	2	0	0	3	1	0	2	2	1	1	1	0	0
90	1	1	0	1	1	1	0	1	1	1	1	0	0	0	0
100	1	1	0	1	1	2	2	1	0	1	0	0	1	0	1
110	1	0	1	2	1	2	2	1	2	1	1	0	1	1	1
120	1	1	1	1	1	1	1	0	1	1	1	1	1	1	1
130	0	0	1	1	1	1	1	1	0	0	0	0	1	1	0
140	2	1	1	1	1	2	2	2	1	2	1	1	1	1	1
150	1	1	1	1	1	2	0	1	0	1	1	1	1	1	1

Table 16b – %RSD for average peak areas of PAHs (n=3) in toluene at varying initial column temperatures

	PAH														
Column T_o (°C)	2	3	4	5	6	7	8	9	10	11	12	13	14	15	16
50	100	100	100	100	100	100	100	100	100	100	100	100	100	100	100
60	103	93	87	98	99	102	104	88	98	97	95	96	100	94	97
70	114	88	101	97	100	95	88	98	99	93	93	96	97	93	98
80	113	93	93	95	98	91	92	100	97	94	97	94	95	88	94
90	101	94	110	97	105	89	100	92	91	94	95	94	93	92	96
100	108	99	102	104	106	109	110	93	90	97	96	94	94	87	89
110	108	87	102	104	103	91	87	105	101	97	96	93	91	89	89
120	94	94	109	96	107	89	103	96	97	95	93	94	89	87	91
130	100	86	104	99	106	103	90	93	93	91	93	90	90	85	89
140	97	88	97	100	108	102	98	101	99	96	92	90	90	84	90
150	91	84	80	98	102	105	98	92	96	94	96	93	87	87	88

Table 17a – Relative average peak heights of PAHs (n=3) in toluene at varying initial column temperatures

	PAH														
Column T_o (°C)	2	3	4	5	6	7	8	9	10	11	12	13	14	15	16
50	6	6	8	7	4	11	7	8	7	3	3	5	4	2	4
60	10	10	10	3	2	3	2	11	4	2	4	2	2	3	4
70	2	3	4	4	3	11	9	2	5	4	3	5	4	6	8
80	3	10	12	6	5	11	14	2	3	1	3	1	6	2	2
90	12	11	2	2	3	7	3	3	6	2	4	2	4	5	3
100	4	4	8	4	1	4	7	4	7	2	2	2	2	2	2
110	5	10	12	5	2	9	4	5	2	3	2	3	2	4	6
120	8	3	2	1	1	11	1	3	5	3	3	3	1	1	2
130	3	7	6	3	4	5	8	7	1	1	4	2	4	4	1
140	2	5	3	8	1	17	5	4	7	3	2	4	5	2	3
150	3	1	3	3	0	4	5	2	3	3	2	0	4	3	2

Table 17b – %RSD for average peak height of PAHs (n=3) in toluene at varying initial column temperatures

	PAH														
Column T_o (°C)	2	3	4	5	6	7	8	9	10	11	12	13	14	15	16
65	100	100	100	100	100	100	100	100	100	100	100	100	100	100	100
75	107	106	99	99	98	100	100	97	97	93	94	93	96	96	95
85	109	109	106	102	100	98	99	99	99	93	94	93	93	94	93
95	101	100	95	105	104	96	98	95	97	92	92	91	90	90	90
105	105	104	101	100	99	97	97	95	96	90	91	90	88	89	88
115	109	107	104	102	101	92	98	92	92	88	89	88	86	86	86
125	112	109	107	106	106	99	98	94	93	87	89	89	84	86	86
135	114	111	107	110	109	104	104	97	97	90	89	89	84	87	88
145	112	110	107	109	110	108	107	97	95	91	90	89	84	86	86
155	111	109	107	108	109	110	110	102	100	95	92	91	83	85	84
165	107	102	104	103	105	114	112	106	105	95	92	91	84	85	84

Table 18a – Relative average peak areas of PAHs (n=3) in n-octane at varying initial column Temperatures

	PAH														
Column T_o (°C)	2	3	4	5	6	7	8	9	10	11	12	13	14	15	16
65	1	1	4	3	3	3	2	2	3	4	5	4	2	2	2
75	1	1	1	0	2	1	2	1	0	1	1	1	1	1	1
85	1	0	1	1	1	0	1	1	1	1	1	0	1	1	1
95	0	1	0	1	0	1	1	2	0	1	1	1	1	2	1
105	1	2	1	1	1	2	2	2	1	1	1	1	0	0	0
115	0	0	2	1	1	2	2	0	0	0	1	1	1	1	1
125	1	1	2	1	2	2	2	1	2	2	0	1	1	1	1
135	1	1	1	1	0	2	1	1	1	1	2	1	1	1	1
145	1	1	0	1	1	3	1	1	0	0	2	1	1	1	2
155	0	1	1	0	0	1	2	0	0	1	1	1	1	1	2
165	0	1	1	0	0	1	3	1	1	2	1	1	1	1	1

Table 18b – %RSD for average peak areas of PAHs (n=3) in n-octane at varying initial column temperatures

	PAH														
Column T_o (°C)	2	3	4	5	6	7	8	9	10	11	12	13	14	15	16
65	100	100	100	100	100	100	100	100	100	100	100	100	100	100	100
75	104	88	96	106	99	99	121	87	93	97	93	91	93	96	96
85	98	106	97	106	104	82	117	85	90	94	91	91	93	95	92
95	94	82	89	103	105	84	119	80	86	92	88	89	92	91	88
105	77	100	92	102	107	99	98	92	97	92	92	90	86	93	91
115	89	97	99	103	103	90	104	87	89	91	85	88	84	90	84
125	89	86	101	112	112	99	116	83	84	88	86	85	83	86	87
135	89	95	101	117	115	100	123	90	90	90	87	88	85	88	88
145	88	87	91	111	116	94	126	89	89	92	87	89	82	91	85
155	69	76	87	102	109	105	123	96	95	93	90	93	82	87	86
165	64	58	79	97	97	106	109	95	99	92	90	92	83	88	84

Table 19a – Relative average peak heights of PAHs (n=3) in n-octane at varying initial column temperatures

	PAH														
Column T_o (°C)	2	3	4	5	6	7	8	9	10	11	12	13	14	15	16
65	2	1	8	3	4	3	3	1	6	6	6	5	11	3	6
75	3	10	11	2	8	7	5	5	8	3	5	4	5	1	9
85	2	0	5	4	3	1	2	8	6	3	1	1	3	3	9
95	2	11	7	5	6	5	1	3	4	4	5	3	3	4	2
105	3	2	2	3	4	5	4	4	4	3	4	2	3	2	4
115	11	2	12	7	6	11	11	5	3	8	3	1	4	1	6
125	10	12	5	6	5	5	6	10	6	1	3	4	3	1	8
135	10	4	8	1	2	10	3	4	6	5	5	5	5	0	6
145	2	6	7	2	3	6	3	6	8	2	2	4	0	4	1
155	3	4	4	1	2	4	12	7	11	3	1	1	1	4	3
165	2	1	2	3	4	7	7	8	7	3	2	0	4	2	5

Table 19b – RSD for average peak height of PAHs (n=3) in n-octane at varying initial column temperatures

For all of the solvents, it was found that the lowest initial column temperature yielded the largest peak areas for the late-eluting peaks. The same conclusion was drawn regarding peak heights. As a result, the lowest initial column temperature for each solvent was chosen as the optimum initial column temperature.

Toluene and n-octane were found to be the most forgiving solvents, in terms of peak areas (of late-eluting PAHs), for the choice of initial column temperature. With these solvents, the smallest changes in peak areas, at all initial column temperatures, were observed. n-Octane was, however, not as forgiving in terms of peak heights as toluene.

For early-eluting peaks, cyclopentanol, n-octane, 1-butanol, and toluene were found to yield the most consistent peak areas with changing initial column temperatures. But, of these solvents, toluene again showed the smallest changes. n-Octane and 1-butanol showed promising results in terms of peak areas, but the peak heights obtained using these solvents were especially poor for PAHs 2-4.

Toluene was found to be the most forgiving solvent overall as it displayed the smallest changes in peak areas and peak heights, for all PAHs, throughout the entire initial column temperature range.

Of all the solvents, 1-pentanol and 1-hexanol were found to be least forgiving in terms of peak areas and peak heights. The development of an optimized temperature program is most essential if these solvents are chosen for PAH analysis by a gas chromatographic technique.

The reproducibility for three replicate injections of all PAHs, at all initial column temperatures tested, is displayed for each solvent in Tables 1b-12b. In all solvents, and at all initial column temperatures, the reproducibility for peak areas is excellent. The relative standard deviation in peak areas are less than or equal to 5%. For peak heights, the reproducibility is not as good. However, as discussed earlier, with syringe injection, relative errors of up to 10% are not uncommon. Although some PAHs, especially the early-eluting ones, exhibit relative standard deviations over 10%, most are within the 10%

range. Since sampling speed is so critical for early-eluting peak heights, small variations in injection speed (resultant of the autosampler) may cause this discrepancy.

Solvent trapping is an important mechanism for increasing the response of PAHs. It appears, based on this work, to be more significant than cold trapping effects. Solvent trapping is described well by Grob [47]. At temperatures well below the boiling point of the solvent, the solvent is trapped at the head of the column after injection. The solvent condenses as it reaches the cool column and forms a layer over the stationary phase called the flooded zone. The flooded zone will continue to grow as long as the carrier gas entering the column is saturated with solvent vapour. As the analytes reach the column, from the injector, they are trapped by the condensed solvent. The condensed solvent acts as a temporary stationary phase. Once all of the solvent and solutes from the injector have been transferred, the carrier gas is no longer saturated with solvent vapour. As the column is heated, the solvent begins to evaporate from the end closest to the injector, and the carrier gas carries the evaporated solvent down the column. Analytes move forward in the flooded zone as it shortens and by the time chromatography begins, they have been focused to a condensed band.

Figures 23a and 23b – 28a and 28b below show the peak areas and peak heights of selected PAHs, and how they are affected by changing initial column temperatures. These figures include: acenaphthylene (Acy), benzo[a]pyrene (BaP), and dibenz[a,h]anthracene (DahA). These PAHs were chosen, as BaP and DahA are two of the most carcinogenic PAHs (of the 16 US EPA priority PAHs) and therefore must be detected at very low levels. These two PAHs are also high-boiling, whereas Acy is low-boiling (relative to other PAHs). This way, the effect of initial column temperature on early and late-eluting PAHs can be evaluated.

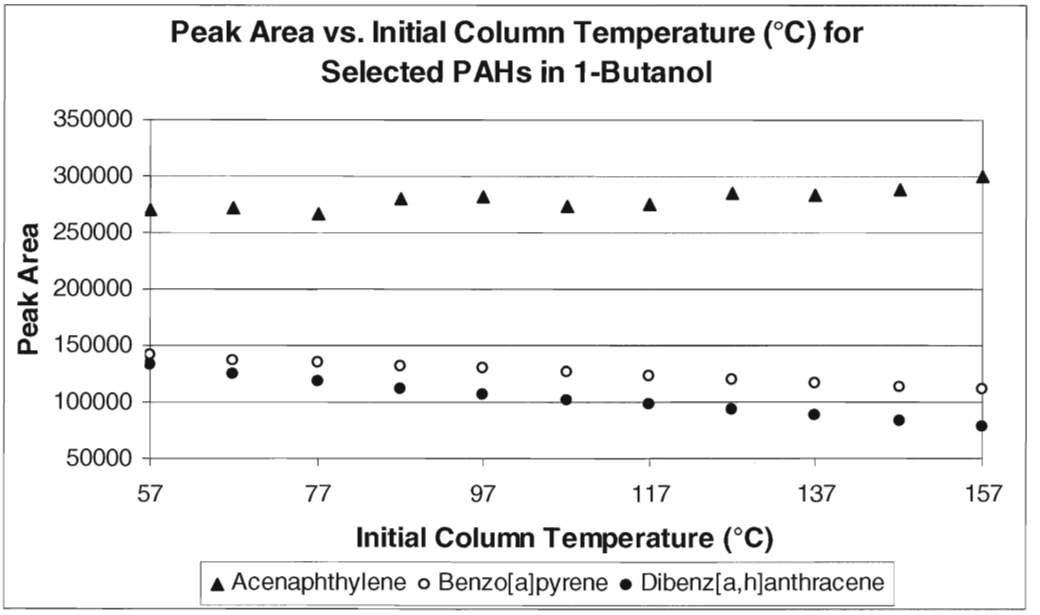

Figure 23a – The effect of initial column temperature on peak area of selected PAHs in 1-butanol

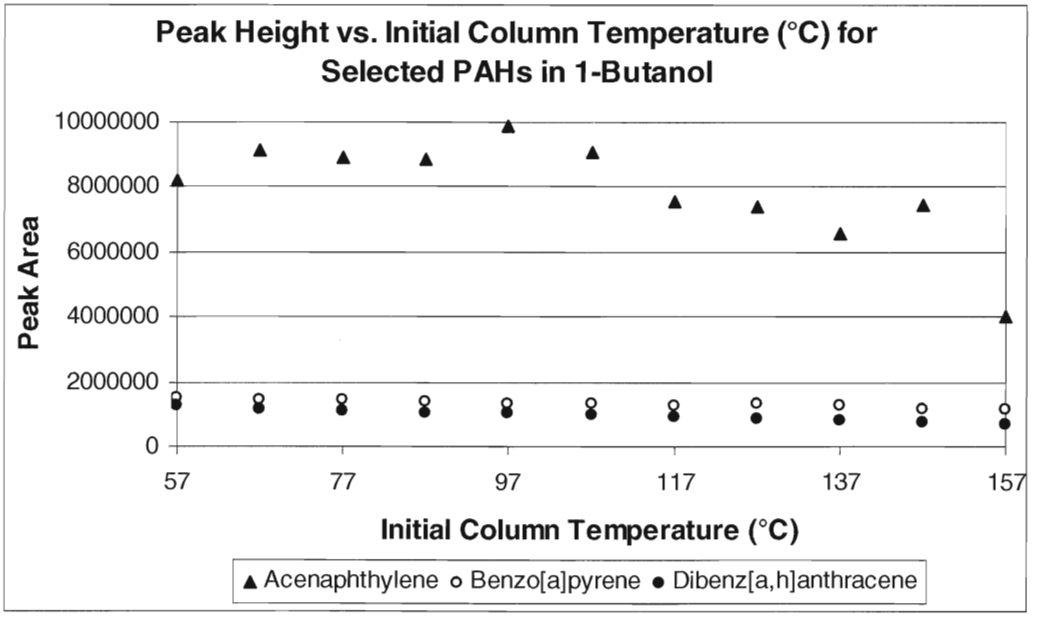

Figure 23b – The effect of initial column temperature on peak height of selected PAHs in 1-butanol

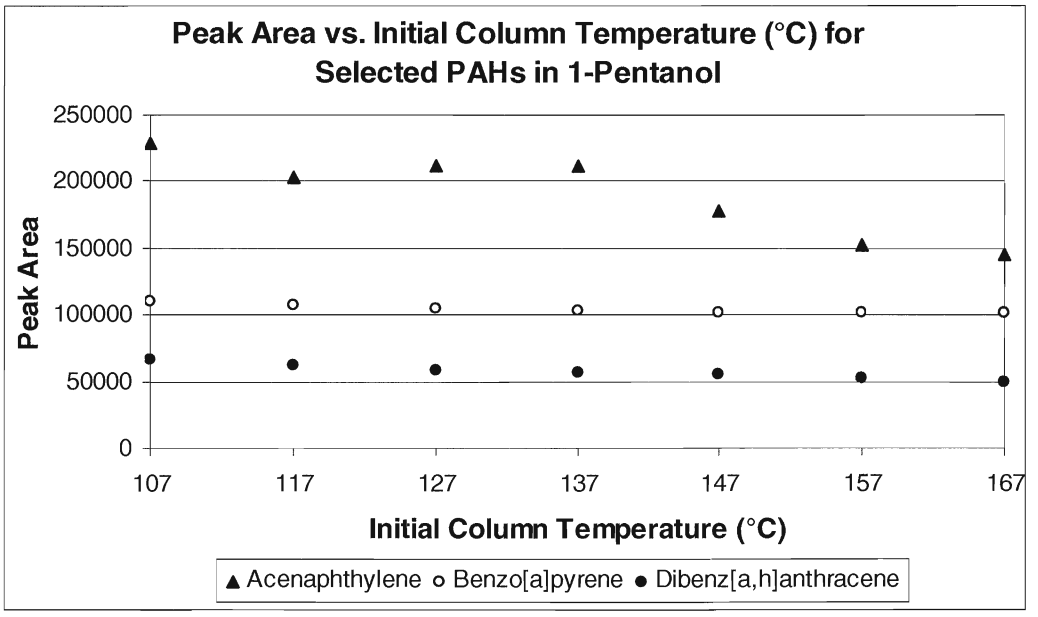

Figure 24a – The effect of initial column temperature on peak area of selected PAHs in 1-pentanol

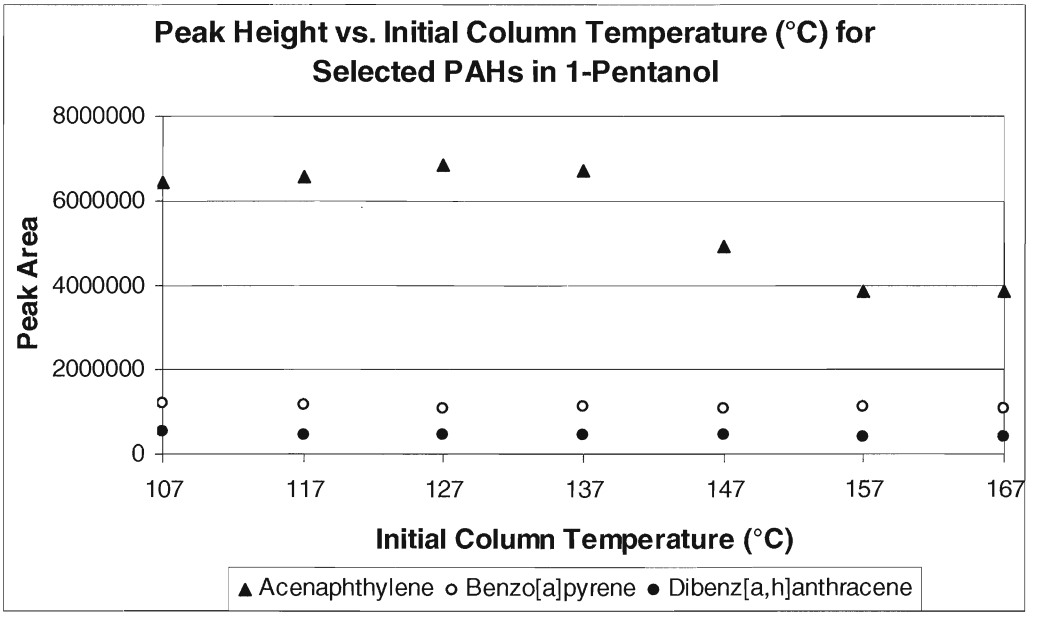

Figure 24b – The effect of initial column temperature on peak height of selected PAHs in 1-pentanol

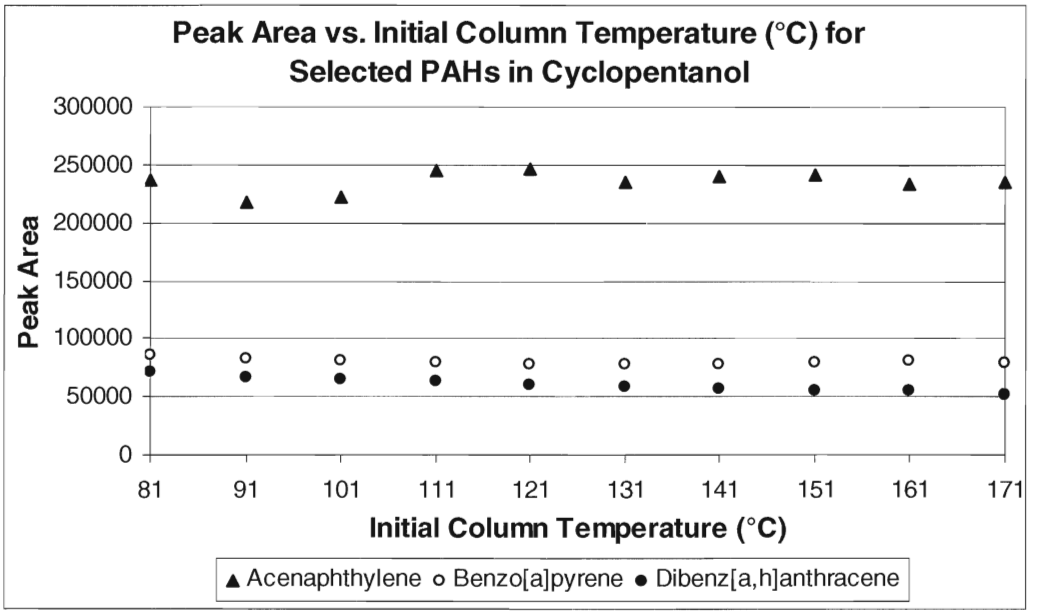

Figure 25a – The effect of initial column temperature on peak area of selected PAHs in cyclopentanol

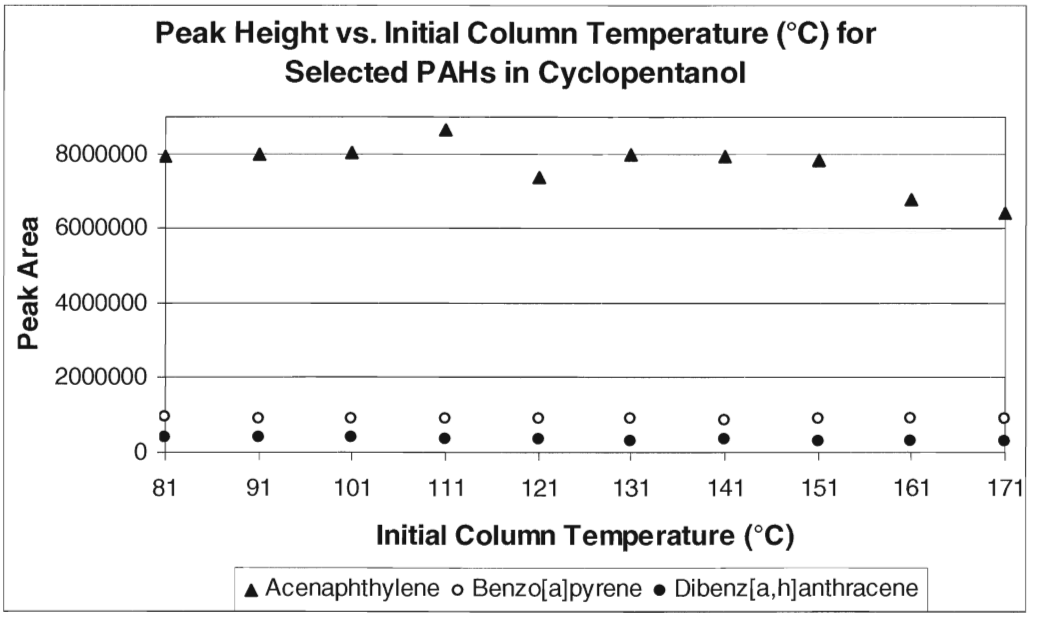

Figure 25b – The effect of initial column temperature on peak height of selected PAHs in cyclopentanol

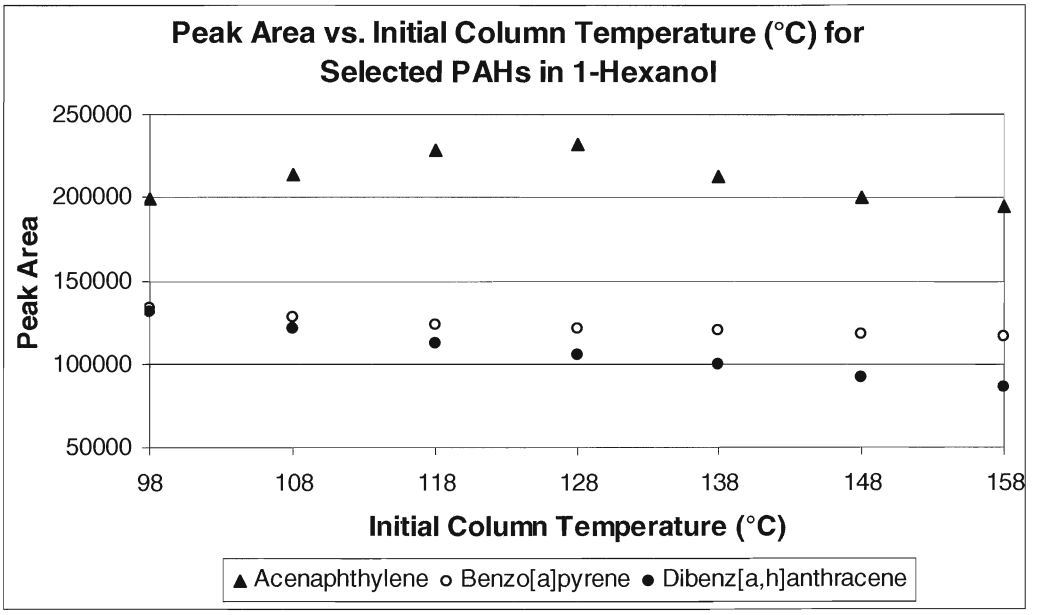

Figure 26a – The effect of initial column temperature on peak area of selected PAHs in 1-hexanol

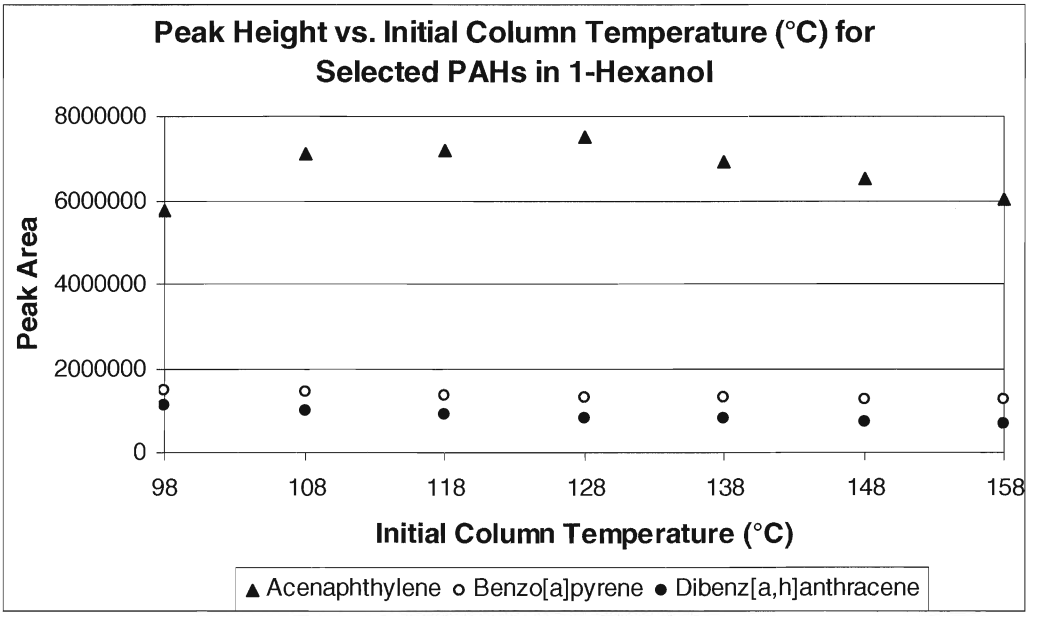

Figure 26b – The effect of initial column temperature on peak height of selected PAHs in 1-hexanol

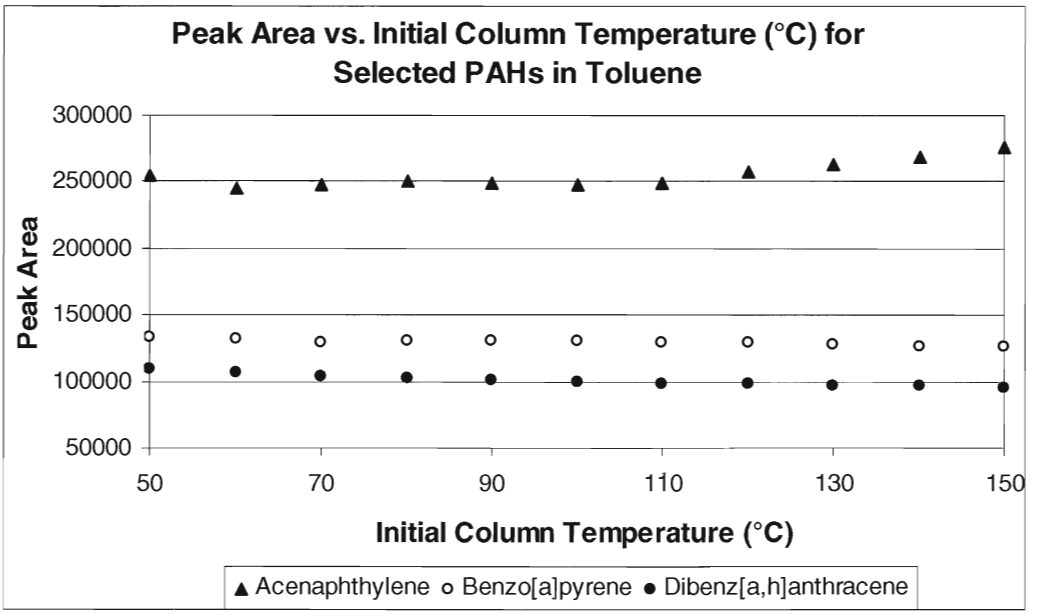

Figure 27a – The effect of initial column temperature on peak area of selected PAHs in toluene

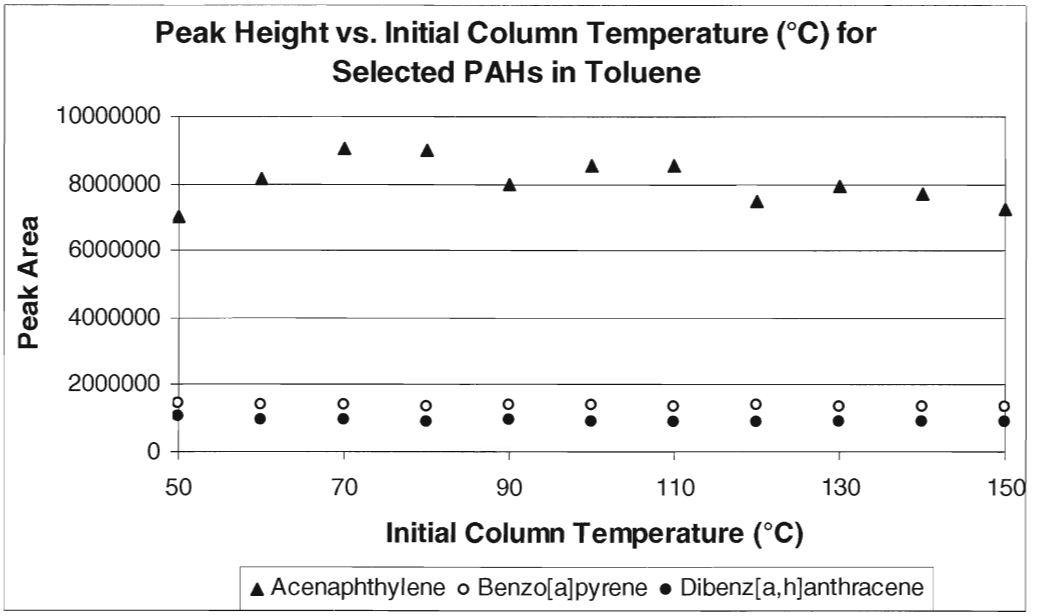

Figure 27b – The effect of initial column temperature on peak height of selected PAHs in toluene

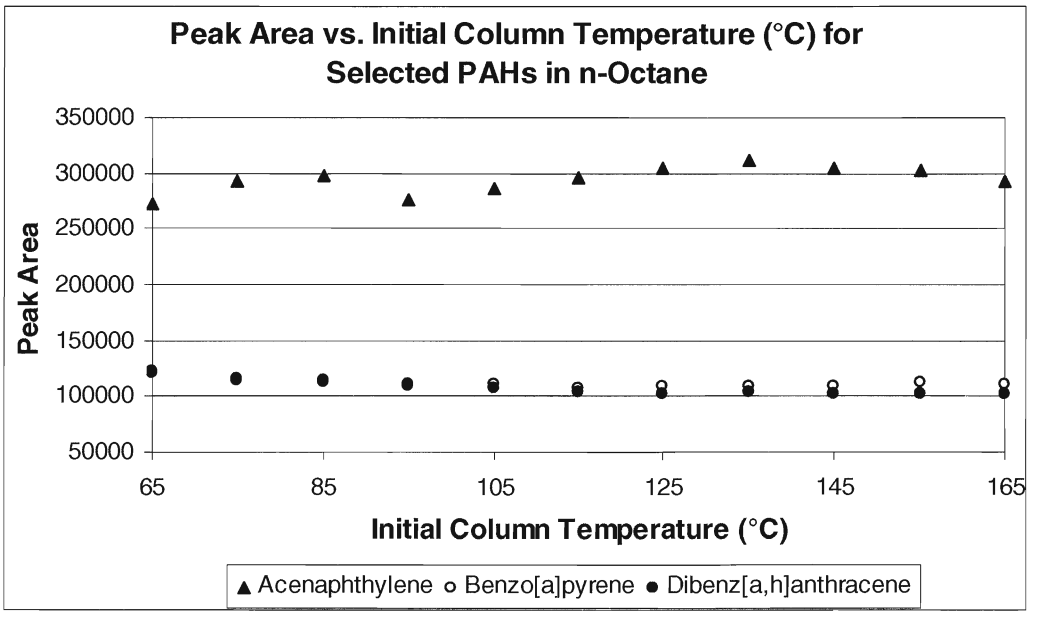

Figure 28a – The effect of initial column temperature on peak area of selected PAHs in n-octane

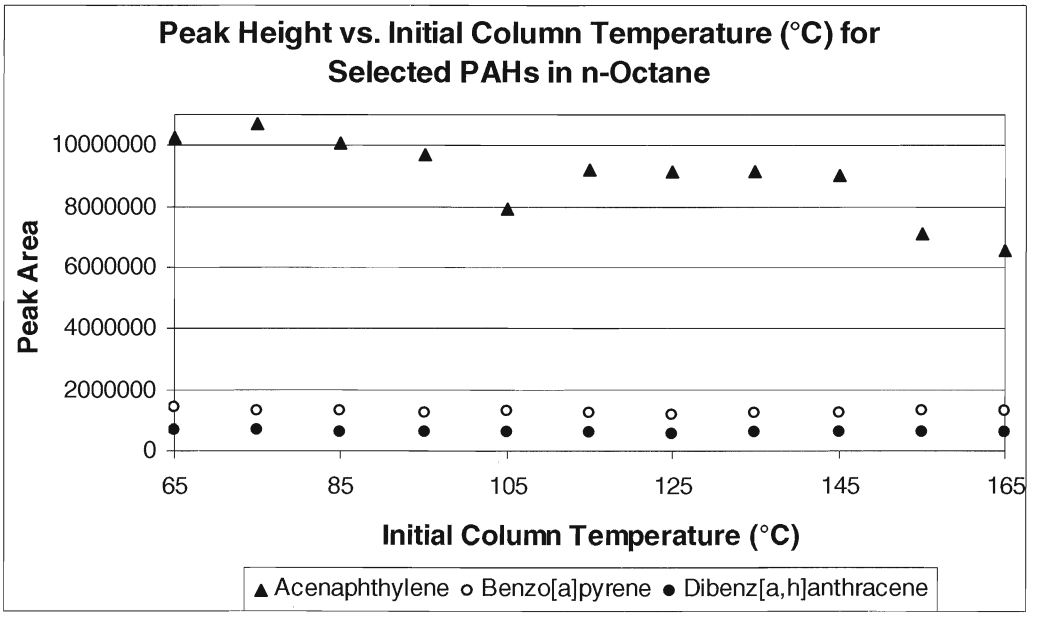

Figure 28b – The effect of initial column temperature on peak height of selected PAHs in n-octane

From these figures it can be seen that BaP and DahA, and therefore late-eluting PAHs, show a consistent decrease in peak area and height with increasing initial column temperature. The decline in response for DahA is usually more significant than for BaP. Acenaphthylene, however, does not behave consistently between solvents. The response of Acy: decreases (with increasing initial column temperature) in pentanol, increases in butanol, and remains steady over the entire initial column temperature range in cyclopentanol.

Effect on Resolution

To determine the effect of initial column temperature on resolution of closely-eluting PAHs, a graph of resolution of anthracene (Ant)/phenanthrene (Phen) and benzo[b]fluoranthene (BbF)/benzo[k]fluoranthene (BkF) vs. initial column temperature was plotted – see Figure 29 below.

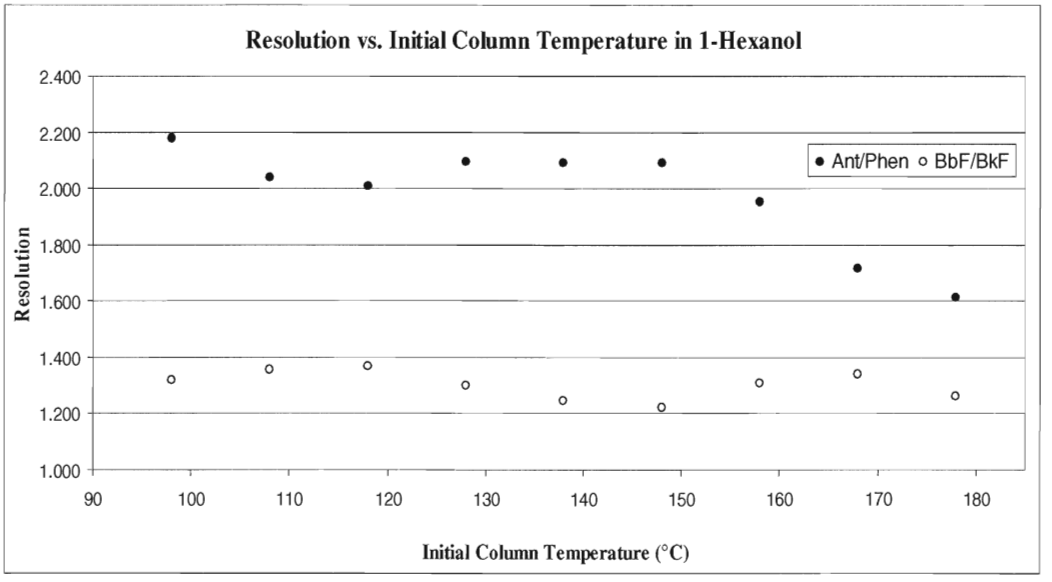

Figure 29 – Effect of initial column temperature on the resolution of PAHs Ant/Phen and BbF/BkF in 1-hexanol

From this figure, it can be seen that the resolution Ant/Phen is temperature dependent. The resolution of this PAH pair decreases with increasing initial column temperature. This decrease in resolution of Ant/Phen with increasing

column temperature can be seen in each of the solvents tested (see Figures 30-35 below). The resolution of BbF/BkF, on the other hand, does not appear to be affected by changing initial column temperature.

Effect on Peak Shape (Symmetry)

As previously mentioned, authors have shown that the initial column temperature can have a significant impact on peak symmetry [90]. In order to explore this effect, PAHs Ant/Phen were shown at all initial column temperatures tested, in each solvent. Anthracene and phenanthrene were chosen because they are early-eluting PAHs, and previous authors have shown that they are susceptible to fronting at low initial column temperatures and tailing at high initial column temperatures [90]. Also, these peaks usually were not affected by peak splitting at high initial column temperatures.

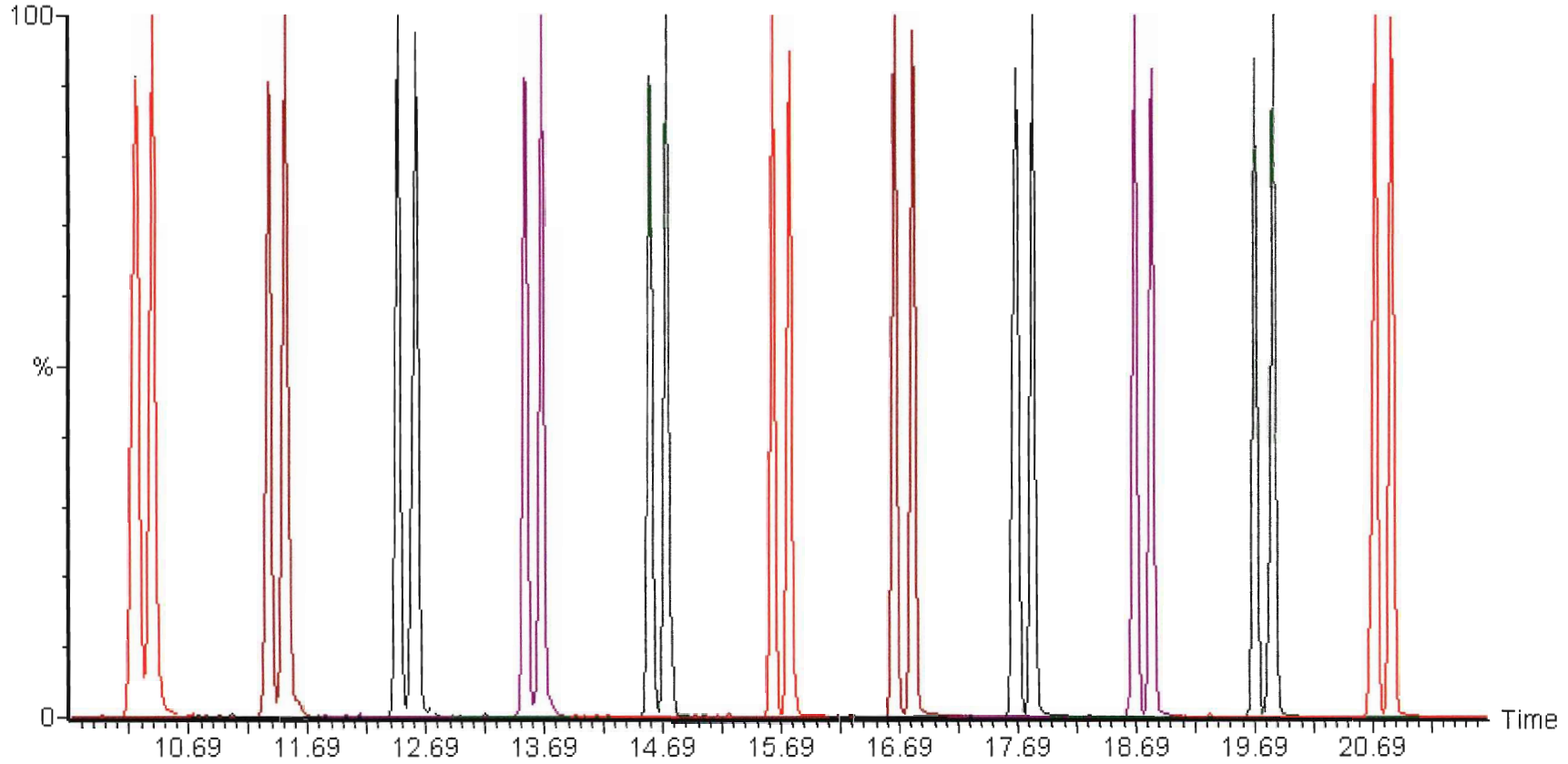

Figure 30 – Effect of initial column temperature on symmetry of Ant/Phen in 1-butanol (T_0=57°C-157°C from right to left)

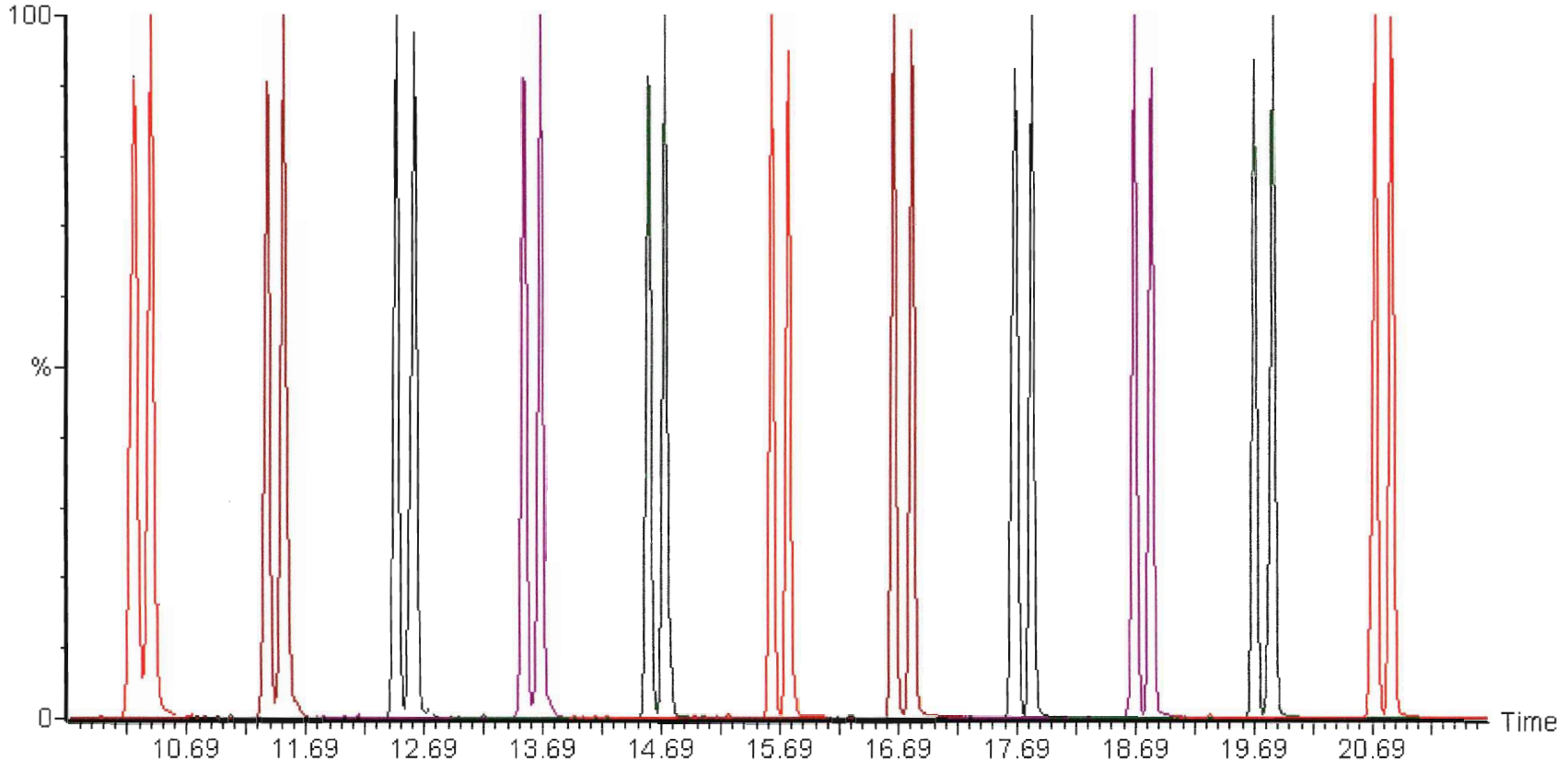

Figure 31 – Effect of initial column temperature on symmetry of Ant/Phen in 1-pentanol (T_0=77°C-177°C from right to left)

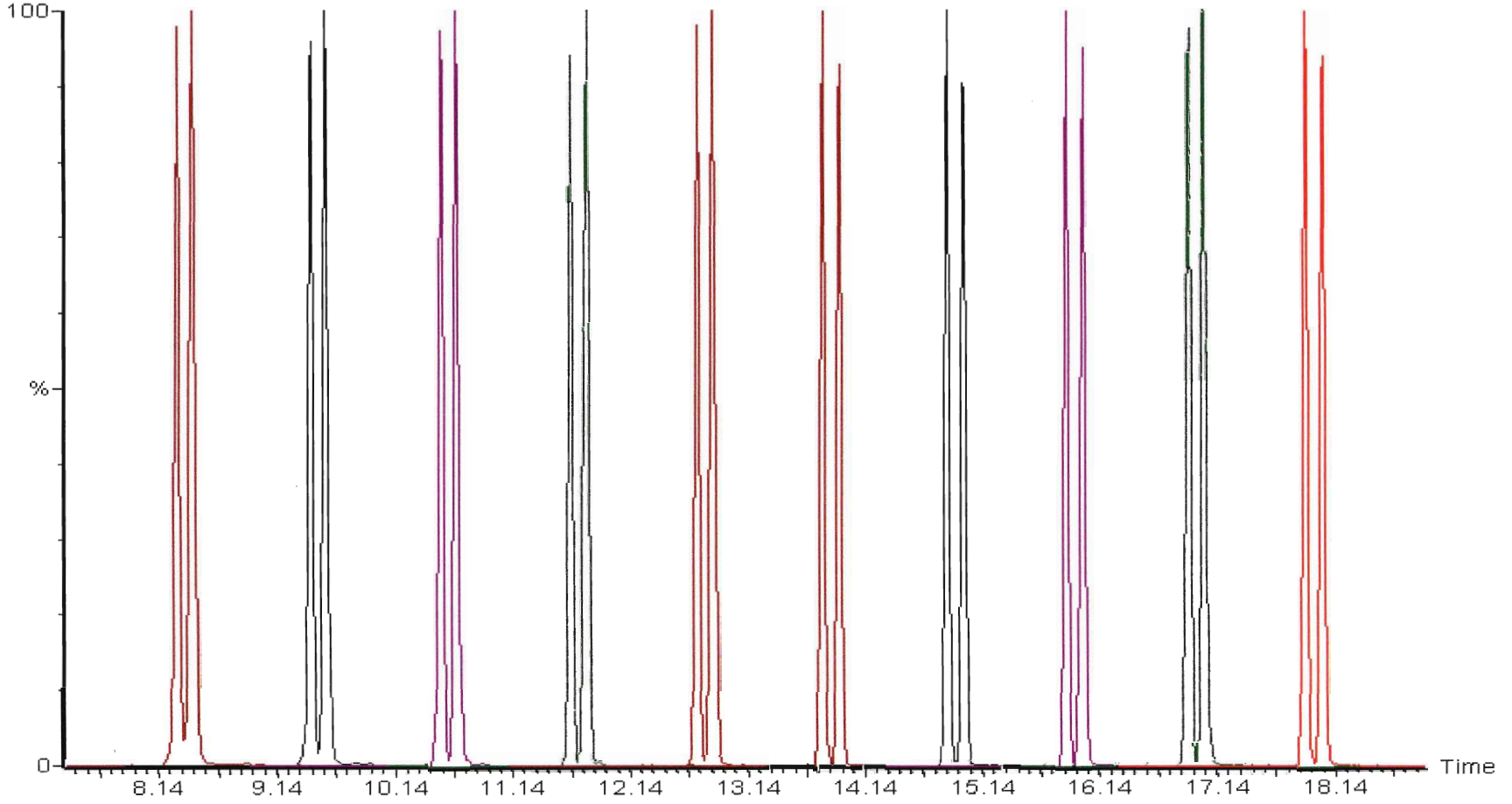

Figure 32 – Effect of initial column temperature on symmetry of Ant/Phen in cyclopentanol (T_0=81°C-171°C from right to left)

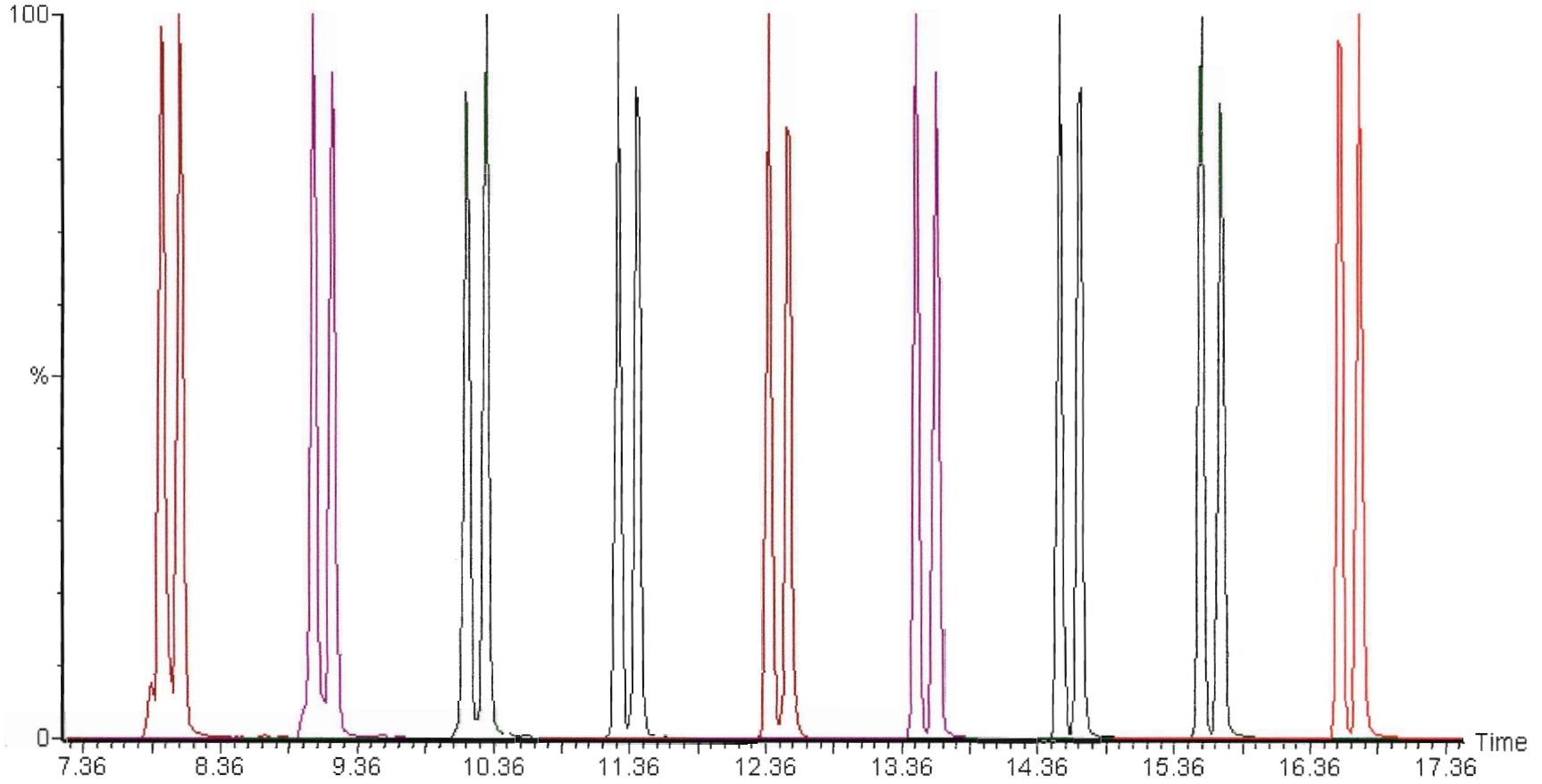

Figure 33 – Effect of initial column temperature on symmetry of Ant/Phen in 1-hexanol (T_0=98°C-178°C from right to left)

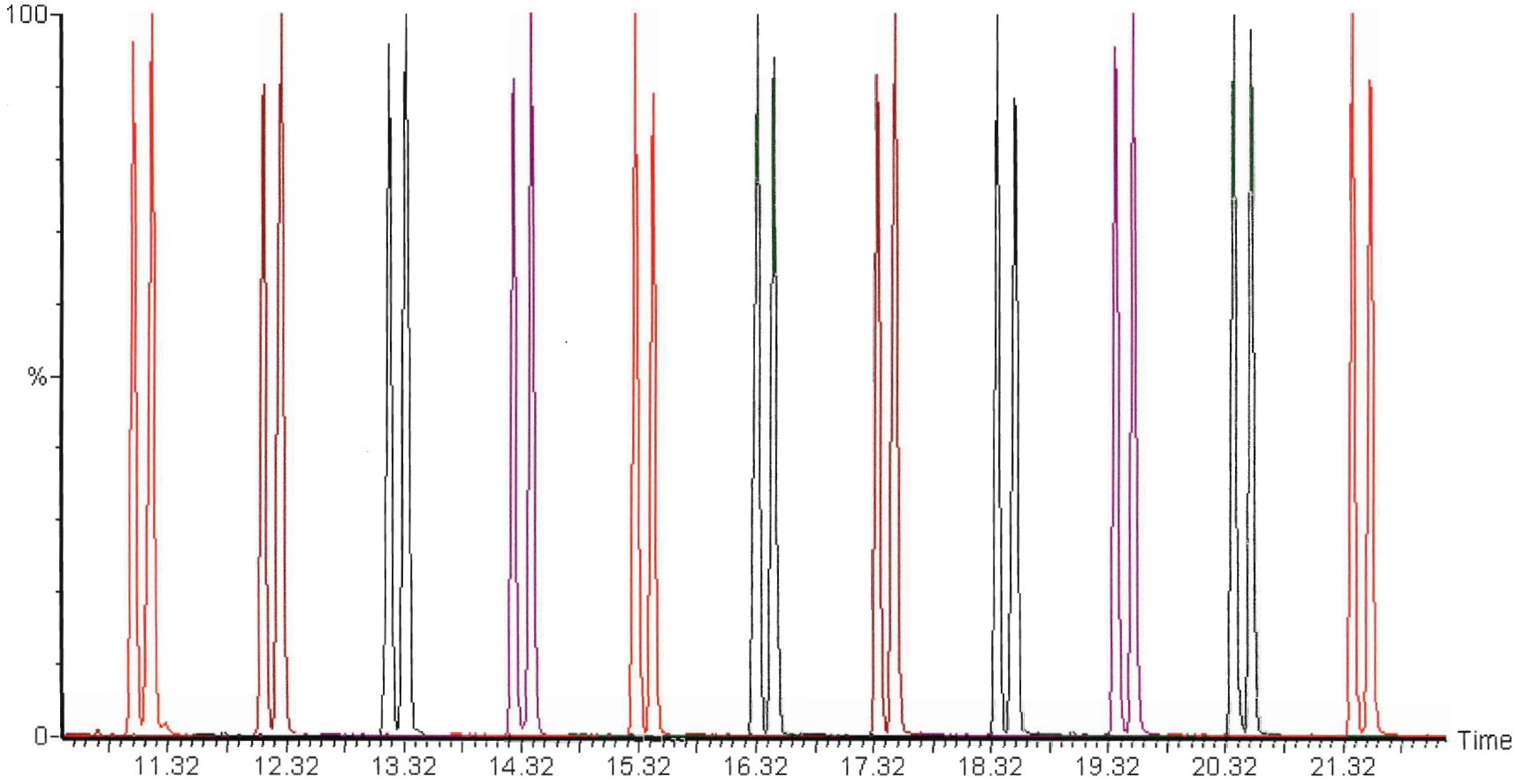

Figure 34 – Effect of initial column temperature on symmetry of Ant/Phen in toluene (T_0=50°C-150°C from right to left)

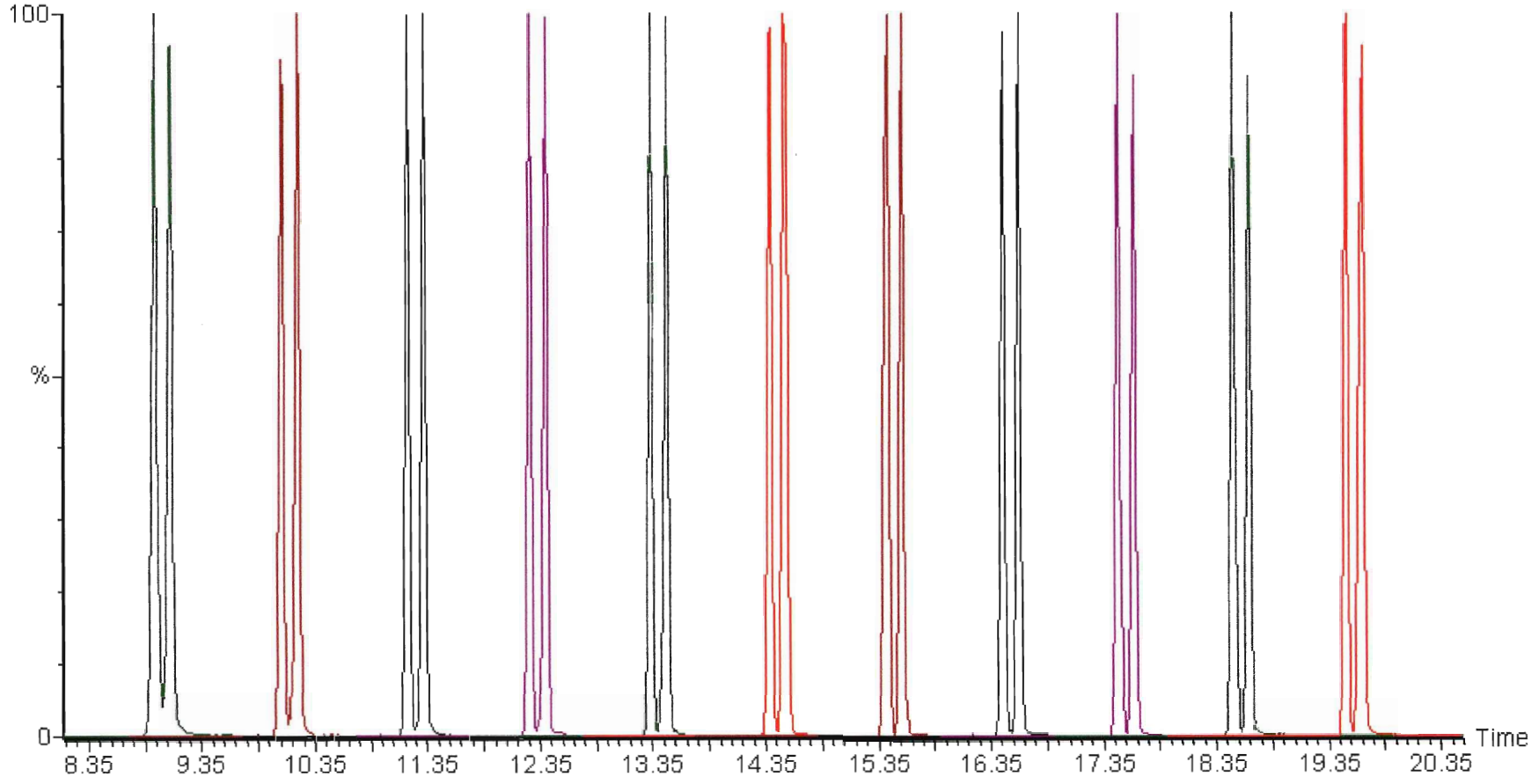

Figure 35 – Effect of initial column temperature on symmetry of Ant/Phen in n-octane (T_0=65°C-165°C from right to left)

Brindle *et al.* [90] explored the effects of initial column temperatures on the 15 US EPA priority PAHs in toluene using a DB-5 (5% phenyl methyl polysiloxane) column. Initial column temperatures of 100-140°C were tested. The authors reported that the optimum initial column temperature for PAHs in toluene was 120°C [90]. It was shown that at initial column temperatures below this value, peaks would exhibit fronting and that at initial column temperatures above 120°C, peak tailing would result. The fronting and tailing was shown to intensify the further the initial column temperature was from the optimum value [90]. In this work, there is no evidence of peak fronting at any initial column temperature, and in any of the solvents tested.

Peak tailing is not observed in cyclopentanol, 1-hexanol, or toluene. Slight peak tailing is observed in 1-hexanol, but it is present throughout the entire temperature range tested and does not intensify with increasing initial column temperatures. This tailing appears unlikely to be caused by the same mechanism as the tailing observed by Brindle *et al.* [90]. Peak tailing that is evident at all initial column temperatures, and that which does not intensify with increasing initial column temperature, may be resultant of the guard column.

Slight peak tailing is observed in 1-butanol, 1-pentanol, and n-octane. In all three solvents, the tailing is minor, and only occurs at high initial column temperatures that are over 70°C above the optimum initial column temperature.

When the initial column temperature reached and surpassed the boiling point of the solvent, peak fronting, then splitting was observed for PAHs 2-5 in all solvents, except toluene. Peak fronting was observed at high initial column temperatures, but splitting was not observed within the initial column temperature range tested.

As an example of peak splitting, consider n-octane (see Figures 36a and 36b). At an initial column temperature of 115°C (10°C below the boiling point of the solvent), symmetric peaks are observed for PAHs 2-5. When the initial column temperature reaches the boiling point of the solvent, 125°C, these same PAHs begin to front (very slightly). Fronting intensifies as the initial column

temperature increases further, and when the initial column temperature reaches 145°C, peak splitting is observed. This peak splitting phenomenon is not expected to be caused by the same mechanism responsible for the fronting and tailing observed at varying initial column temperatures by Brindle *et al.*, as the fronting in this case is observed at high initial column temperatures. Brindle *et al.* observed peak fronting at low initial column temperatures (below the boiling point of the solvent) [90].

1-pentanol and 1-hexanol were the solvents that made the PAHs most susceptible to splitting. In these solvents, as the initial column temperature increased beyond that at which the splitting occurred, tailing and splitting (on the tailing side) of the peak occurred as well. For a more extreme example of peak splitting at high initial column temperatures, see Figure 37. Again, this splitting only occurs at temperatures well above the optimum initial column temperature.

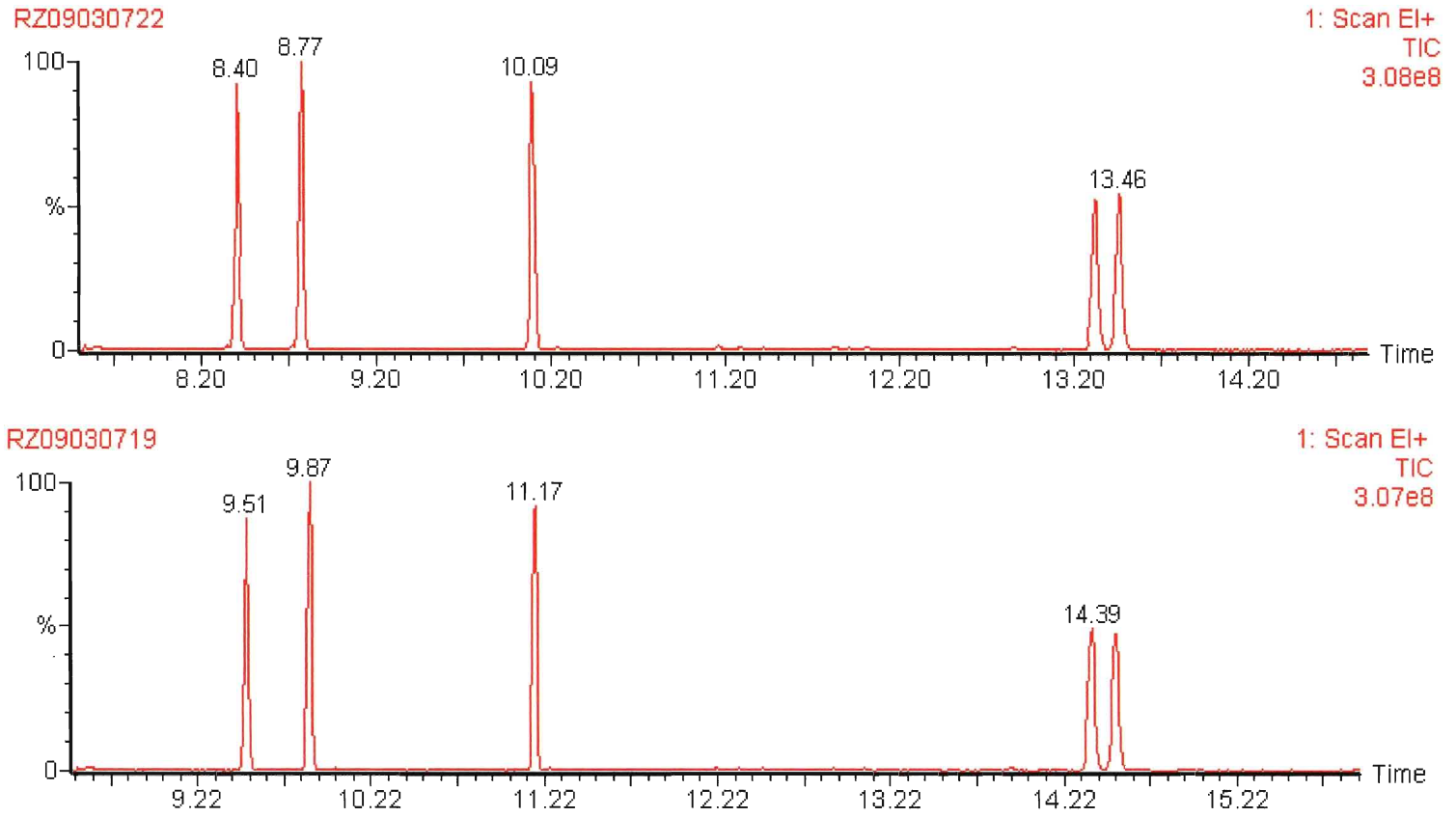

Figure 36a – Effect of initial column temperature on peak splitting in n-octane (from bottom T_0=115°C, 125°C)

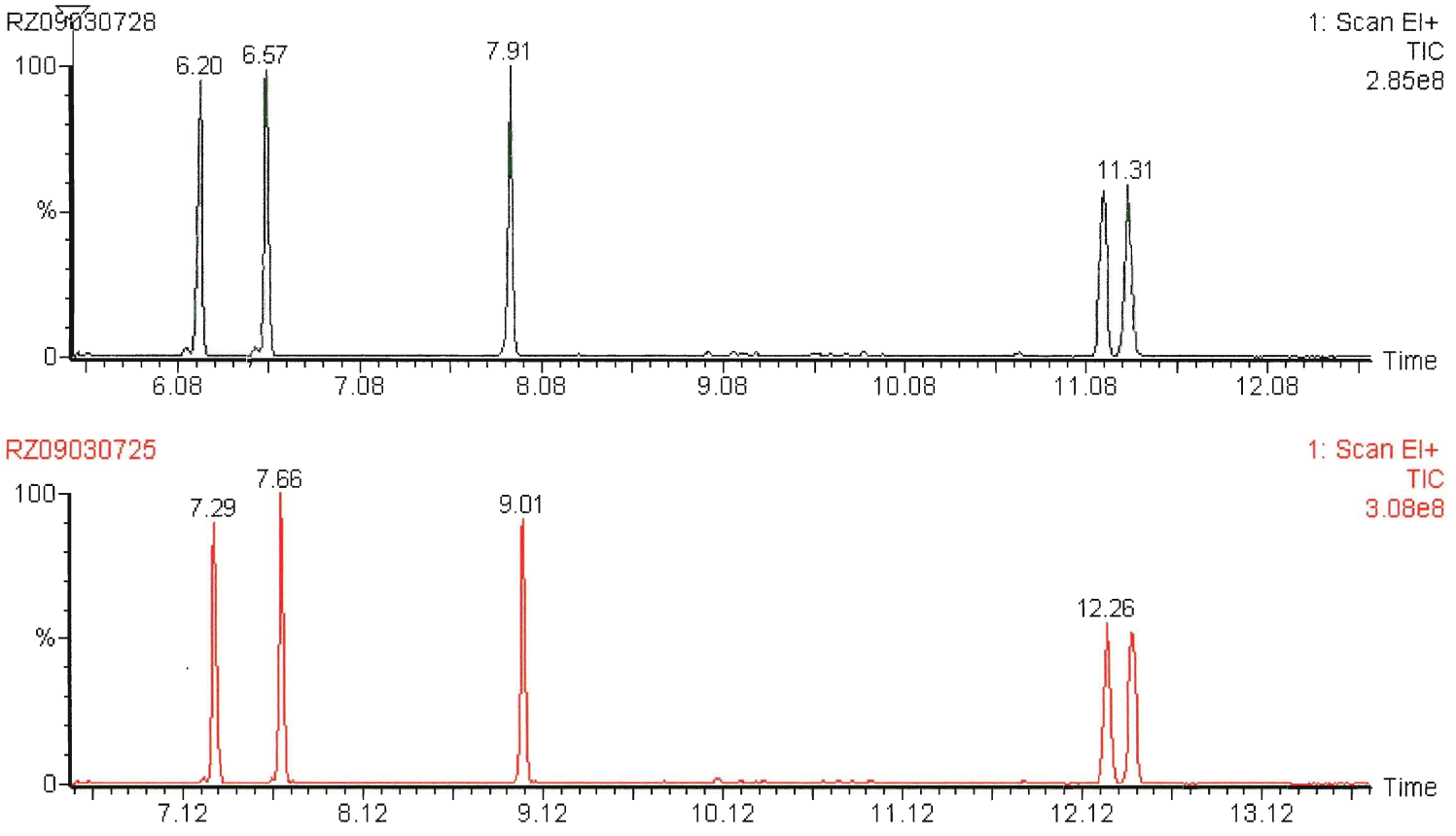

Figure 36b – Effect of initial column temperature on peak splitting in n-octane (from bottom: T_0=135°C, 145°C)

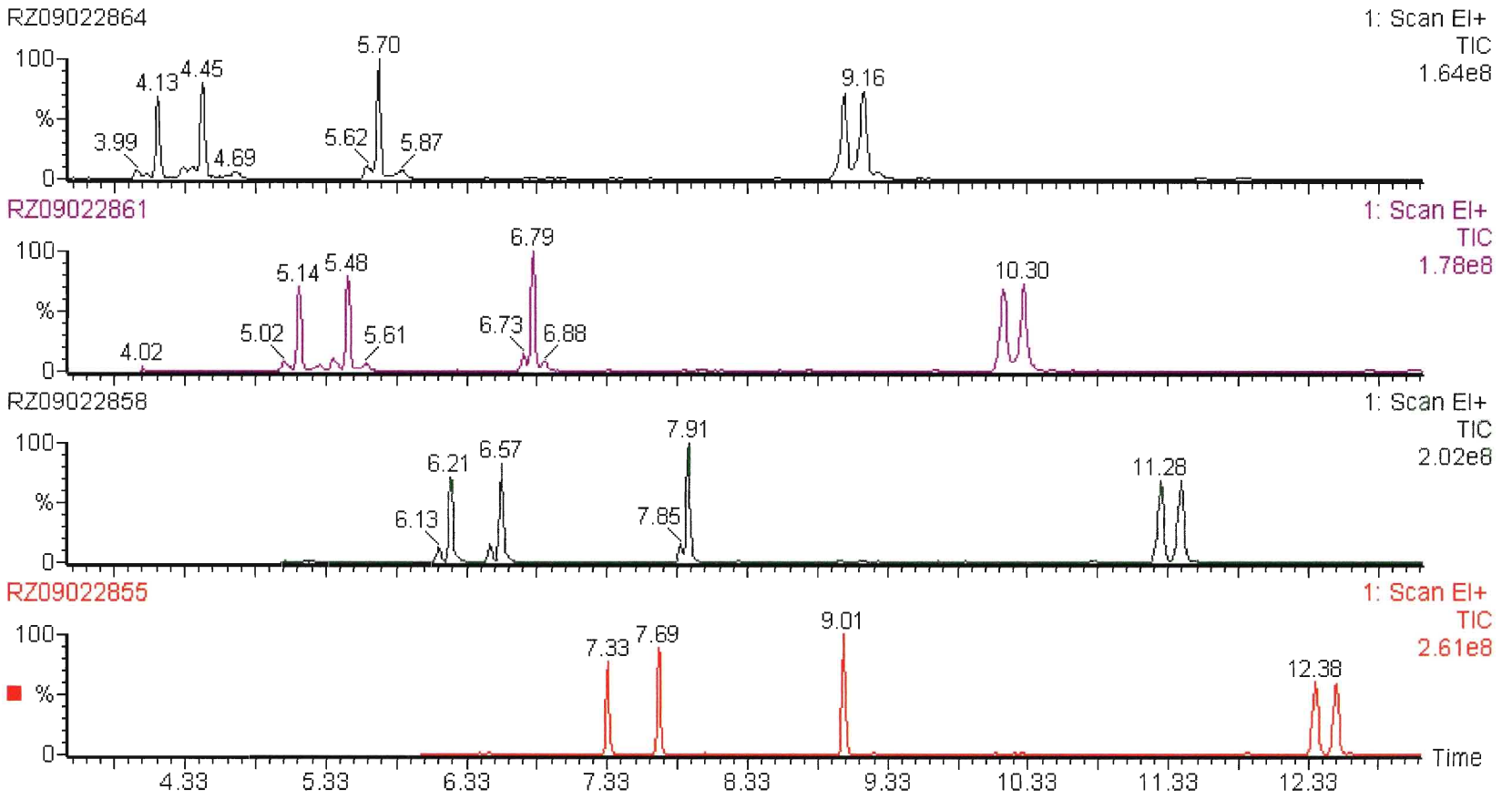

Figure 37 – Effect of initial column temperature on peak splitting in 1-pentanol (from bottom: T_0=137°C, 147°C, 157°C, 167°C)

Injector Liner

Effect on Response

The effect of a dirty injector liner on PAH response was tested. A PAH standard in toluene was injected into an injector liner that had been exposed to over 100 injections (of 4ppm PAH solutions). The peak areas and heights of the 15 PAHs for 3 replicate injections were tabulated and the average values were plotted against the corresponding PAH number (see Table 1). For comparison, the injector liner was cleaned, and then the same PAH standard was rerun and the results plotted in the same way. Figures 38a and 38b show a comparison of the results obtained using a clean and dirty injector liner.

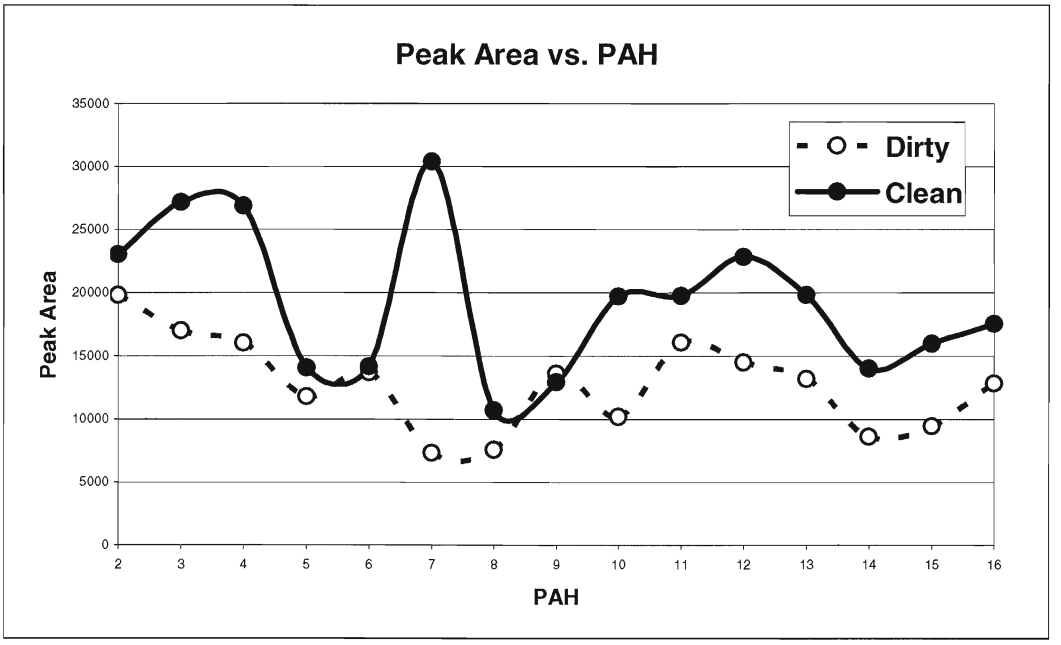

Figure 38a – The peak area of PAHs determined with a dirty injector liner vs. the peak area of PAHs determined with a freshly cleaned liner

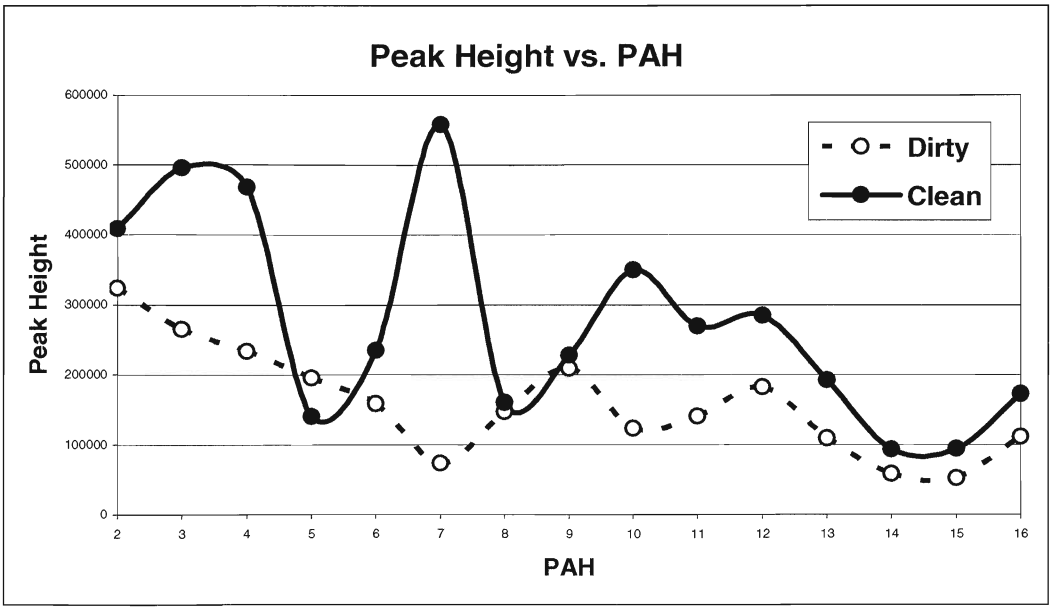

Figure 38b – The peak height of PAHs determined with a dirty injector liner vs. the peak height of PAHs determined with a freshly cleaned liner

It has been found that the cleanliness of the injector liner has a significant impact on the response of PAHs. It can be seen in Figures 38a and 38b that a dirty liner results in decreased responses of all PAHs in terms of peak area and peak height. This effect is more significant for the early-eluting PAHs than the late-eluting PAHs. For unknown reasons the response of fluorene, PAH 7, appears to be most significantly impacted by the dirty liner.

Effect of Solvent on Chromatographic Behaviour

Response

High-Boiling Alcohols

In order to determine the effect of the solvent on chromatographic response, the peak areas and peak heights of 15 US EPA priority PAHs were compared at the optimum initial column temperature in each of the high-boiling alcohols. The results are tabulated as the relative average peak areas and heights for the 15 PAHs in the high-boiling alcohol solvents (see Tables

20a and 20b). See Figure 39 for a graphical comparison of the peak areas of the late-eluting PAHs in the high-boiling alcohols.

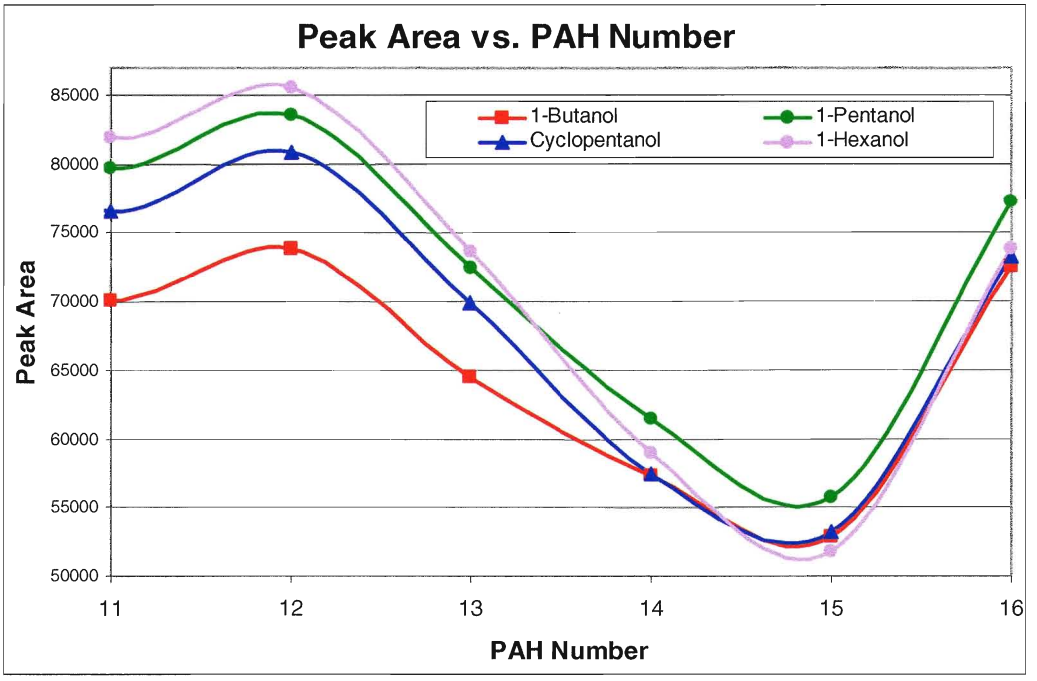

Figure 39 – Comparison of peak areas of PAHs 11-16 in high-boiling alcohols

			PAH													
Solvent	**bp (°C)**	**T_o Opt (°C)**	**2**	**3**	**4**	**5**	**6**	**7**	**8**	**9**	**10**	**11**	**12**	**13**	**14**	**15**	**16**
1-butanol	117	57	97	96	86	82	82	82	82	84	83	86	86	88	97	102	98
1-pentanol	137	77	119	116	102	97	95	94	96	97	95	97	98	98	104	107	105
cyclopentanol	141	81	122	116	100	94	94	89	92	94	93	93	95	95	98	103	99
1-hexanol	158	98	100	100	100	100	100	100	100	100	100	100	100	100	100	100	100

Table 20a – Relative average peak areas of PAHs (n=3) in high-boiling alcohols at varying initial column temperatures

			PAH													
Solvent	**bp (°C)**	**T_o Opt (°C)**	**2**	**3**	**4**	**5**	**6**	**7**	**8**	**9**	**10**	**11**	**12**	**13**	**14**	**15**	**16**
1-butanol	117	57	102	87	79	76	76	77	83	83	85	84	83	88	98	102	91
1-pentanol	137	77	128	107	106	93	92	88	101	97	94	98	97	99	103	109	101
cyclopentanol	141	81	145	108	106	91	90	80	99	105	102	96	95	95	102	103	94
1-hexanol	158	98	100	100	100	100	100	100	100	100	100	100	100	100	100	100	100

Table 20b – Relative average peak heights of PAHs (n=3) in high-boiling alcohols at varying initial column temperatures

1-Hexanol was found to yield the highest peak areas and peak heights of the late-eluting PAHs of all the high-boiling alcohols. Once it was determined which of the high-boiling alcohols made the best injection solvent, the response (in terms of peak areas and heights) of PAHs in this alcohol was compared to the response of PAHs in toluene. Before this investigation on the use of alcohols as injection solvents, toluene was proposed by Brindle *et al.* to be the best solvent for the determination of PAHs by gas chromatography [90].

Toluene

In a direct comparison of 1-hexanol to toluene (see Tables 21a and 21b), 1-hexanol was found to yield higher peak areas and peak heights of all 15 of the US EPA priority PAHs tested, except dibenz[*ah*]anthracene. As a result, 1-hexanol was found to be the better of the two solvents. See also Figure 40.

n-Octane

In addition to the high-boiling alcohols, a high-boiling aliphatic solvent, n-octane, was tested as an injection solvent for the PAHs. Since the alcohols were shown to be effective injection solvents, it was important to determine whether the alcohols make good solvents solely due to their high boiling points.

n-Octane was compared directly to both toluene and 1-hexanol – see Tables 22a and 22b (below). n-Octane fared better than toluene in this determination, but 1-hexanol, again, was the clear winner. n-Octane yielded higher peak areas and heights than toluene. 1-Hexanol, however, still gave the largest peak areas and heights for the late-eluting PAHs, and is therefore favoured in this test. This effect is shown graphically in Figure 41. These data suggest that the boiling point of the solvent does play an important role on the response of PAHs. Higher-boiling solvents have been shown here to yield improved responses for PAHs over solvents with lower boiling points.

All Solvents

As the best solvent for the determination of PAHs had been determined, a comparison of all solvents (tested in this study) was executed. Tables 23a and 24a show a comparison of relative peak areas and peak heights of the 15 PAHs in each solvent. A comparison of the peak areas of the late-eluting PAHs is shown graphically in Figure 42. From these data, it can be seen that 1-hexanol is the best injection solvent. Another interesting observation is made from these data. It is noted that as the boiling point of the solvent increases, the range of PAHs for which it yields the best response increases. In other words, the solvent of lowest boiling point shows the lowest response for the largest number of PAHs, and the solvent with the highest boiling point shows the best response for the largest number of PAHs.

The type of solvent, (i.e. alkane, aromatic, alcohol) does not seem to have an impact on the effectiveness of the solvent. Based on the results in Tables 23a and 24a, the increased response of PAHs from one solvent to another is governed by boiling point.

			PAH														
Solvent	**bp (°C)**	**T_o Opt (°C)**	**2**	**3**	**4**	**5**	**6**	**7**	**8**	**9**	**10**	**11**	**12**	**13**	**14**	**15**	**16**
toluene	110	50	87	87	79	79	78	81	83	83	83	86	85	87	99	109	99
1-hexanol	158	98	100	100	100	100	100	100	100	100	100	100	100	100	100	100	100

Table 21a – Relative average peak areas of PAHs (n=3) in toluene and 1-hexanol at varying initial column temperatures

			PAH														
Solvent	**bp (°C)**	**T_o Opt (°C)**	**2**	**3**	**4**	**5**	**6**	**7**	**8**	**9**	**10**	**11**	**12**	**13**	**14**	**15**	**16**
toluene	110	50	84	85	76	77	70	66	91	90	90	83	84	87	99	111	96
1-hexanol	158	98	100	100	100	100	100	100	100	100	100	100	100	100	100	100	100

Table 21b – Relative average peak heights of PAHs (n=3) in toluene and 1-hexanol at varying initial column temperatures

			PAH														
Solvent	**bp (°C)**	**T_o Opt (°C)**	**2**	**3**	**4**	**5**	**6**	**7**	**8**	**9**	**10**	**11**	**12**	**13**	**14**	**15**	**16**
toluene	110	50	87	87	79	79	78	81	83	83	83	86	85	87	99	109	99
n-octane	125	65	115	110	87	83	83	83	87	88	87	90	90	92	107	117	105
1-hexanol	158	98	100	100	100	100	100	100	100	100	100	100	100	100	100	100	100

Table 22a – Relative average peak areas of PAHs (n=3) in toluene, n-octane, and 1-hexanol at varying initial column temperatures

			PAH														
Solvent	**bp (°C)**	**T_o Opt (°C)**	**2**	**3**	**4**	**5**	**6**	**7**	**8**	**9**	**10**	**11**	**12**	**13**	**14**	**15**	**16**
toluene	110	50	84	85	76	77	70	66	91	90	90	83	84	87	99	111	96
n-octane	125	65	126	98	85	81	80	74	99	91	93	91	89	93	106	120	105
1-hexanol	158	98	100	100	100	100	100	100	100	100	100	100	100	100	100	100	100

Table 22b – Relative average peak heights of PAHs (n=3) in toluene, n-octane, and 1-hexanol at varying initial column temperatures

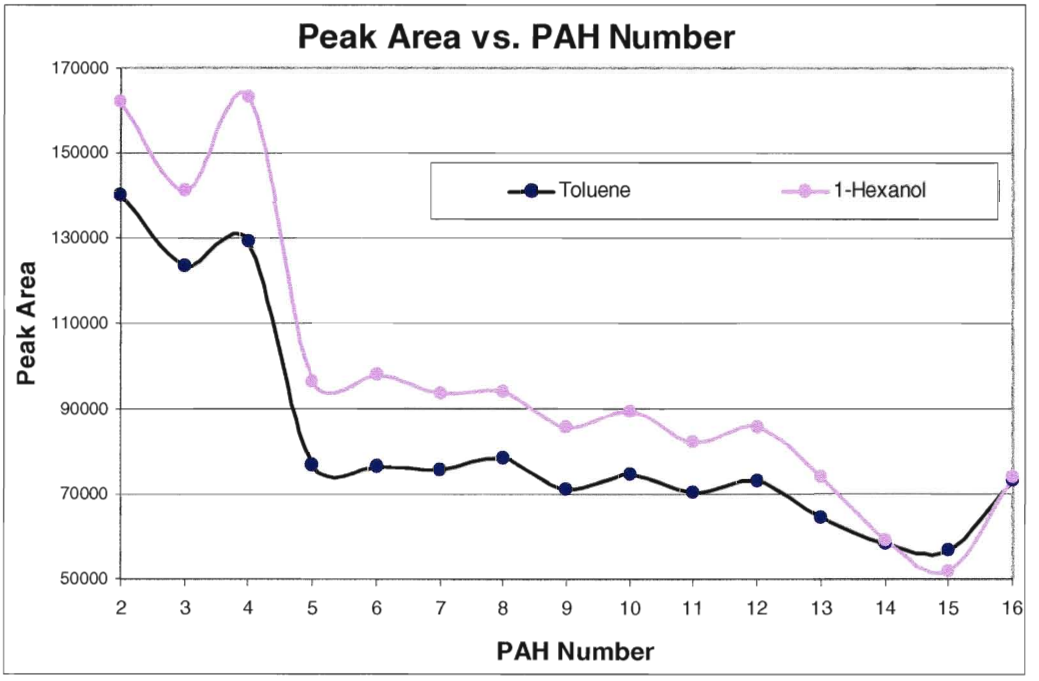

Figure 40 – Peak areas of all PAHs in toluene and 1-hexanol

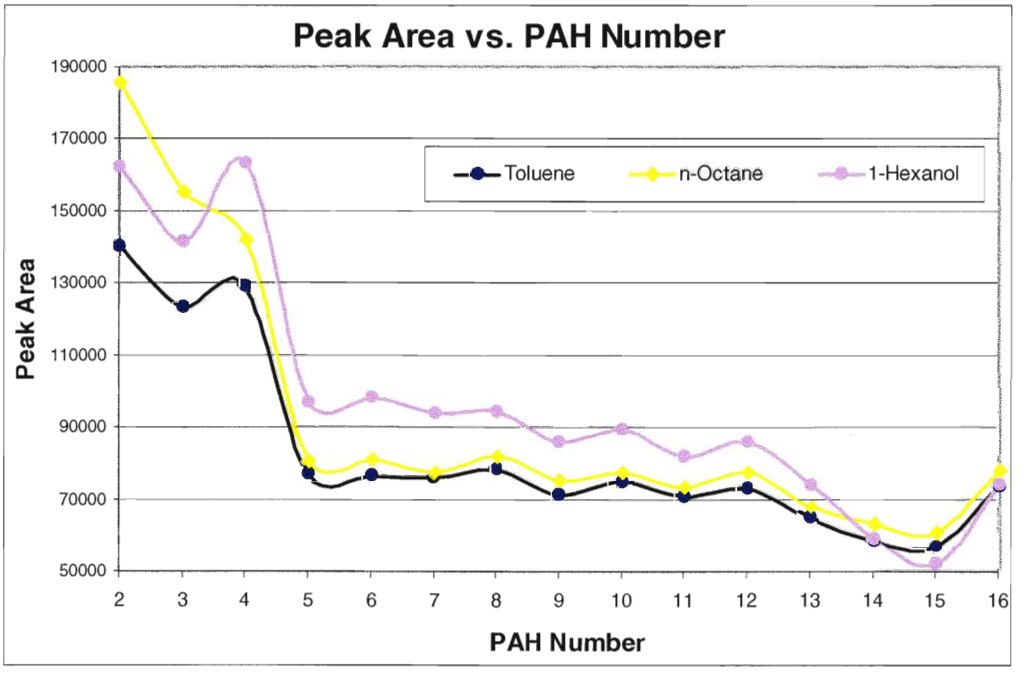

Figure 41 – Peak areas of all PAHs in toluene, n-octane, and 1-hexanol

			PAH														
Solvent	**bp (°C)**	**T_o Opt (°C)**	**2**	**3**	**4**	**5**	**6**	**7**	**8**	**9**	**10**	**11**	**12**	**13**	**14**	**15**	**16**
toluene	110	50	87	87	79	79	78	81	83	83	83	86	85	87	99	109	99
1-butanol	117	57	97	96	86	82	82	82	82	84	83	86	86	88	97	102	98
n-octane	125	65	115	110	87	83	83	83	87	88	87	90	90	92	107	117	105
1-pentanol	137	77	119	116	102	97	95	94	96	97	95	97	98	98	104	107	105
cyclopentanol	141	81	122	116	100	94	94	89	92	94	93	93	95	95	98	103	99
1-hexanol	158	98	100	100	100	100	100	100	100	100	100	100	100	100	100	100	100

Table 23a – Relative average peak areas for 15 PAHs (n=3) in various solvents at optimum initial column temperatures

		PAH														
Solvent	**Column T_o (°C)**	**2**	**3**	**4**	**5**	**6**	**7**	**8**	**9**	**10**	**11**	**12**	**13**	**14**	**15**	**16**
toluene	110	0	1	2	1	0	1	2	1	1	2	1	0	1	0	1
n-butanol	117	0	0	1	1	1	1	1	1	1	2	1	0	0	1	2
n-octane	125	2	2	2	2	1	2	2	1	0	2	1	2	3	3	1
n-pentanol	137	1	1	0	1	0	0	1	2	1	1	1	1	1	1	1
cyclopentanol	141	1	0	1	0	1	2	1	1	1	2	1	1	1	1	2
n-hexanol	158	3	3	2	2	1	1	2	1	2	3	2	3	3	3	2

Table 23b – %RSD for average peak areas of 15 PAHs (n=3) in various solvents at optimum initial column temperatures

			PAH														
Solvent	**bp (°C)**	**T_o Opt (°C)**	**2**	**3**	**4**	**5**	**6**	**7**	**8**	**9**	**10**	**11**	**12**	**13**	**14**	**15**	**16**
toluene	110	50	87	87	79	79	78	81	83	83	83	86	85	87	99	109	99
1-butanol	117	57	97	96	86	82	82	82	82	84	83	86	86	88	97	102	98
n-octane	125	65	115	110	87	83	83	83	87	88	87	90	90	92	107	117	105
1-pentanol	137	77	119	116	102	97	95	94	96	97	95	97	98	98	104	107	105
cyclopentanol	141	81	122	116	100	94	94	89	92	94	93	93	95	95	98	103	99
1-hexanol	158	98	100	100	100	100	100	100	100	100	100	100	100	100	100	100	100

Table 24a – Relative average peak heights for 15 PAHs (n=3) in various solvents at optimum initial column temperatures

		PAH														
Solvent	**Column T_o (°C)**	**2**	**3**	**4**	**5**	**6**	**7**	**8**	**9**	**10**	**11**	**12**	**13**	**14**	**15**	**16**
toluene	110	10	3	10	3	2	8	7	2	2	2	1	2	6	2	2
n-butanol	117	13	11	4	3	2	3	14	10	4	1	2	4	2	6	4
n-octane	125	10	17	3	4	3	10	5	12	5	6	0	1	4	4	3
n-pentanol	137	11	17	4	7	9	13	15	8	7	4	3	4	1	2	4
cyclopentanol	141	3	9	1	4	5	12	11	3	1	3	2	3	2	4	1
n-hexanol	158	18	11	7	2	1	1	14	9	10	3	2	4	4	3	5

Table 24b – %RSD for average peak heights of 15 PAHs (n=3) in various solvents at optimum initial column temperatures

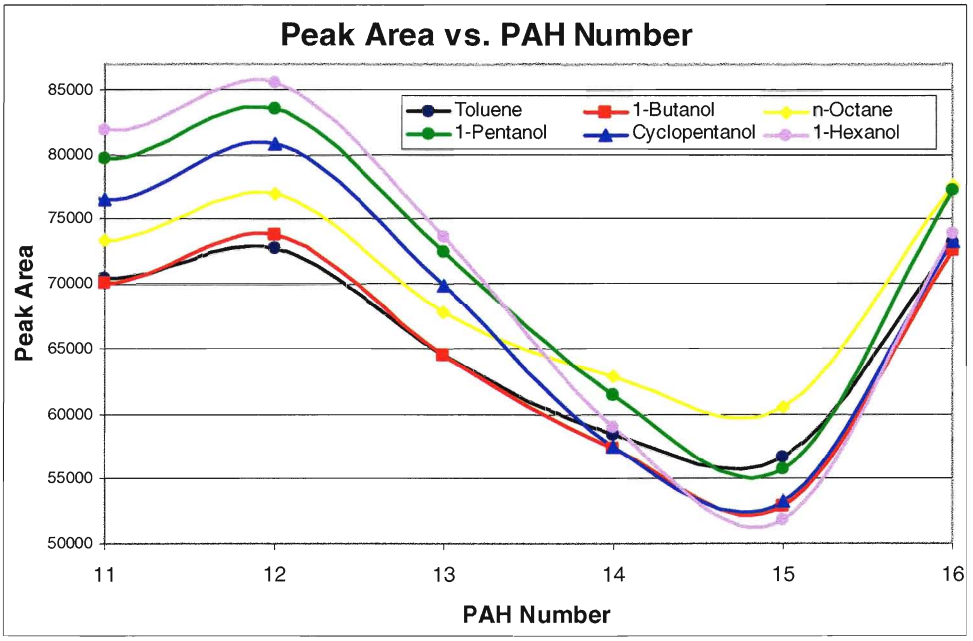

Figure 42 – Comparison of peak areas of late-eluting PAHs in all solvents

The peak areas and heights of four PAHs: anthracene (Ant), benzo[a]anthracene (BaA), benzo[a]pyrene (BaP), and dibenz[ah]anthracene (DahA) in each solvent were plotted against the boiling points of the solvents. See Figures 39a and 39b below. These PAHs were chosen to represent a range of volatilities of the PAHs and also because these PAHs are all known to be carcinogenic [78].

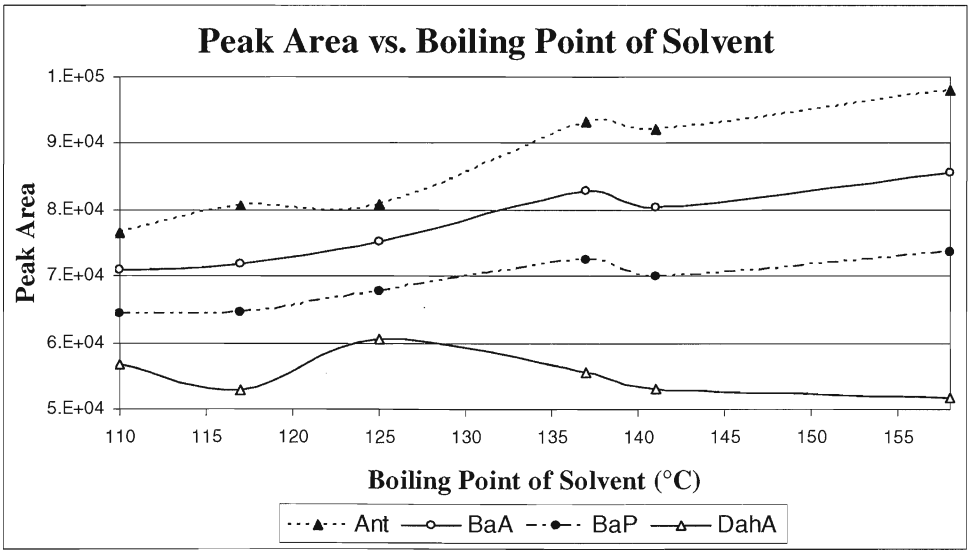

Figure 43a – Peak area vs. boiling point of solvent for selected PAHs

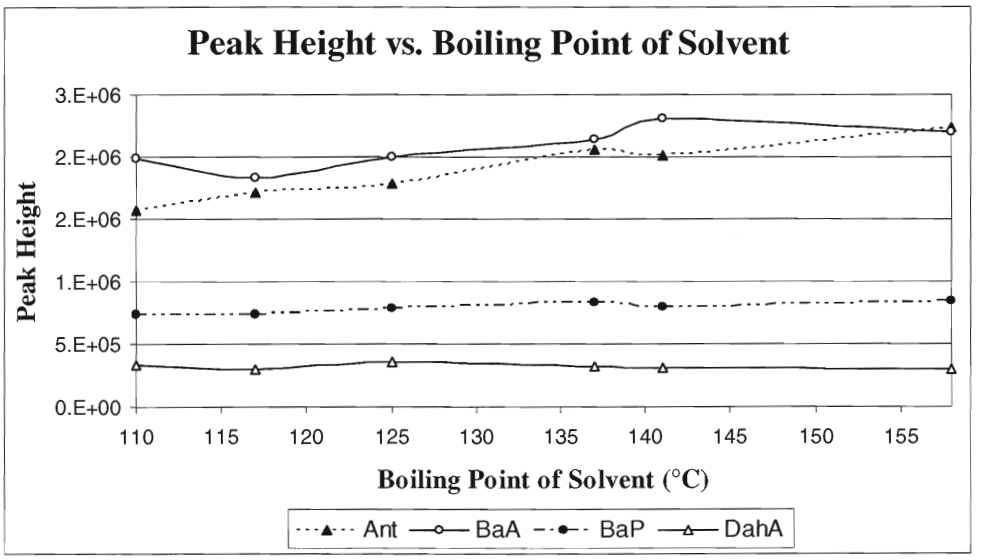

Figure 43b – Peak height vs. boiling point of solvent for selected PAHs

These figures clearly show that the response of all PAHs, except DahA, is increased through the use of higher boiling injection solvents. Dibeno[*ah*]anthracene showed the best response in n-octane.

Resolution

The resolution of two pairs of commonly coeluting PAHs, in each solvent, was plotted against the boiling point of the respective solvents in order to determine if the boiling point of the solvent has any effect on the resolution of these PAH pairs. The result is shown below in Figure 44.

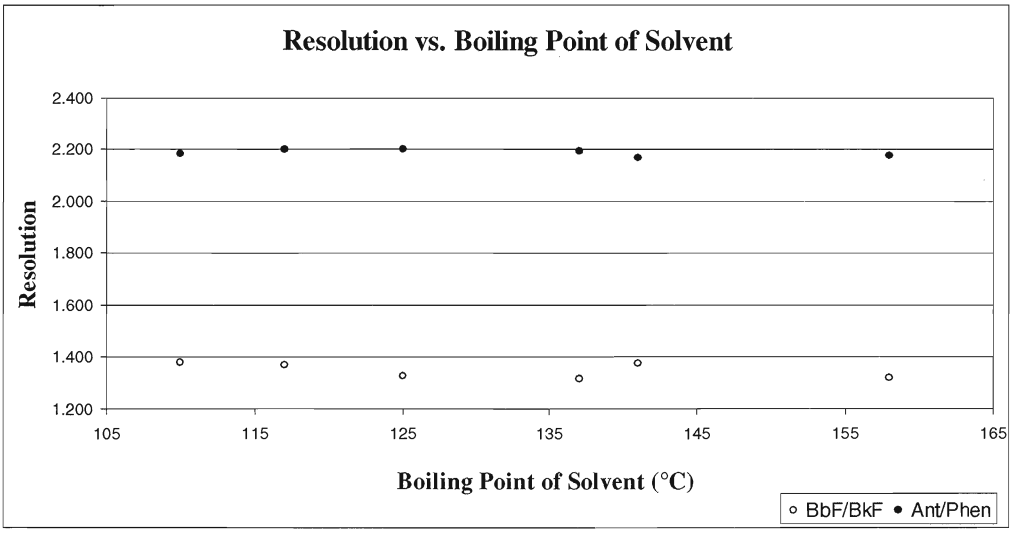

Figure 44 – Effect of solvent volatility on resolution of Ant/Phen and BbF/BkF

It can be seen that neither the resolution of Ant/Phen or BbF/BkF are affected by the boiling point of the solvent. There is no significant change in resolution, for either PAH pair, observed in solvents of different volatilities.

Peak Shape (Symmetry)

The choice of injection solvent has been found to affect peak symmetry. This effect is not controlled by the volatility of the solvent. 1-Butanol, n-octane, and 1-pentanol exhibited peak tailing at high initial column temperatures, while toluene, cyclopentanol, and 1-hexanol did not. As toluene has the lowest boiling point of all the solvents, and 1-hexanol the highest, the volatility of the solvent cannot be what governs this behaviour.

Peak splitting is also observed at high initial column temperatures. Polycyclic aromatic hydrocarbons 1-5 exhibit this behaviour in all solvents except toluene. In toluene, the early peaks show evidence of fronting, but not splitting. As toluene is the lowest boiling solvent, it is possible that the volatility of the solvent does affect this phenomenon.

Effect of Stationary Phase on Chromatographic Behaviour

Peak Symmetry

The range of initial column temperatures that yield symmetric peaks (no fronting or tailing) for the 15 PAHs was determined. The results (GC runs) from the experiment run to determine the optimum initial column temperature were used for this test. For each solvent, and at each initial column temperature, all 15 PAH peaks were evaluated for symmetry. For each PAH (and in each solvent) the minimum temperature, and maximum temperature for which symmetric peaks were obtained were recorded. Results obtained in this work, were attained using an RTX-50 column (50% phenyl methyl polysiloxane). Previous work done by Elrutb [111] determined the symmetry range for these same PAHs using a DB-5 column (5% phenyl methyl polysiloxane). Results from the RTX-50 column are compared to the results of the DB-5 column in Figures 45-49. The symmetry range for the PAHs in toluene, using the RTX-50 column, is shown in Figure 50. Symmetry data for toluene, using the DB-5 column, was not reported by Elrubt [111].

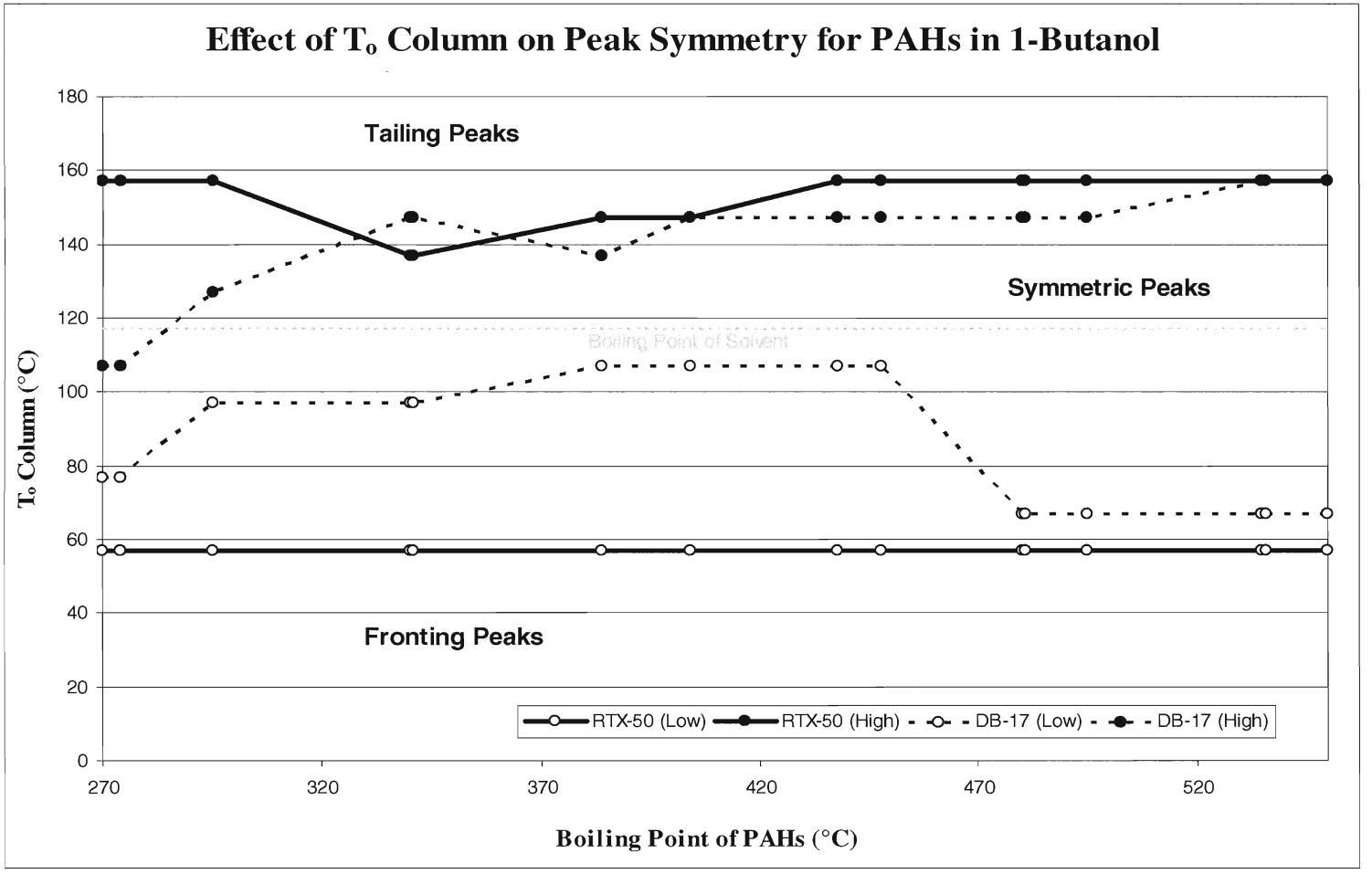

Figure 45 – The effect of initial column temperature on peak symmetry for 15 PAHs in 1-butanol

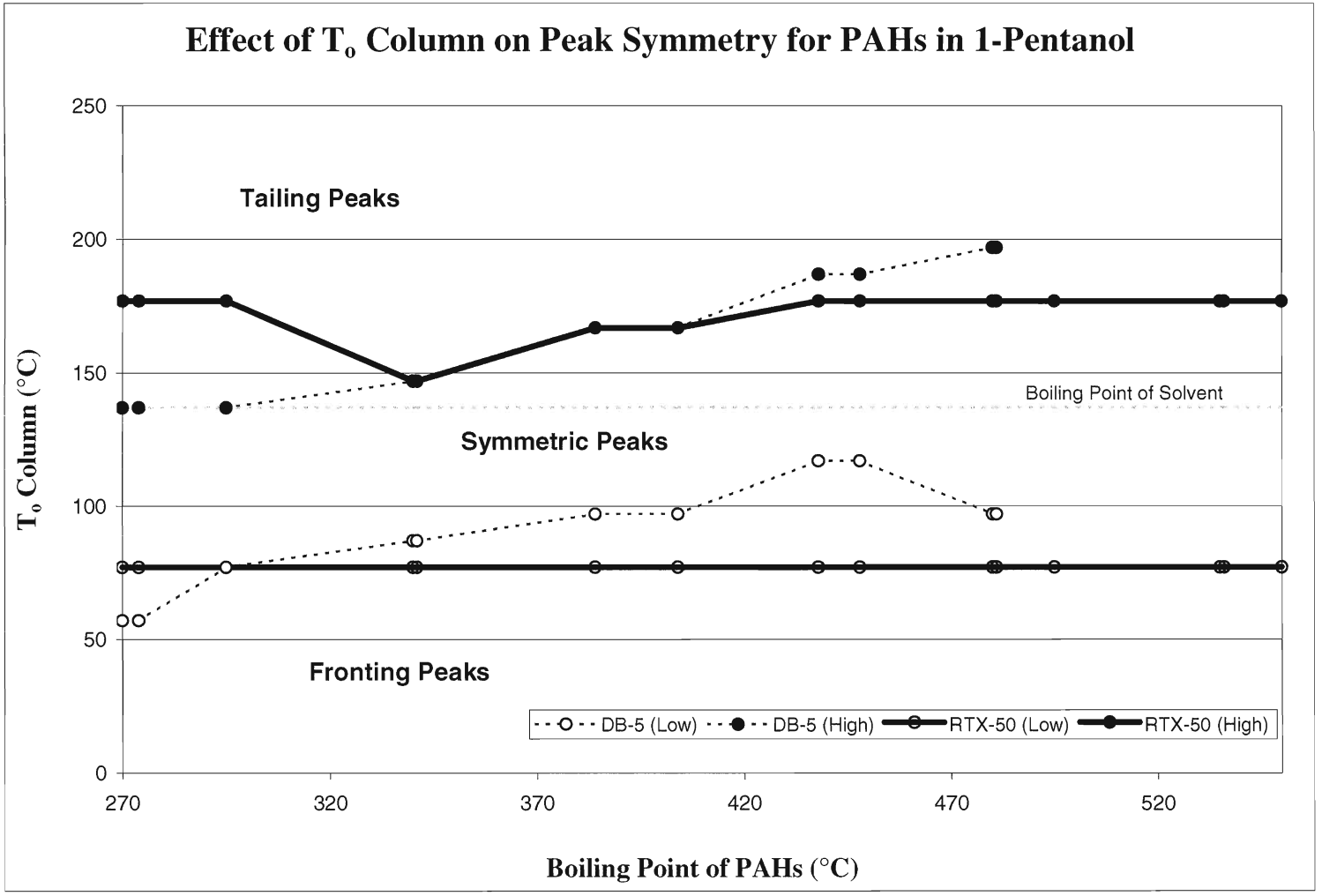

Figure 46 – The effect of initial column temperature on peak symmetry for 15 PAHs in 1-pentanol

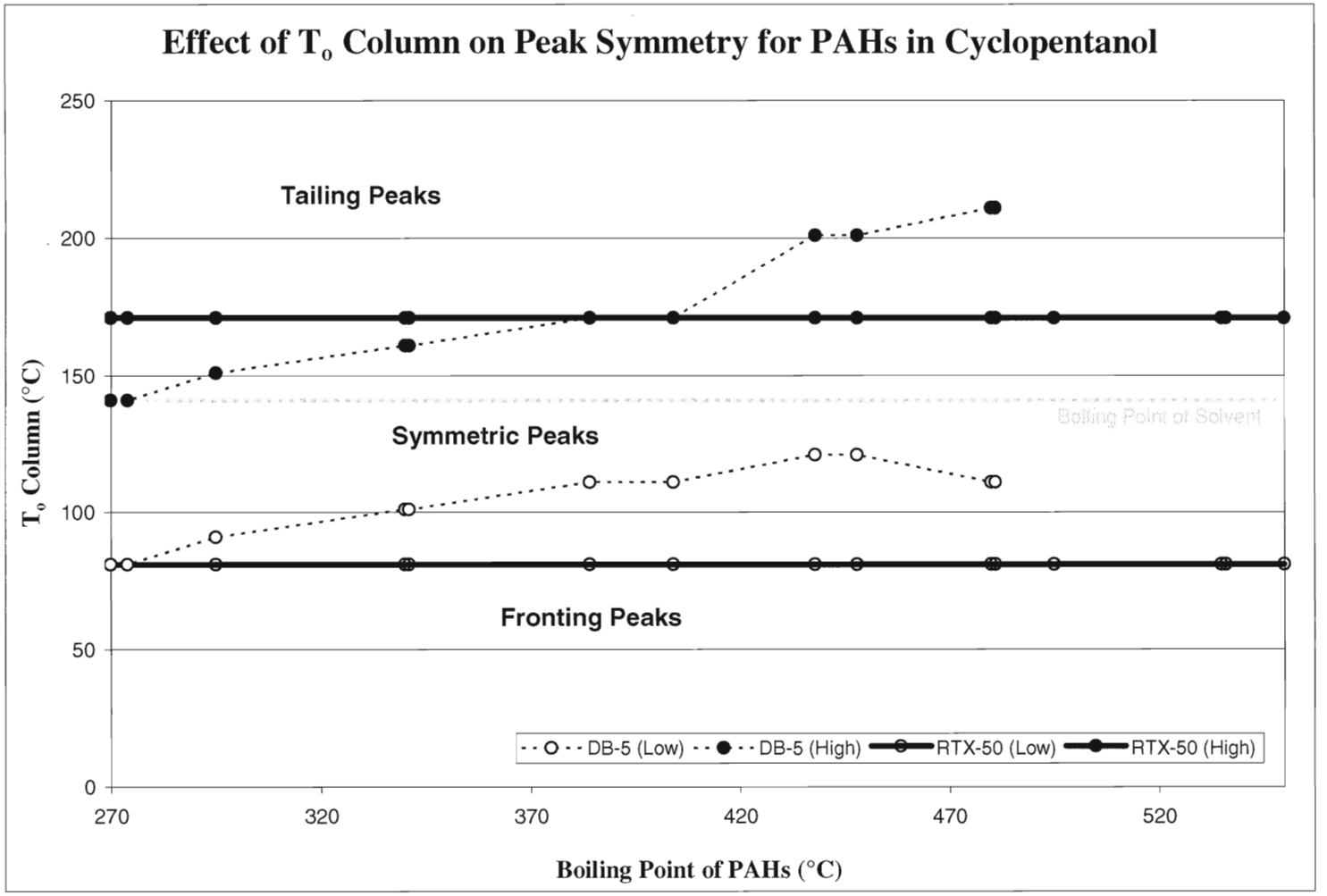

Figure 47 – The effect of initial column temperature on peak symmetry for 15 PAHs in cyclopentanol

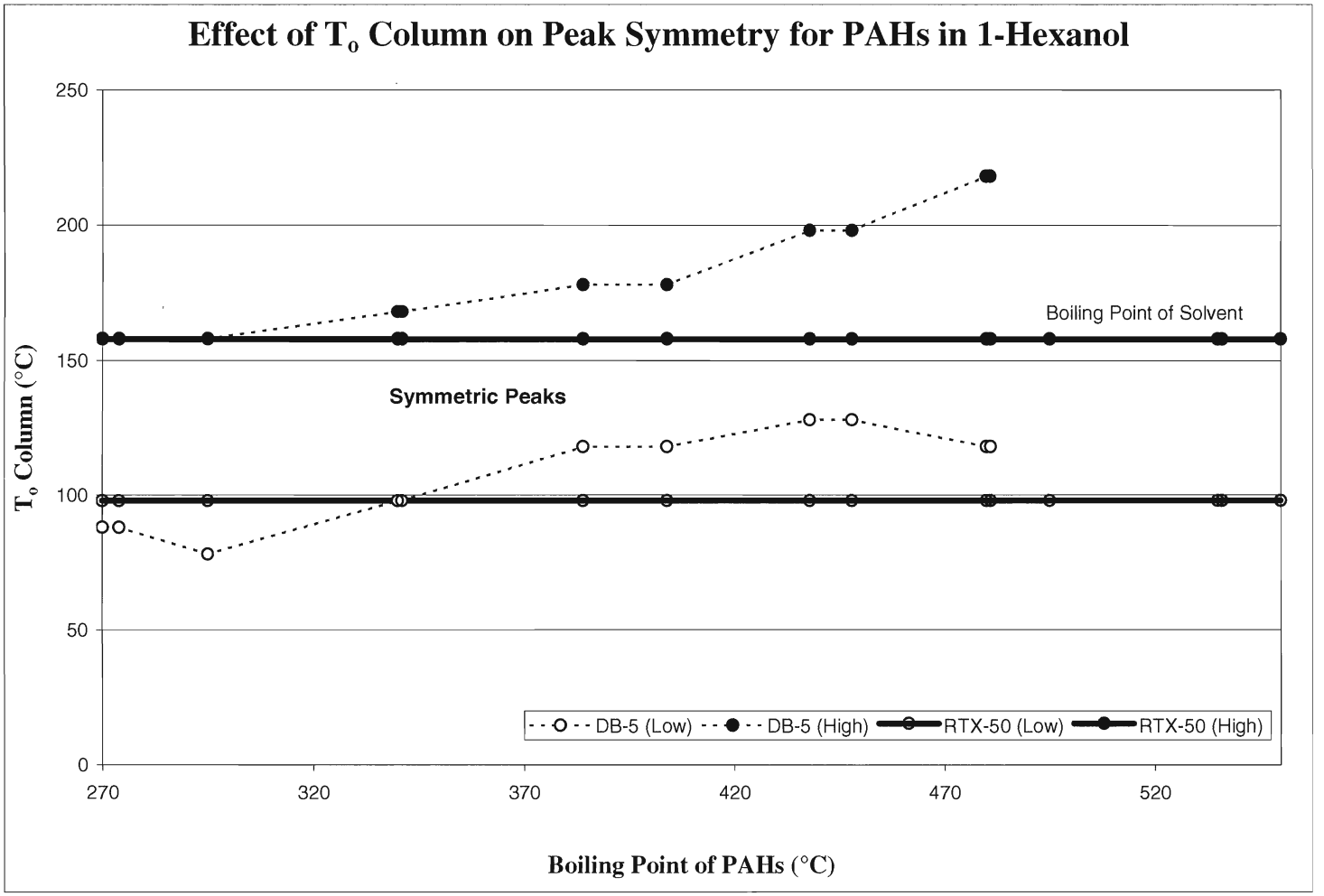

Figure 48 – The effect of initial column temperature on peak symmetry for 15 PAHs in 1-hexanol

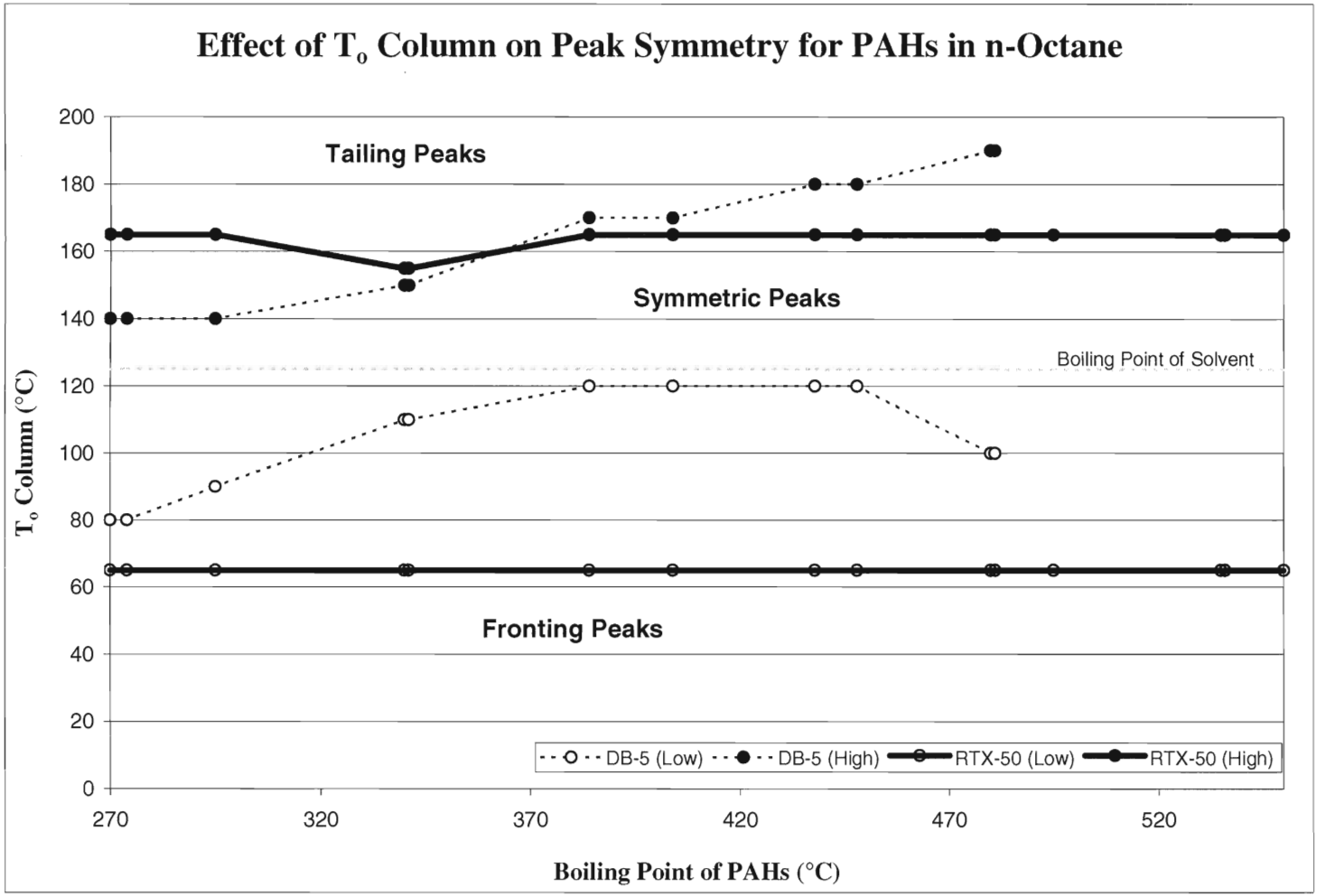

Figure 49 – The effect of initial column temperature on peak symmetry for 15 PAHs in n-octane

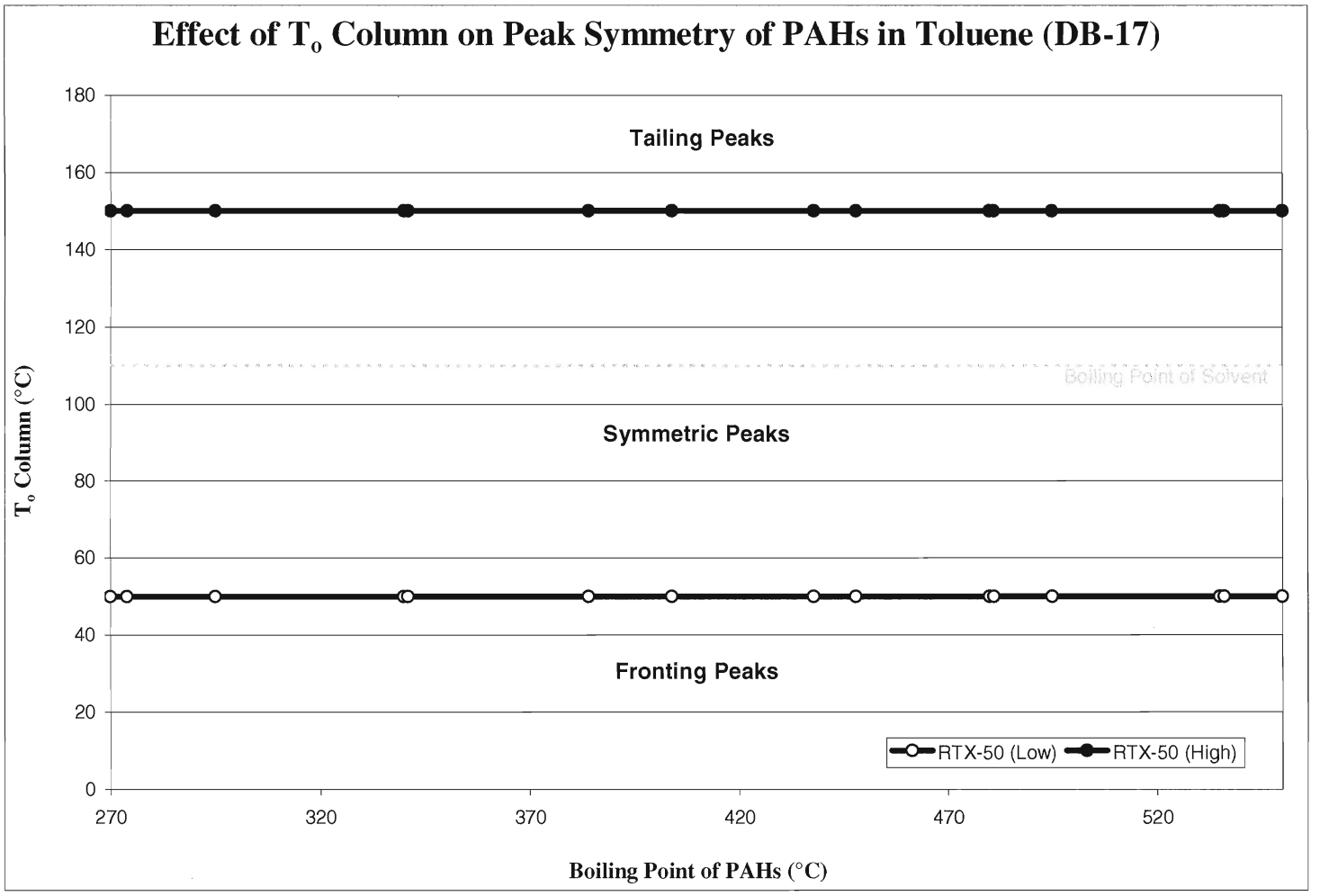

Figure 50 – The effect of initial column temperature on peak symmetry for 15 PAHs in toluene

In Figures 45-49 above, it is evident that the RTX-50 column allows a larger, and in some solvents much larger, initial column temperature range over which symmetric peaks can be obtained. Factors which affect the fronting and tailing of chromatographic peaks are therefore solvent and column dependent.

Not All Columns are Created Equal

Early experiments in the determination of PAHs were performed on a 50% phenyl methyl polysiloxane column manufactured by Agilent Technologies Canada Inc. (DB-17). At a later time, a column of the same stationary phase but manufactured by Restek Corporation (RTX-50) was used to perform these same experiments. It was found that although both columns contain the same stationary phase, they did not promote the same chromatographic behaviour from the PAHs in same solvent. Although limited results were obtained from the DB-17 column, a symmetry profile of the 15 PAHs in 1-butanol was compiled. This symmetry profile is compared to the symmetry profile obtained, for the same PAH standard, using the RTX-50 column in Figure 51.

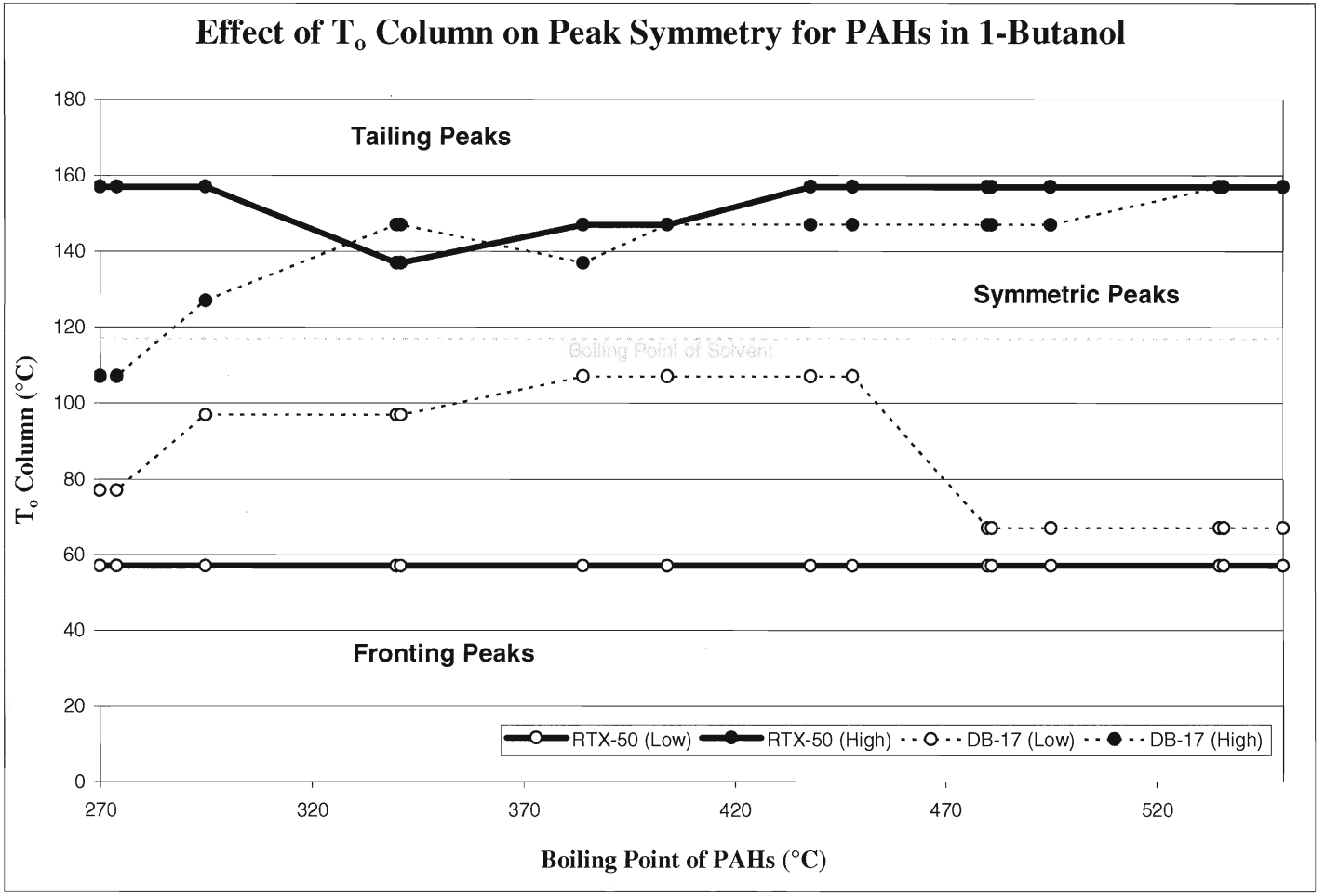

Figure 51 – A comparison of the symmetry profiles of 15 PAHs in 1-butanol determined from DB-17 and RTX-50 columns

As seen in Figure 51, the symmetry profile for the PAHs in 1-butanol determined using the RTX-50 column is very different from the symmetry profile determined using the DB-17 column. The RTX-50 column permits a wider range of initial column temperatures over which symmetric peaks can be obtained.

Differences in the stationary phases probably arise as the result of different synthetic procedures used in their formation. As these processes are proprietary to each manufacturer, and are not released to the public, it cannot be known what difference causes the discrepancy observed here. But it is clear from the data shown here, that a significant difference exists.

Chapter 4 – Conclusions

Part I – Fluorinated Compounds

The method developed here was shown to be not viable for compound A. It is not certain, what part of the method failed in this regard, but the extraction is highly suspect. More method development is still necessary.

The depositional profile for compound B is reflective of the operation of the Hyde Park Landfill. The obtained profile shows that compound B, at present, has not returned to background levels. This may be due to the disturbance and redistribution of previously deposited contaminated sediments.

The increased levels of compound B at present also may suggest that the Hyde Park Landfill is still leaking. This is a concern as the Hyde Park Landfill is the largest dioxin dump in the world. The depositional profile of compound B would then also be reflective of one known path of entry for TCDD into Lake Ontario.

These results are based only on the data from one sediment core, and cannot draw any definitive conclusions about the Hyde Park Landfill. But the results of this core do suggest that these compounds are worth looking into.

Part II – Polycyclic Aromatic Hydrocarbons

Solvent trapping has been shown to be a more significant mechanism for increasing the response of late-eluting PAHs than cold trapping.

Toluene was found to be the most forgiving solvent overall. It displayed the smallest discrepancies in peak area and peak height for all PAHs throughout the entire initial column temperature range explored.

The response (peak area and peak height) of late-eluting PAHs tends to decrease constantly with increasing initial column temperature. Early-eluting PAHs do not behave consistently between solvents. Some early-eluting PAHs will show an increase in response with increasing initial column temperature in some solvents, and show a decrease in response with increasing initial column temperature in other solvents.

The resolution of closely-eluting PAH pair Ant/Phen is temperature dependent. The resolution of these PAHs decreases with increasing initial column temperature. The resolution of BbF/BkF is not affected by initial column temperature.

The initial column temperature does have an impact on peak shape for PAHs. Although there was no evidence of peak fronting, for any of the 15 PAHs, at any initial column temperature, in any solvent, some subtle peak tailing was observed for 1-butanol, 1-pentanol, and n-octane. Peak splitting is observed at initial column temperatures at or above the boiling point of the solvent, for all solvents. Again, the tailing and splitting observed only occurred at initial column temperatures well above the optimum value.

A dirty injector liner can have a significant impact on the response of PAHs. The peak areas and heights of most of the 15 PAHs were found to be reduced when determined using a dirty injector liner. More importantly, the dirty liner did not affect the response of the PAHs equally.

1-Hexanol produced the highest response for the late-eluting PAHs, but it was one of the least forgiving solvents for early-eluting PAHs. Method

development, in terms of temperature program optimization is especially critical if this solvent is chosen for the determination of PAHs by a gas chromatographic method.

The boiling point of the solvent impacts the response of all PAHs. Higher-boiling solvents were shown to yield a higher response for the largest number of PAHs.

It has been shown that the resolution of closely-eluting PAHs is not affected by the boiling point of the injection solvent. There is no significant change in resolution observed for either Ant/Phen or BbF/BkF in solvents of differing volatilities.

Peak tailing is a solvent-dependent phenomenon, but it is not governed by the boiling point of the solvent. Peak tailing of early-eluting PAHs is observed at high initial column temperatures in some solvents but not in others.

It has been found that different manufactures of the same stationary phase can have different effects on chromatographic behaviour. An RTX-50 column has been shown to allow symmetric peaks for PAHs in 1-butanol over a wider range of initial column temperatures than a DB-17 column. The differences in the stationary phase between the two columns cannot be known as they are the result of proprietary formulation of the columns. But, as it has been shown, a difference does exist.

References

[1] Niagara Falls – Environmental Impact. http://www.iaw.com/~falls/environment.html (accessed July 2008).

[2] The Niagara River Secretariat. *Niagara River Toxics Management Plan: Progress Report and Work Plan: May 1999*; United States Environmental Protection Agency: New York, New York, USA, 1999.

[3] Elder, V.A., Proctor, B.L., and Hites, R.A. Organic Compounds Found Near Dump Sites in Niagara Falls, New York *Environ. Sci. Technol.* **1981**, 15(10), 1237-1243.

[4] Kemp, A.L.W., and Harper, N.S. Sedimentation Rates and a Sediment Budget for Lake Ontario. *J. Great Lakes Res.* **1976**, 2(2), 324-340.

[5] Eadie, B.J., and Robertson, A. An IFYGL Carbon Budget for Lake Ontario. *J. Great Lakes Res.* **1976**, 2(2), 307-323.

[6] Robertson, A., and Jenkins, C.F. Canadian-American Study of Lake Ontario. *Ambio*. **1978**, 7,106-112.

[7] Government of Canada and United States Environmental Protection Agency. *The Great Lakes: An Environmental Atlas and Resource Book, 3rd Edition*; Government of Canada: Toronto, and the Great Lakes National Program Office, Chicago, Illinois, USA, 2002.

[8] Sosa, G.M. *Third Five-Year Review Report for Hyde Park Landfill Superfund Site*; United States Environmental Protection Agency, Region 2: New York, New York, USA, 2006.

[9] *Hooker – Hyde Park Fact Sheet*; United States Environmental Protection Agency, Region 2: New York, New York, USA, 2008.

[10] Howdeshell, M.J. and Hites, R.A. Is the Hyde Park Dump, near the Niagara River, Still Affecting the Sediment of Lake Ontario? *Environ. Sci. Technol.* **1996**, 30, 969-974.

[11] Niagara: A River to Save. *Pollution Probe* **1999**.

[12] United States Environmental Protection Agency and the New York State Department of Environmental Conservation. *Reduction of Toxic Loadings to the Niagara River from Hazardous Waste Sites in the United States*; United States Environmental Protection Agency Region 2: New York, New York, USA, 2007.

[13] Pohl, H.R., Liados, F., Ingerman, L., Cunningham, P., Raymer, J.H., Wall, C., Gasiewicz, T., and De Rosa, C.T. ATSDR Evaluation of Health Effects of Chemicals VII: Chlorinated Dibenzo-*p*-dioxins. *Toxicol. Ind. Health* **2000**, 16, 85-201.

[14] Jaffe, R. and Hites, R.A. Identification of New, Fluorinated Biphenyls in the Niagara River-Lake Ontario Area. *Environ. Sci. Technol.* **1985**, 19, 736-740.

[15] Environment Canada, Environmental Conservation Branch. *The Niagara River Upstream/Downstream Program 1986/87-1996/97: Concentrations, Loads, Trends*; Ecosystem Health Division Technical Report EHD/ECB-OR/00-01/I; Environment Canada: Burlington, Ontario, Canada 1999.

[16] Yurawecz, M.P. Gas-Liquid Chromatographic and Mass Spectrometric Identification of Chlorinated Trifluorotoluene Residues in Niagara River Fish. *J. Assoc. Off. Anal. Chem.* **1979**, 62, 36-40.

[17] Kaminsky, R., Kaiser, K.L., Hites, R.A. Fates of Organic Compounds from Niagara Falls Dumpsites in Lake Ontario. *J. Great Lakes Res.* **1983**, 9(2), 183-189.

[18] Jaffe, R. and Hites, R.A. Fate of hazardous Waste Derived Organic Compounds in Lake Ontario. *Environ. Sci. Technol.* **1986**, 20(3), 267-274.

[19] Smith, D.W. and Weston, A.P. Comment on "Is the Hyde Park Dump, near the Niagara River, Still Affecting the Sediment of Lake Ontario?" *Environ. Sci. Technol.* **1997**, 31, 1246-1247.

[20] Qiao, M., Huang, S., and Wang, Z. Partitioning Characteristics of PAHs Between Sediment and Water in a Shallow Lake. *J. Soils Sediments* **2008**, 8, 69-73.

[21] *LOG K_{ow} Criteria of 5 is Equivalent to BCF Criteria of 5000*; ICCA Briefing Paper; International Council of Chemical Associations: Brussels, Belgium, 1998.

[22] Dearden, J.C. and Shinnawei, N.M. Improved Prediction of Fish Bioconcentration Factor of Hydrophobic Chemicals. *SAR and QSAR in Environmental Research* **2004**, 15, 449-455.

[23] Meylan, W.M. and Howard, P.M. Atom/Fragment Contribution Method for Estimating Octanol-Water Partition Coefficients. *J. Pharm. Sci.* **1995**, 84, 83-92.

[24] Schwarzenbach, R.P.; Gschwend, P.M.; Imboden, D.M. *Environmental Organic Chemistry*, 2nd Edition; Wiley: Hoboken, NJ, 2003.

[25] Syracuse Research Corporation. Simulation of Software KowWin (2003). http://dino.wiz.uni-kassel.de/dain/ddb/x343.html (accessed December 2008).

[26] US EPA. Estimation Programs Interface Suite™ for Microsoft® Windows, v 4.00. United States Environmental Protection Agency, Washington, DC, USA, 2009.

[27] Pawliszyn, J. *CHEM 425 Analytical Separations Course Notes*; Universtiy of Waterloo: Waterloo, Ontario, Canada, 2005

[28] Kou, D. and Mitra, S. Extraction of Semivolatile Organic Compounds from Solid Matrices. In *Sample Preparation Techniques in Analytical Chemistry*; Mitra, S., Chemical Analysis, Volume 162; John Wiley and Sons Inc.: Hoboken, New Jersey, USA, 2003; 139-178.

[29] Peres, V.F., Saffi, J., Melecci, M.I.S., Abad, F.C., De Assis Jacques, R., Martinez, M.M. Conceicao Oliveira, E., and Caramao, E.B. Comparison of soxhlet, ultrasound-assisted and pressurized liquid extraction of terpenes, fatty acids and Vitamin E from *Piper gaudichaudianum* Kunth. *J. Chromatogr. A* **2006**, 1105, 115-118.

[30] Shen, J. and Shao, X. A comparison of accelerated solvent extraction, Soxhlet extraction, and ultrasonic-assisted extraction for analysis of terpenoids and sterols in tobacco. *Anal. Bioanal. Chem.* **2005**, 383, 1003-1008.

[31] Takashi, Y. Extraction Behaviour of Accelerated Solvent Extraction of DDT Metabolite from Fish Matrix. *Analytical Sciences* **2001**, 17, i913-i915.

[32] Herrero, M., Martin-Alvarez, P.J., Senorans, F.J., Cifuentes, A., and Ibanez, E. Optimization of accelerated solvent extraction of antioxidants from *Spirulina platensis* microalga. *Food Chemistry* **2005**, 93, 417-423.

[33] US Environmental Protection Agency. Method 3545A – Pressurized Fluid Extraction, Revision 1, US Environmental Protection Agency, Washington D.C, USA, 2007.

http://www.epa.gov/waste/hazard/testmethods/sw846/pdfs/3545a.pdf (accessed August 2008).

[34] Gan, J., Papiernik, S.K., Koskinen, W.C., and Yates, S.R. Evaluation of Accelerated Solvent Extraction (ASE) for Analysis of Pesticide Residues in Soil. *Environ. Sci. Technol.* **1999**, 33, 3249-3253.

[35] Popp, P., Keil, P., Moder, M., Paschke, A., and Thuss, U. Application of accelerated solvent extraction followed by gas chromatography, high-performance liquid chromatography and gas chromatography-mass spectrometry for the determination of polycyclic aromatic hydrocarbons, chlorinated pesticides and polychlorinated dibenzo-*p*-dioxins and dibenzofurans in solid wastes. *J. Chromatogr. A.* **1997**, 774, 203-211.

[36] Kuriki, K., Tajima, K., and Tokudome, S. Accelerated Solvent Extraction for Quantitative Measurement of Fatty Acids in Plasma and Erythrocytes. *Lipids* **2006**, 41(6), 605-614.

[37] Preud'homme, H and Potin-Gauthier, M. Optimization of Accelerated Solvent Extraction for Polyhalogenated Dibenzo-p-Dioxins and Benzo-p-Furans in Mineral and Environmental Matrices Using Experimental Designs. *Analytical Chemistry* **2003**, 75(22), 6109-6118.

[38] Fojtova, F., Lojkova, L., and Kuban, V. GC/MS of terpenes in walnut-tree leaves after accelerated solvent extraction. *J. Sep. Sci.* **2008**, 31, 162-168.

[39] Shao, B., Han, H., Li, D., Ma, Y., Tu, X., and Wu, Y. Analysis of alkylphenol and bisphenol A in meat by accelerated solvent extraction and liquid chromatography with tandem mass spectrometry. *Food Chemistry* **2007**, 105, 1236-1241.

[40] Wahlen, R and Catterick, T. Simultaneous co-extraction of organometallic species of different elements by accelerated solvent extraction and analysis by inductively coupled plasma mass spectrometry coupled to liquid and gas chromatography. *Rapid Commun. Mass Spectrom.* **2003**, 18, 211-217.

[41] Sporring, S., Bowadt, S., Svensmark, B., and Borklund, E. Comprehensive comparison of classic Soxhlet extraction with Soxtec extraction, ultrasonic extraction, supercritical fluid extraction, microwave assisted extraction and accelerated solvent extraction for the determination of polychlorinated biphenyls in soil. *J. Chromatogr. A* **2005**, 1090, 1-9.

[42] Antunes, P., Viana, P., Vinhaz, T., Capelo, J.L., Rivera, J., and Gaspar, E.M.S.M. Optimization of pressurized liquid extraction (PLE) of dioxin-furans and dioxin-like PCBs from environmental samples. *Talanta* **2008**, 75, 916-925.

[43] Tavazzi, S., Benfenati, E., and Barcelo, D. Accelerated Solvent Extraction then Liquid Chromatography Coupled with Mass Spectrometry for Determination of 4-t-Octylphenol, 4-Nonylphenols, and Bisphenol A in Fish Liver. *Chromatographia* **2002**, 56, 463-467.

[44] Masucci, J.A. and Caldwell, G.W. Techniques for Gas Chromatography/Mass Spectrometry. In *Modern Practice of Gas Chromatography*; Grob, R.L. and Barry, E.F., 4th Edition; John Wiley & Sons, Inc.: Hoboken, NJ, 2004; pp 339-401.

[45] Johnstone, R.A.W., and Rose, M.E. *Mass Spectrometry for Chemists and Biochemists*, 2nd Edition; Cambridge University Press: Cambridge, United Kingdom, 1996.

[46] Harris, D.C. *Quantitative Chemical Analysis*, 5th Edition; W.H. Freeman and Company: New York, NY, 2000.

[47] Grob, K. *Split and Splitless Injection for Quantitative Gas Chromatography: Concepts, Processes, Practical Guidelines, Sources of Error*, 4th Edition; Wiley-VCH: Weinheim, Germany, 2001.

[48] Grob Jr., K.; Neukom, H.P. Glass Wool in the Injector Insert for Quantitative Analysis in Splitless Injection. *Chromatographia* **1984**, 18, 517-519.

[49] Tswett, M.S. Adsorption analysis and chromatographic method. Application on the chemistry of the Chlorophylls [machine translation]. *Ber. Deut. Bot. Ges.* **1906**, 24, 384-393.

[50] Scott, R.P.W. *Principles and Practice of Chromatography*; Book1 in Chrom-Ed Book Series; Library for Science, LLC, 2003.

[51] Skoog, D.A.; Holler, F.J.; Nieman, T.A. *Principles of Instrumental Analysis*, 5th Edition; Thomson Learning, Inc.: Toronto, ON, 1998.

[52] de Hoffman, E. and Stroobant, V. *Mass Spectrometry: Principles and Applications*; John Wiley & Sons Ltd.: Toronto, Ontario, Canada, 2002.

[53] Barker, J. *Mass Spectrometry: Analytical Chemistry by Open Learning*, 2nd Edition; John Wiley and Sons Ltd.: Chichester, West Sussex, United Kingdom, 1999.

[54] Gross, J.H. *Mass Spectrometry – A Textbook*; Springer: Heidelberg, Germany, 2004.

[55] Worton, D.R., Mills, G.P., Dram, D.E., and Sturges, W.T. Gas Chromatography negative ion chemical ionization mass spectrometry: Application to the detection of alkyl nitrates and halocarbons in the atmosphere. *J. Chromatogr. A* **2008**, 1201, 112-119.

[56] Schulz, H.J. Pesticide Analysis Using the Agilent GC/MSD – a Compendium of EI/PCI and NCI data; Agilent Technologies: Oberhaching, Germany, 2004.

[57] Knighton, W.B., Sears, L.J., and Grimsrud, E.P. High-Pressure Electron Capture Mass Spectrometry. *Mass Spectrom. Rev.* **1995**, 14, 327-343.

[58] Ong, V.S. and Hites, R.A. Electron Capture Mass Spectrometry of Organic Environmental Contaminants. Mass Spectrom. Rev. **1994**, 13, 259-283.

[59] Stemmler, E.A and Hites, R.A. *Electron Capture Negative Ion Mass Spectra of Environmental Contaminants and Related Compounds*; VCH: New York, New York, USA, 1988.

[60] Agilent Technologies. Choosing the Right Column. (2000) http://www.chem.agilent.com/cag/cabu/gccolchoose.htm (accessed March 2009).

[61] Parrott, H.C and Scott, G.W.S. *Polynuclear Aromatic Hydrocarbons*; Report No. 58-79; Ministry of the Environment: Toronto, ON, 1979.

[62] National Research Council of Canada. *Polycyclic Aromatic Hydrocarbons in the Aquatic Environment: formation, sources, fate, and effect on the aquatic environment*; NRCC No. 18981; Associate Committee on Scientific Criteria for Environmental Quality, Ottawa, ON, 1983.

[63] Li, X.F. Investigations into the Determination of Polycyclic Aromatic Hydrocarbons (PAHs) and Polychlorinated Biphenyls (PCBs) by Capillary Gas Chromatography. MSc. Thesis, Brock University, St. Catharines, ON, 1989.

[64] Harvey, R.G. Polycyclic Aromatic Hydrocarbons, Wiley-VCH, Inc.: New York, NY, 1997.

[65] Bordajandi, L.R., Dabrio, M., Ulberth, F., and Emons, H. Optimization of the GC-MS conditions for the determination of the 15 EU foodstuff priority polycyclic aromatic hydrocarbons. *J. Sep. Sci.* **2008**, 31, 1769-1778.

[66] Bjorseth, A. and Ramdahl, T. *Handbook of Polycyclic Aromatic Hydrocarbons: Emission Sources and Recent Progress in Analytical Chemistry*, Volume 2; Marcel Dekker Inc., New York, New York, USA 1983.

[67] Itoh, N., Numata, M., Aoyagi, Y., and Yarita, T. Effect of residues remaining in the injection liner of a gas chromatograph on the quantification of polycyclic aromatic hydrocarbons by isotope dilution mass spectrometry using deuterium-labeled internal standards. *J. Chromatogr. A* **2006**, 1134, 246-252.

[68] Radding, S.B., Mill, T., Gould, C.W., Liu, D.H., Johnson, H.L., Bomberger, D.C., and Fojs, C.V. *The Environmental Fate of Selected Polynuclear Aromatic Hydrocarbons*, U.S. Environmental Protection Agency, Office of Toxic Substances, Washington, DC, EPA 560/5-75-009, 1976.

[69] Moret, S, and Conte, L.S. Polycyclic aromatic hydrocarbons in edible fats and oils: occurrence and analytical methods. *J. Chromatogr. A.* **2000**, 882, 245-253.

[70] Wise, S.A., Sander A.C., and May, W.E. Determination of polycyclic aromatic hydrocarbons by liquid chromatography. *J. Chromatogr.* **1993**, 642, 329-349.

[71] Graf, W. and Diehl, H. About the natural background of carcinogenic polycyclic aromatics and its cause. *Arch. Hyg. Bakt.* **1966**, 150, 49-59.

[72] Hancock, J.L. Applegate H.G., and Dodd, J.D. Polynuclear aromatic hydrocarbons on leaves. *Atmos. Environ.* **1970**, 4, 363-370.

[73] Graf, W. and Nowak, W. Growth promotion of lower and higher plants by carcinogenic polycyclic aromatics. *Arch. Hyg. Bakt.* **1966**, 150, 513-528.

[74] Harrison, R.M., Perry, R., and Wellings, R.A. Polynuclear Aromatic Hydrocarbons in Raw, Potable and Waste Waters. *Water Res.* **1975**, 9, 331-346.

[75] Karickhoff, S.W., Brown, D.S., and Scott, T.A. Sorption of Hydrophobic Pollutants on Natural Sediments. *Water Res.* **1979**, 13, 241-248.

[76] Chen, B.H., Wang, C.Y., and Chiu, C.P. Evaluation of Analysis of Polycyclic Aromatic Hydrocarbons in Meat Products by Liquid Chromatography. J. Agric. Food Chem. 1996, 44, 2244-2251.

[77] Chiu, C.P., Lin, Y.S., and Chen, B.H. Comparison of GC-MS and HPLC for Overcoming Matrix Interferences in the Analysis of PAHs in Smoked Food. *Chromatographia* **1997**, 44, 497-504.

[78] Poster, D.L., Schantz, M.M., Sander, L.C., and Wise, S.A. Analysis of polycyclic aromatic hydrocarbons (PAHs) in environmental samples: a critical review of gas chromatographic (GC) methods. *Anal. Bioanal. Chem.* **2006**, 368, 859-881.

[79] US Environmental Protection Agency. Compendium method TO-13A: determination of polycyclic aromatic hydrocarbons (PAHs) in ambient air using gas chromatography/mass spectrometry (GC/MS), compendium of methods for the determination of toxic organic compounds in ambient air, second edition, EPA/625/R-96/010b, US Environmental Protection Agency, Cincinnati, OH, USA, 1999. http://www.epa.gov/ttn/amtic/files/ambient/airtox/to-13arr.pdf (accessed April 2009).

[80] National Environmental Methods Index. Methods for the determination of organic compounds in drinking water – supplement I, EPA/600/R-95-131, National Technical Information Service, PB95-261616, Washington D.C., USA, 1995. http://www.nemi.gov/apex/f?p=237:38:1707853104718420::::P38_METHOD_ID:4782 (accessed April 2009).

[81] National Environmental Methods Index. Methods for the determination of organic compounds in drinking water – supplement III, EPA/600/R-95-131, National Technical Information Service, PB95-261616, Washington D.C., 1995. http://www.nemi.gov/apex/f?p=237:38:1707853104718420::::P38_METHOD_ID:4783 (accessed April 2009).

[82] US Environmental Protection Agency. Method 8310 – Determination of PAHs in groundwater and wastes, US Environmental Protection Agency, Washington D.C, USA, 1986. http://www.epa.gov/waste/hazard/testmethods/sw846/pdfs/8310a.pdf (accessed March 2009).

[83] National Environmental Methods Index. Method 610 - polynuclear aromatic hydrocarbons, Part 136 guidelines establishing test procedures for the analysis of pollutants; appendix A: methods for organic chemical

analysis of municipal and industrial wastewater, 40CFR136.1, US Environmental Protection Agency, Washington D.C, USA, 2005. http://www.nemi.gov/apex/f?p=237:38:1707853104718420::::P38_METHOD_ID:4713 (accessed April 2009).

[84] US Environmental Protection Agency. Method 8275A - Semivolatile Organic Compounds (PAHs AND PCBs) In Soils/Sludges and Solid Wastes Using Thermal Extraction/Gas Chromatography/Mass Spectrometry (TE/GC/MS), Revision 1, US Environmental Protection Agency, Washington D.C, USA, 1996. http://www.epa.gov/osw/hazard/testmethods/sw846/pdfs/8275a.pdf (accessed April 2009).

[85] US Environmental Protection Agency. Methods for sampling and analyzing contaminants in fish and shellfish tissue, guidance for assessing chemical contaminant data for use in fish advisories, volume 1: fish sampling and analysis – third edition, EPA 823/B-00-007, US Environmental Protection Agency, Office of Water, Washington D. C., USA, 1993. http://www.epa.gov/waterscience/fish/advice/volume1/index.html (accessed April 2009).

[86] Nemcik, M. *Low-Level PAH Analysis using the Finnigan Surveyor HPLC System with PDA Detection*; Application Note 341; Thermo Electron Corporation: San Jose, California, 2004.

[87] Chee, K.K., Wong, M.K., and Lee, H.K. Optimization of microwave-assisted solvent extraction of polycyclic aromatic hydrocarbons in marine sediments using a microwave extraction system with high-performance liquid chromatography-fluorescence detection and gas chromatography-mass spectrometry. J. Chromatogr. A. **1996**, 723, 259-271.

[88] Shibamoto, T. *Chromatographic Analysis of Environmental and Food Toxicants*; CRC Press: Boca Raton, Florida, USA, 1998, pp. 170.

[89] de Boer, J., and Law, R.J. Developments in the use of chromatographic techniques in marine laboratories for the determination of halogenated contaminants and polycyclic aromatic hydrocarbons. *J. Chromatogr. A.* **2003**, 1000, 223-251.

[90] Brindle, I.D. and Li, X.F. Investigation into the Factors Affecting Performance in the Determination of Polycyclic Aromatic Hydrocarbons Using Capillary Gas Chromatography-Mass Spectrometry with Splitless Injection. *J. Chromatogr.* **1990**, 498, 11-24.

[91] Grob, K. and Grob, G. Splitless Injection on Capillary Columns, Part 1. The Basic Technique; Steroid Analysis as an Example. *J. Chromatogr. Sci.* **1969**, 7, 584-6.

[92] Berset, J.D. and Holzer, R. Separation of Important PCBs and PAHs on a Prototype Smectic Liquid-Crystalline Polysiloxane Stationary Phase Capillary Column. *Chemosphere* **1994**, 28, 2087-2099.

[93] Godula, M., Hajslova, J., and Alterova, K. Pulsed Splitless Injection and the Extent of Matrix Effects in the Analysis of Pesticides. *J. High Resol. Chromatogr.* **1999**, 22, 395-402.

[94] Ruikang, H., Lifeng, Z., and Zhaoguang, Y. Picogram determination of N-nitrosodimethylamine in water. *Water Science & Technology* **2008**, 58.1, 143-151.

[95] Russell, M., Webster, L., Walsham, P., Packer, G., Dalgarno, E.J., Mcintosh, A.D., and Moffat, C.F. The effects of oil exploration and production in the Fladen Ground: Composition and concentration of hydrocarbons in sediment samples collected during 2001 and their comparison with sediment samples collected in 1989. *Marine Pollut. Bull.* **2005**, 50, 638-651.

[96] Castello, G. and Gerbino, T.C. Analysis of polycyclic aromatic hydrocarbons with an ion-trap mass detector and comparison with other gas chromatographic and high-performance liquid chromatographic techniques. *J. Chromatogr.* **1993**, 642, 351-357.

[97] Lee, H.B., Szawiola, R., and Chau, A.S. Solvent Effects on Response Factors for Polynuclear Aromatic Hydrocarbons Determined by Capillary Gas Chromatography Using Splitless Injections. *J. Assoc. Off. Anal. Chem.* **1987**, 70, 929-930.

[98] Trotter, W.J. Effect of the Solvent on the Response to Organophosphorus Pesticides Determined using Gas Chromatography with Flame Photometric Detection. *Intern. J. Environ. Anal. Chem.* **1985**, 21, 171-178.

[99] Gebhart, J.E., Hayes, T.L., Alford-Stevens, A.L., and Budde, W.L. Mass Spectrometric Determination of Polychlorinated Biphenyls as Isomer Groups. *Anal. Chem.* **1985**, 57, 2458-2463.

[100] Grob, K. Solvent Effects on Response Factors – Problems in Performing Splitless Injection. *J. Assoc. Off. Anal. Chem.* **1988**, 71, 76A-78A.

[101] Trevelin, W.R., Vidal, R.H., Landgraf, M.D., Silva, I.C.E., and Rezende, M.O.O. Optimization of parameters for the gas chromatographic determination of polycyclic aromatic hydrocarbons. *Analytica Chimica Acta* **1992**, 268, 67-71.

[102] Grob, K. and Grob, K. Jr. Isothermal Analysis on Capillary Columns without Stream Splitting: The Role of the Solvent. *J. Chromatogr.* **1974**, 94, 53-64.

[103] Brindle, I.D., Elrutb, M., and Li, X.F. An Investigation of High Boiling Alcohols as Injection Solvents for the Determination of Polynuclear Aromatic Hydrocarbons. Unpublished data

[104] Zoccolillo, L., Babi, D., and Felli, M. Evaluation of Polycyclic Aromatic Hydrocarbons in Gasoline by HPLC and GC-MS. *Chromatographia* **2000**, 52, 373-376.

[105] Grob, K. and Grob, K. Jr. Splitless Injection and the Solvent Effect. *J. High Resolut. Chromatogr. Chromatogr. Commun.* **1978**, 1, 57-64.

[106] Yang, F. *^{207}Pb Dating of Lacustrine Sediments from Lake Ontario (Core 298), Ontario*; NWRI Report 07-01; National Water Research Institute, Burlington, ON, Canada, 2007.

[107] Standard Operating Procedure for the Analysis of 9 Chlorobenzenes, 17 Organochlorine Pesticides, Total Polychlorinated Biphenyls and 23 Polynuclear Aromatic Hydrocarbons in Sediment Using Ultrasonic Extraction and Gas Chromatography with Electron Capture and Mass Selective Detectors; SOP 03-3751, Version 1; National Laboratory for Environmental Testing: Burlington, ON, Canada, 2005.

[108] Crozier, P., Lega, R., Kolic, T., Macpherson, K., Gewurtz, S., Shen, L., Helm, P., Reiner, E., Brindle, I., and Marvin, C. Temporal Trends of Legacy and Emerging Persistent Organic Pollutants in a Sediment Core from Lake Ontario. In *Global Environment and Sustainability: Sound Science in a World of Diversity*, CETAC North America 27th Annual Meeting, Montreal, QC, Canada, November 5-9, 2006.

[109] Helm, P., Lega, R., Crozier, P., Reiner, E., Howell, T., Gewurtz, S., Shen, L., Brindle, I., and Marvin, C. Polychlorinated Naphthalenes in the Laurentian Great Lakes: Occurrence in Nearshore Sediments and Historical Profiles in Lake Ontario Sediment Cores. In *Environmental Stewardship: Integrating Science and Management*, CETAC North America 29th Annual Meeting, Tampa, FL, USA, November 16-20, 2008.

[110] Guide to Preparing and Analyzing Semivolatile Organic Compounds. Restek Corporation Literature Catalogue #59411A. http://www.restek.com/restek/images/external/59411A.pdf (accessed January 2008).

[111] Elrutb, M. Investigations into the Extraction and the Determination of Polycyclic Aromatic Hydrocarbons (PAHs) from Water by Solid-Phase Extraction and Capillary Gas Chromatography/Mass Spectrometry. MSc. Thesis, Brock University, St. Catharines, ON, 1993.

Appendix 1 – Synthesis of Fluorinated Compounds

All synthesis was performed at Brock University by **Bradford Sullivan** of Tomas Hudlicky's research group.

The fluorinated benzamides were synthesized according to the following reactions:

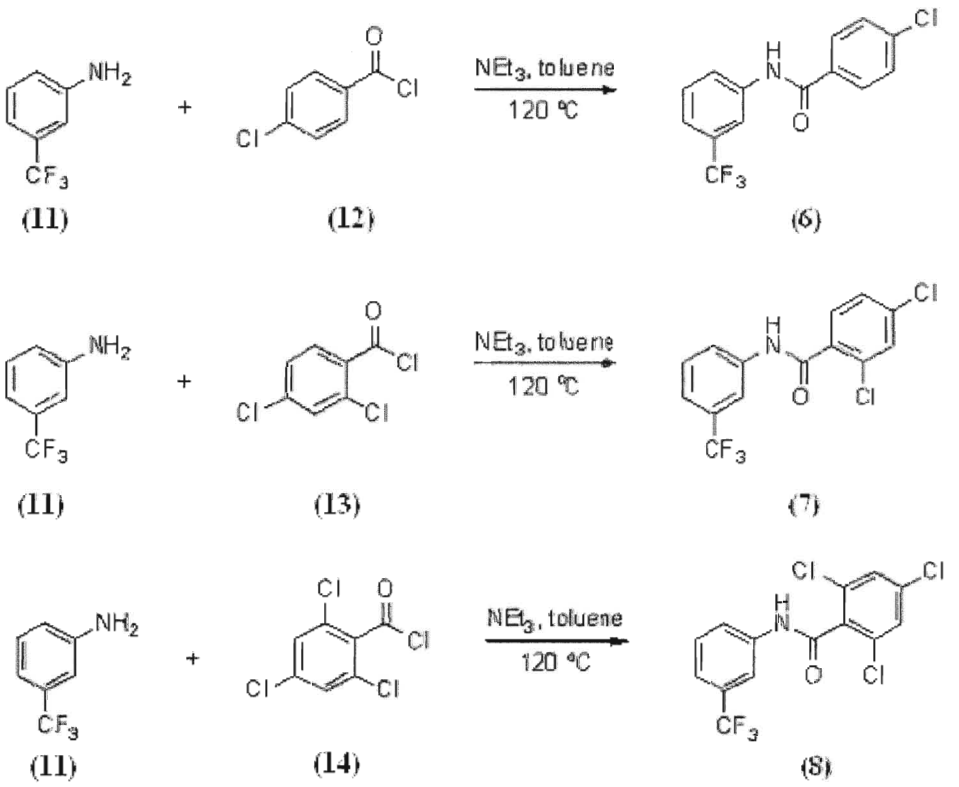

Figure 52 – Mechanism for synthesis of fluorinated benzamides

All fluorinated benzamides were synthesized by the same general procedure, as described below.

General Procedure

3-(trifluoromethyl)aniline (**11**) (1.8g, 11.2mmol) and triethylamine (3.11mL, 22.3mmol) were dissolved into 5mL of toluene. While stirring, chlorinated benzoyl chloride (1.96g, 2.34g, and 2.72g for **12**,**13**, and **14** resp., 11.2mmol)

was added and the solution was then heated and allowed to reflux for 12 hours. Once cooled, the solution was concentrated under reduced pressure. The resulting residue was added to 5mL of water, dissolved, and stirred for 2 hours. Liquid-liquid extraction was performed, with ethyl acetate (3×3mL). The combined solvent extracts were washed with a saturated NH_4Cl solution (1×3mL), and a saturated NaCl solution (1×2mL), and was then dried with Mg_2SO_4. The crude solid was recrystallized from ethyl acetate, by the addition of hexanes. The yield, melting point, and spectral information for the three products are listed below. See Appendix 2 for relevant spectra.

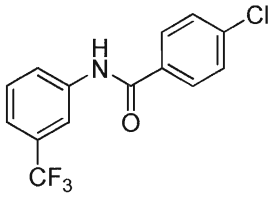

4-chloro-N-[3-(trifluoromethyl)phenyl]benzamide (**6**)

The title compound was a white crystalline solid (2.91 g, 87%): R_f 0.41 (4:1 hexanes-ethyl acetate); mp 114-116 °C (ethyl acetate-hexanes); IR (film) ν 3434, 2095, 1652, 1333, 1124 cm^{-1}; ^1H NMR (600 MHz, $CDCl_3$) δ 8.02 (s, 1NH), 7.90-7.92 (m, 1H), 7.84 (d, *J* = 8.2 Hz, 1H), 7.80 (d, *J* = 8.3 Hz, 2H), 7.48 (t, *J* = 8.1 Hz, 1H), 7.45 (d, *J* = 8.3 Hz, 2H), 7.41 (d, *J* = 8.1 Hz, 1H) ppm; ^{13}C NMR (150 MHz, $CDCl_3$) δ 164.9, 138.6, 138.2, 132.7, 131.6 (q, *J* = 32.6 Hz, 1C), 129.7 (2 x C), 129.2, 128.5 (2 x C), 123.8 (q, *J* = 272.4 Hz, 1C), 123.4, 121.4 (q, *J* = 3.4 Hz, 1C), 117.0 (q, *J* = 3.6 Hz, 1C) ppm; MS (EI) *m/z* (%): 299 (M), 75(10), 111(24), 139(100), 141(30), 299(14); HRMS calculated for $C_{14}H_9ClF_3NO$ 299.0325, found 299.0324.

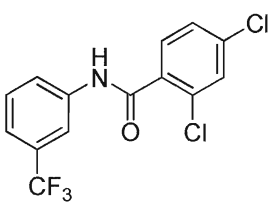

2,4-dichloro-N-[3-(trifluoromethyl)phenyl]benzamide (**7**)

The title compound was a white crystalline solid (3.12 g, 84%): R_f 0.41 (4:1 hexanes-ethyl acetate); mp 128-130 °C (ethyl acetate-hexanes); IR (film) ν 3430, 1655, 1447, 1333, 1127 cm^{-1}; ^1H NMR (600 MHz, $CDCl_3$) δ 8.16 (s, 1NH), 7.92-7.94 (m, 1H), 7.83 (d, *J* = 7.9 Hz, 1H), 7.69 (d, *J* = 8.3 Hz, 1H), 7.49 (t, *J* = 8.3 Hz, 1H), 7.47 (d, *J* = 1.8 Hz, 1H), 7.44 (d, *J* = 7.9 Hz, 1H), 7.36 (dd, *J* = 1.8, 8.3 Hz, 1H) ppm; ^{13}C NMR (150 MHz, $CDCl_3$) δ 163.7, 137.8, 137.7, 132.9, 131.6 (q, *J* = 32.7 Hz, 1C), 131.5, 131.4, 130.3, 129.8, 127.9, 123.8 (q, *J* = 272.3 Hz, 1C), 123.2, 121.6 (q, *J* = 3.4 Hz, 1C), 116.9 (q, *J* = 3.4 Hz, 1C) ppm; MS (EI) *m/z* (%): 333 (M), 145(17), 147(11), 173(100), 175(62), 177(10), 333(15), 335(10); HRMS calculated for $C_{14}H_8Cl_2F_3NO$ 333.9935, found 333.9934.

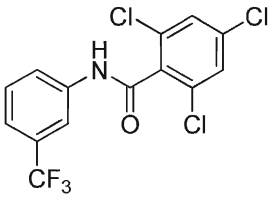

2,4,6-trichloro-N-[3-(trifluoromethyl)phenyl]benzamide (**8**)

The title compound was a white crystalline solid (3.71 g, 90%): R_f 0.49 (4:1 hexanes-ethyl acetate); mp 132-134 °C (ethyl acetate-hexanes); IR (film) ν 3434, 2094, 1657, 1578, 1333, 1127 cm^{-1}; ^1H NMR (600 MHz, $CDCl_3$) δ 7.97 (s, 1NH), 7.84-7.86 (m, 1H), 7.83 (d, *J* = 7.9 Hz, 1H), 7.50 (t, *J* = 7.9 Hz, 1H), 7.45 (d, *J* = 7.9 Hz, 1H), 7.34 (s, 2H) ppm; ^{13}C NMR (150 MHz, $CDCl_3$) δ 162.1, 137.5, 136.5, 133.9, 132.9 (2 x C), 131.6 (q, *J* = 32.5 Hz, 1C), 129.8, 128.3 (2 x C), 123.7 (q, *J* = 272.6 Hz, 1C), 123.4, 121.9 (q, *J* = 3.4 Hz, 1C), 117.1 (q, *J* = 3.4 Hz, 1C) ppm; MS (EI) *m/z* (%): 367 (M), 179(12), 181(12), 207(100), 209(98), 211(32), 367(18), 369(17); HRMS calculated for $C_{14}H_7Cl_3F_3NO$ 366.9545, found 366.9542.

Compounds 9 and 10 were synthesized according to the reaction scheme shown below. See Appendix 2 for relevant spectra.

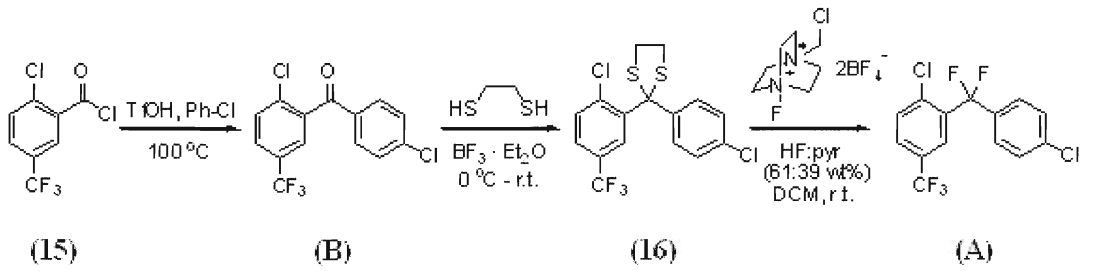

Figure 53 – Mechanism for synthesis of compounds A and B

Procedure

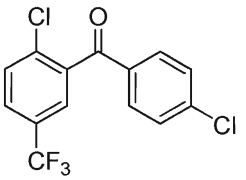

2,4'-dichloro-5-(trifluoromethyl)-benzophenone **(B)**

Trifluoromethanesulfonic (50µL, 0.514mmol) acid was added to a solution of 2-chloro-5-(trifluoromethyl)benzoyl chloride (**15**) (250mg, 1.03mmol) in chlorobenzene (1.25mL), while stirring. The resulting mixture was heated for 6 hours, at 100°C, before cooling to room temperature. The cooled mixture was then combined with 5mL of ice water and extracted with chloroform (5×1mL). The chloroform layers were combined, washed with 2mL of saturated NaCl solution, and dried with Na_2SO_4. Compound 9 was separated from the reaction mixture via column chromatography. The mixture was applied to a column containing 30g of silica gel and then eluted first with 600mL of 200:1 hexanes:ethyl ether, and then with 800mL of 50:1 hexanes:ethyl ether - in which compound 9 was extracted. The 50:1 hexanes:ethyl ether fraction was reduced under vacuum to yield the title compound, 2,4'-dichloro-5-(trifluoromethyl)-benzophenone **(B)**, as a clear and colourless oil (267 mg, 81%): R_f 0.43 (30:1 hexanes-ethyl acetate); IR (film) ν 3432, 2088, 1642, 1335, 1253, 1081, 771 cm^{-1}; ^1H NMR (600 MHz, $(CD_3)_2CO$) δ 7.94 (dd, J = 1.8, 8.3 Hz, 1H), 7.92 (d, J = 1.8 Hz, 1H), 7.82-7.85 (m, 3H), 7.59-7.63 (m, 2H) ppm; ^{13}C NMR (150 MHz, $(CD_3)_2CO$) δ 192.0, 140.1, 139.2,

134.7, 134.6, 131.5 (2 x C), 131.1, 129.3 (2 x C), 129.2 (q, J = 99.6 Hz, 1C), 128.4 (q, J = 3.3 Hz, 1C), 126.1 (q, J = 3.3 Hz, 1C), 123.7 (q, J = 271.8 Hz, 1C) ppm; MS (EI) *m/z* (%): 318 (M), 75(18), 111(26), 139(100), 179(12), 207(24), 318(28), 320(18); HRMS calculated for $C_{14}H_7Cl_2F_3O$ 317.9826, found 317.9822.

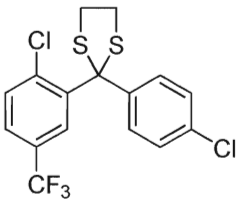

2,4'-dichloro-5-(trifluoromethyl)-diphenyldithiolane **(16)**

BF_3•Et_2O (36μL, 0.295mmol) was added to a solution of 2,4'-dichloro-5-(trifluoromethyl)-benzophenone **(B)** (94mg, 0.295mmol) in 1,2-ethanedithiol (600μL) at 0°C while stirring. The mixture was then stirred for 12 hours at room temperature. It was then filtered through a SiO_2/celite plug, and reduced under vacuum. The resulting compound, 2,4'-dichloro-5-(trifluoromethyl)-diphenyldithiolane **(16)**, was a pale yellow oil (111 mg, 96%): R_f 0.56 (30:1 hexanes-ethyl acetate); IR (film) ν 3425, 2099, 1645, 1327, 1128, 1084, 772 cm^{-1}; ^1H NMR (600 MHz, $CDCl_3$) δ 8.60 (d, J = 1.5 Hz, 1H), 7.53 (dd, J = 1.5, 8.3 Hz, 1H), 7.49 (d, J = 8.3 Hz, 1H), 7.37 (d, J = 8.3 Hz, 2H), 7.22 (d, J = 8.3 Hz, 2H), 3.53-3.59 (m, 2H), 3.30-3.36 (m, 2H) ppm; ^{13}C NMR (150 MHz, $CDCl_3$) δ 143.4, 140.8, 138.9, 133.3, 132.4, 128.9 (q, J = 33.8 Hz, 1C), 128.4 (2 x C), 128.3 (2 x C), 125.8 (q, J = 3.4 Hz, 1C), 125.3 (q, J = 3.4 Hz), 123.8 (q, J = 272.4 Hz, 1C), 74.9, 41.2 (2 x C) ppm; MS (EI) *m/z* (%): 394 (M), 61(22), 75(14), 111(23), 139(100), 141(37), 155(12), 179(14), 207(35), 209(12), 299(13), 318(39), 320(26), 331(60), 332(10), 333(25), 334(10); HRMS calculated for $C_{16}H_{11}Cl_2F_3S_2$ 393.9631, found 393.9632.

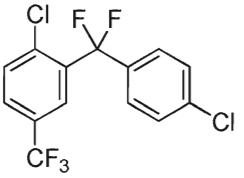

difluoro-2,4'-dichloro-5-(trifluoromethyl)-diphenylmethane **(A)**

Selectfluor® (1-Chloromethyl-4-fluoro-1,4-diazoniabicyclo[2.2.2]-octane bis-{tetrafluoroborate}) (2.51g, 7.08mmol) and HF:pyridine (61:39 wt%) (3.5mL) were combined in a 25mL poly(tetrafluoroethene) round-bottomed flask. The solution was cooled to 0°C and then, by dropwise addition, a solution of 2,4'-dichloro-5-(trifluoromethyl)-diphenyldithiolane **(16)** (700mg, 1.77mmol) in dichloromethane (2mL) was added over 10 minutes. The resulting mixture was stirred for 12 hours at room temperature. Next, the mixture was added to 2mL of H_2O, and then extracted with chloroform (5×1mL). The chloroform layers were combined and washed with saturated NaCl solution (2×2mL) and dried with Mg_2SO_4. The title compound, difluoro-2,4'-dichloro-5-(trifluoromethyl)-diphenylmethane **(A)** was separated by column chromatography. The chloroform extract was applied to a column containing 40g of silica gel. The column was eluted with 600mL of 400:1 hexanes:ethyl ether and then 800mL of 50:1 hexanes:ethyl ether in which the title compound was contained. The 50:1 hexanes:ethyl ether fraction was reduced under vacuum to yield the title compound, difluoro-2,4'-dichloro-5-(trifluoromethyl)-diphenylmethane **(A)**, as a clear and colourless oil (355 mg, 59%): R_f 0.71 (70:1 hexanes-ethyl acetate); IR (film) ν 3430, 2090, 1644, 1333, 1272, 1134, 1093 cm^{-1}; ^1H NMR (600 MHz, $CDCl_3$) δ 8.11 (d, J = 1.5 Hz, 1H), 7.69 (dd, J = 1.5, 8.3 Hz, 1H), 7.56 (d, J = 8.3 Hz, 1H), 7.39-7.41 (m, 4H) ppm; ^{13}C NMR (150 MHz, $CDCl_3$) δ 136.6 (t, J = 2.0 Hz, 1C), 136.5, 135.2 (t, J = 27.9 Hz, 1C), 134.2 (t, J = 27.3 Hz, 1C), 132.2, 129.5 (q, J = 33.6 Hz, 1C), 128.8 (2 x C), 128.4 (q, J = 3.2 Hz, 1C), 127.5 (t, J = 5.4 Hz, 2C), 124.8 (tq, J = 3.6, 4.3 Hz, 1C), 123.4 (q, J = 272.4 Hz, 1C), 118.6 (q, J = 244.1 Hz, 1C) ppm; MS (EI) *m/z* (%): 340(M), 161(100), 163(32), 229(15), 285(11), 305(10), 340(62), 342(40); HRMS calculated for $C_{14}H_7Cl_2F_5$ 339.9845, found 339.9841.

Appendix 2 – Spectra

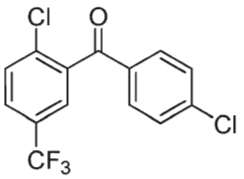

Compound B – ^{1}H and ^{13}C NMR

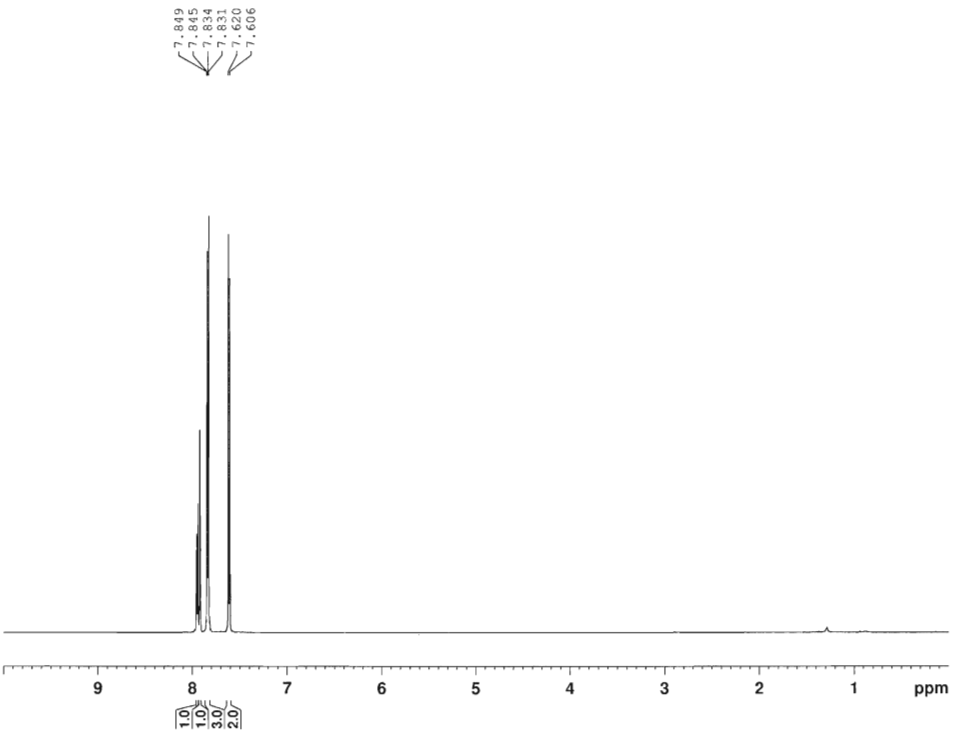

Figure 54 – ^{1}H NMR spectrum for Compound B

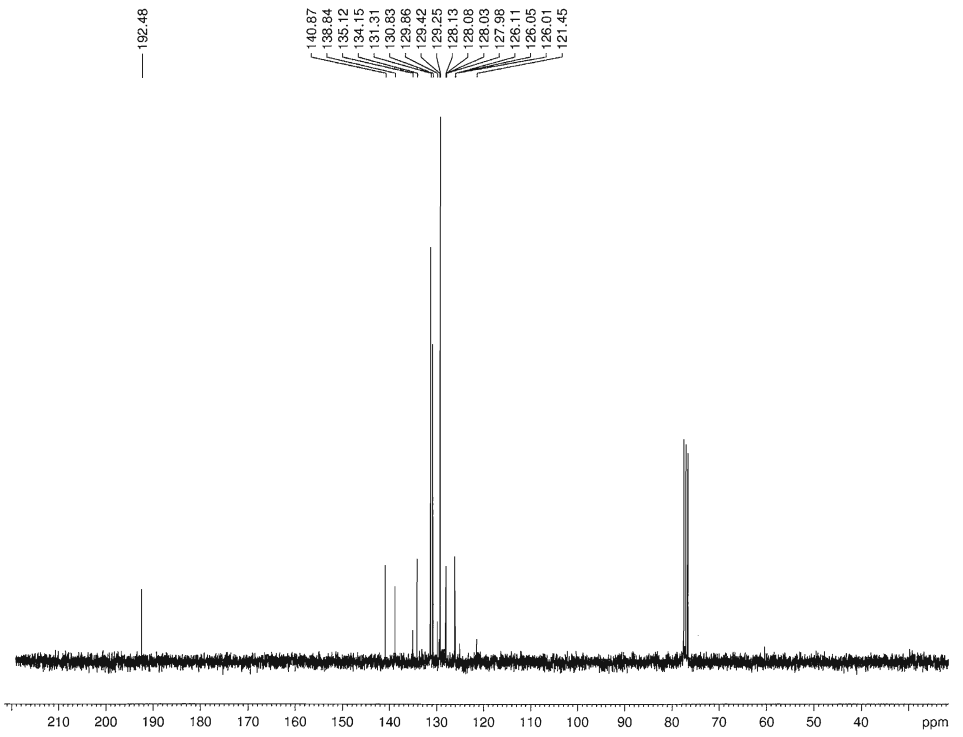

Figure 55 – ^{13}C NMR spectrum for Compound B

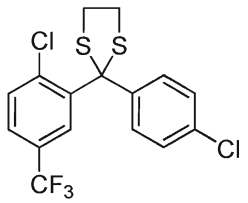

Compound 10 – ^{1}H and ^{13}C NMR

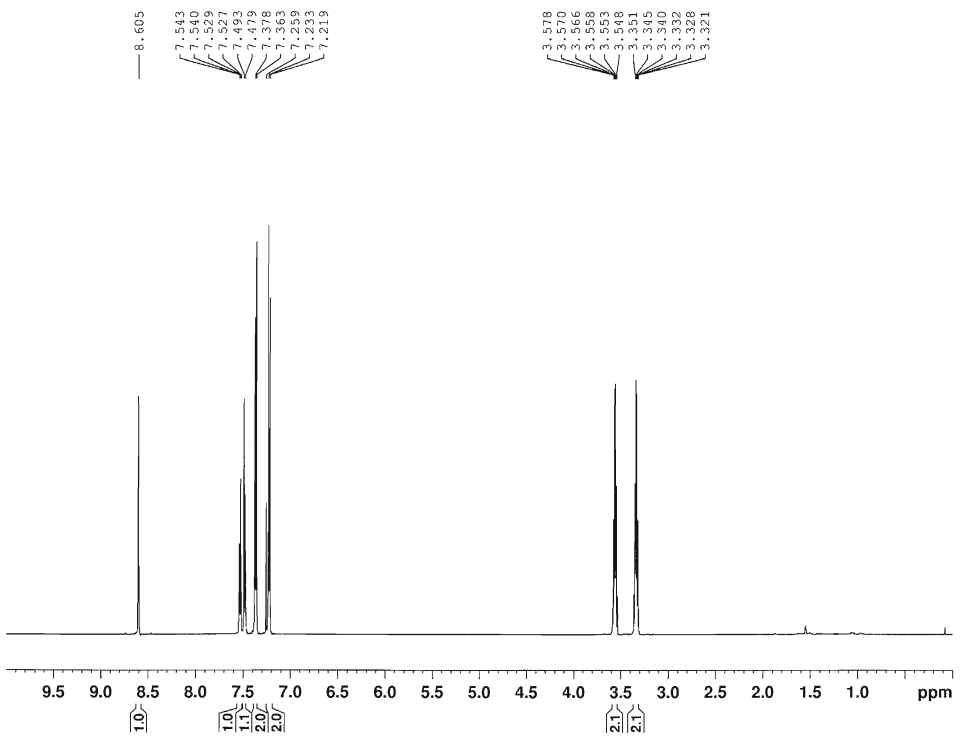

Figure 56 – ^{1}H NMR spectrum for Compound 10

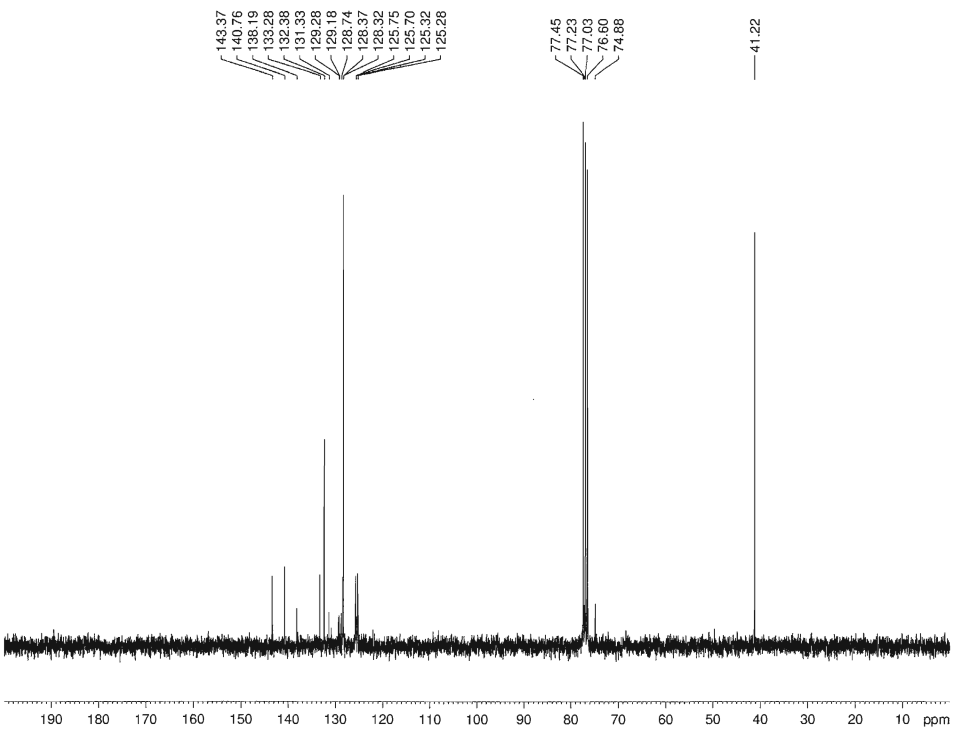

Figure 57 – ^{13}C NMR spectrum for Compound 10

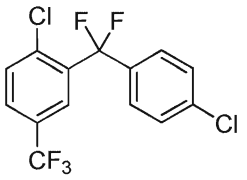

Compound A – ^{1}H and ^{13}C NMR

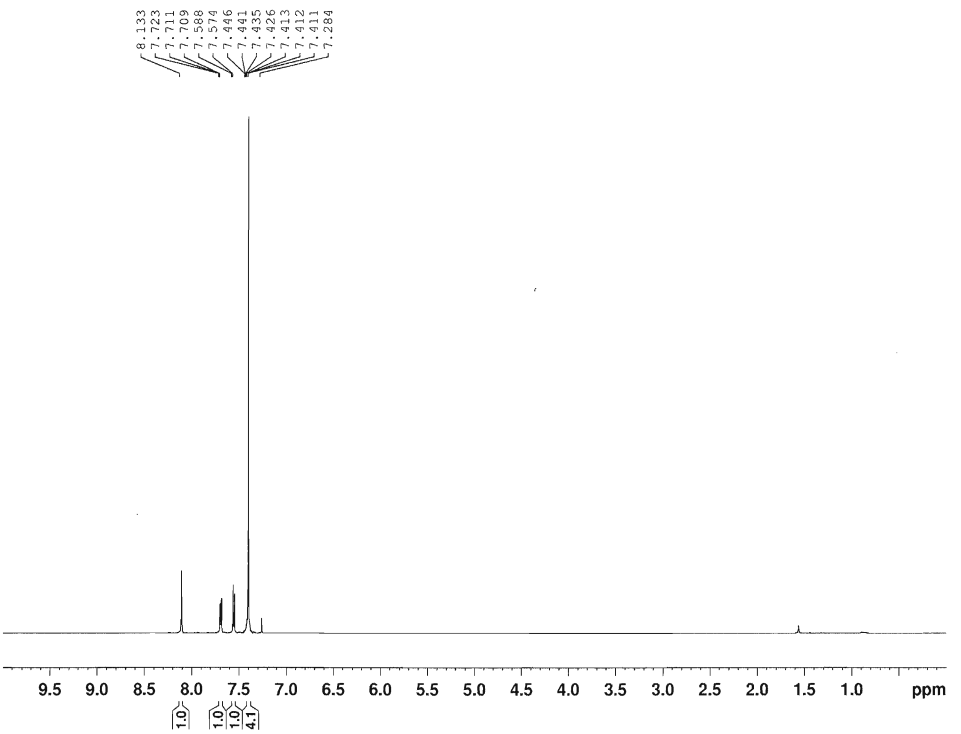

Figure 58 – ^{1}H NMR spectrum for Compound A

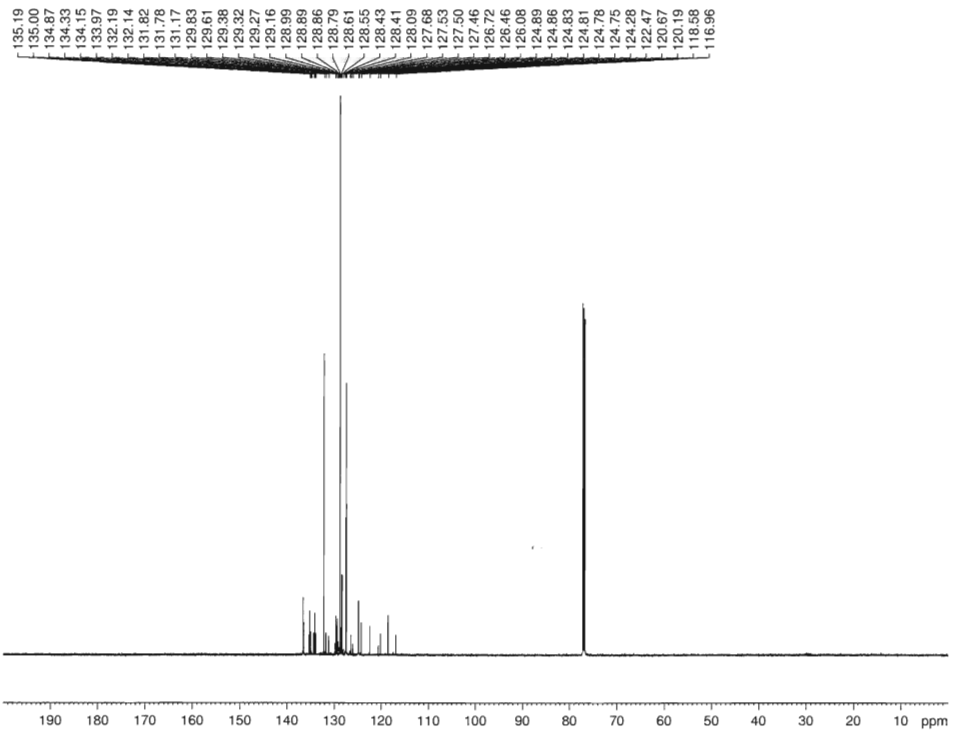

Figure 59 – ^{13}C NMR spectrum for Compound A

Appendix 3 – Additions and Revisions

After completion of this thesis, additional experiments revealed an error in some of the findings. New results indicate that the guard column, used throughout the experiments performed for this work, behaved as a retention gap. The guard column was shown to significantly affect peak symmetry and resolution. See Figure 60.

The additional focusing provided by the guard column almost completely negates the effects of peak fronting and tailing. This explains the superior symmetry ranges observed for the PAHs using the RTX-50 column, in comparison to the results from the DB-5 column determined by Elrutb [111]. New results suggest that symmetry ranges for the PAHs from the RTX-50 column are very similar to those of the DB-5 column [111]. These results also show that both fronting and tailing can occur due to anomalies in the transfer of analytes from the injector to the column.

Recent experiments also suggest that, similar to the findings of Brindle and Li [90], the optimum initial column temperature for the PAHs in the various injection solvents lies near the boiling point of the solvent. As the initial column temperature rises above or falls below this temperature, fronting or tailing, respectively, occur. This trend is also found to intensify as initial column temperatures further from the optimum value are chosen. These new results have also shown that the RTX-50 column has a very similar affect on chromatography as the DB-17ms column, and that one column is not superior to the other.

Recent results suggest additional benefits in the use of guard columns. In addition to protecting the analytical column and MS from non-volatile contamination, the guard column can provide analyte focusing which leads to improved peak symmetry and resolution. The increased analyte symmetry ranges observed will simplify method development.

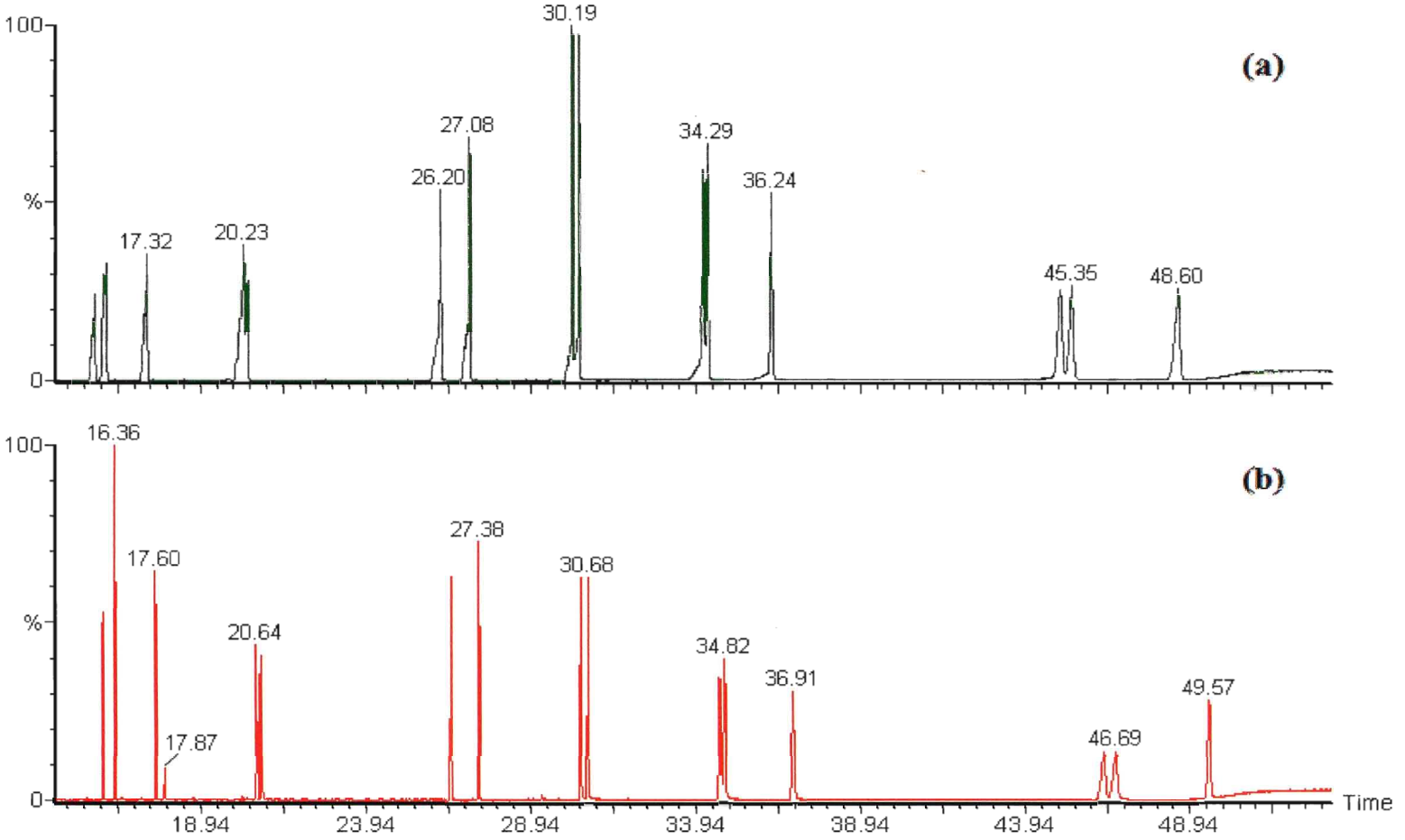

Figure 60 – 15 US EPA priority PAHs in toluene using RTX-50 column (a) without guard column, (b) with 5m × 0.53mmID guard column

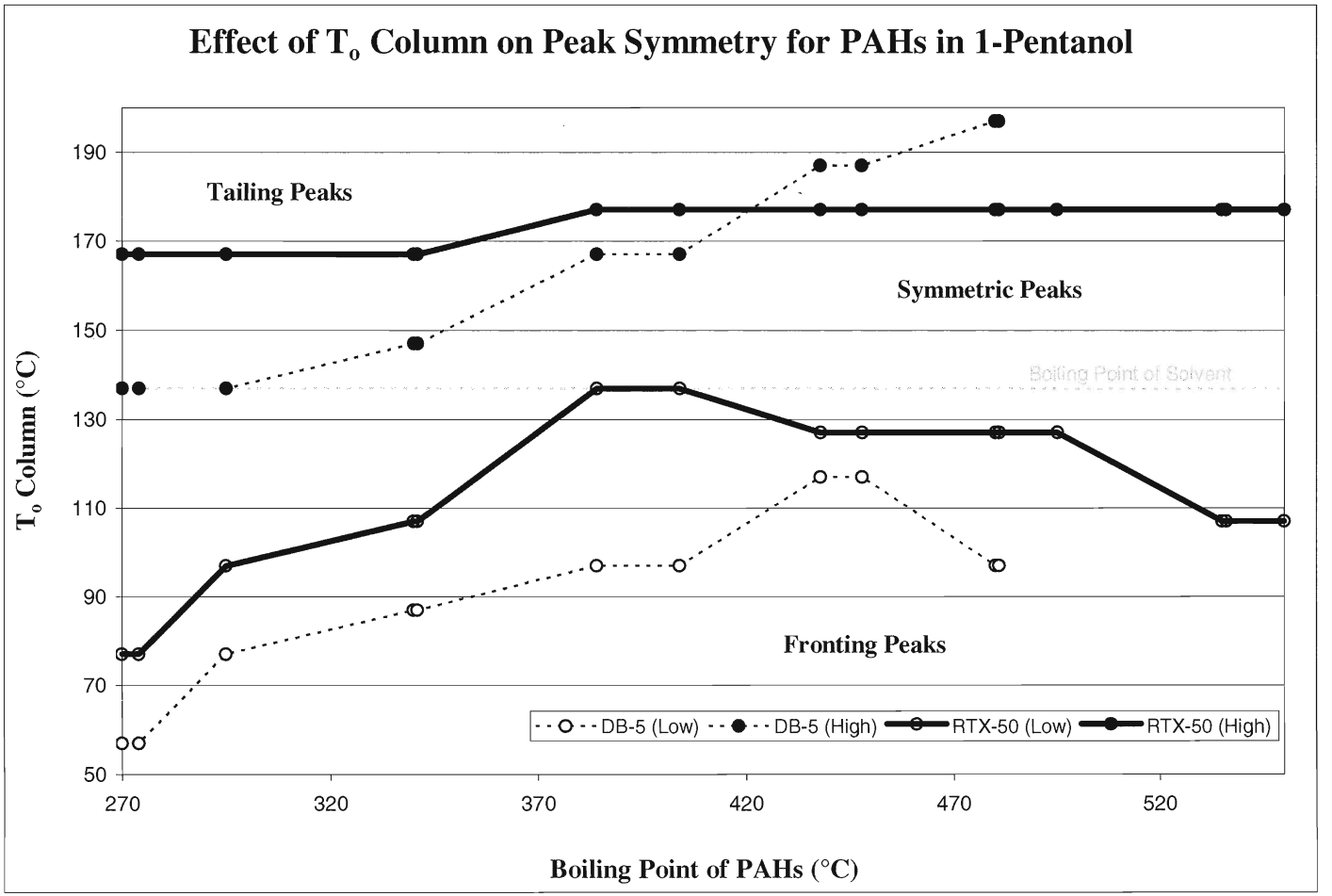

Figure 61 – The effect of initial column temperature on peak symmetry for 15 PAHs in 1-pentanol

As seen in Figures 60 and 61, significant fronting and tailing occurs with the RTX-50 column when used without a guard column. Neither solvent trapping nor cold trapping appear to be important focusing mechanisms. There is a narrower range of initial column temperatures under which symmetric peaks are obtained. The symmetry range observed for the RTX-50 column (without a guard column) is more comparable to the symmetry range for the DB-5 column. See Figure 61.

With the use of a guard column, fronting is eliminated as analytes are trapped twice – once at the inlet to the guard column (solvent or cold trapping) and then again at the inlet to the analytical column (retention gap effect). Peak tailing is minimized as well because analytes are held up at the inlet to the analytical column (retention gap effect) and this provides the opportunity for analytes that were slow to travel from injector to column, to catch up.